THE UNIVERSITY OF CHICAGO

DENDRITIC CELLS PRIME ANTI-TUMOR CD8 T CELL RESPONSES THROUGH MHC-DRESSING

A DISSERTATION SUBMITTED TO
THE FACULTY OF THE DIVISION OF THE BIOLOGICAL SCIENCES
AND THE PRITZKER SCHOOL OF MEDICINE
IN CANDIDACY FOR THE DEGREE OF
DOCTOR OF PHILOSOPHY

COMMITTEE ON IMMUNOLOGY

BY

BRENDAN WILLIAM MACNABB

CHICAGO, ILLINOIS

MARCH 2022

Table of Contents

List of Figures

List of Tables

List of Abbreviations

APC	Antigen Presenting Cell
BMDC	Bone Marrow-Derived DC
cDC1	type 1 conventional Dendritic Cell
cDC2	type 2 conventional Dendritic Cell
CDP	Common DC Progenitor
CDR	Complementarity Determining Region
CLP	Common Lymphoid Progenitor
CMP	Common Myeloid Progenitor
cTEC	cortical Thymic Epithelial Cell
DAMP	Danger-Associated Molecular Pattern
DC	Dendritic Cell
dLN	draining Lymph Node
ERAD	ER-Associated Degradation
ERAAP	ER Aminopeptidase associated with Antigen Processing
Flt3	Fms-Like Tyrosine Kinase 3
GM-CSF	Granulocyte-Macrophage Colony-Stimulating Factor
HLA	Human Leukocyte Antigen
IFN	Interferon
IL	Interleukin
IRAP	Insulin Regulated Aminoprotease
i.v.	Itravenous
LMPP	Lymphomyeloid-Primed Progenitor
LN	Lymph Node
MHC	Major Histocompatibility Complex
MHC-I	class I MHC
MHC-II	class II MHC
mTEC	medullary Thymic Epithelial Cell
PAMP	Pathogen-Associated Molecular Pattern
PLC	Peptide Loading Complex
pMHC	peptide/Major Histocompatibility Complex
PRR	Pattern Recognition Receptor
RAG	Recombination Activating Genes
RSS	Recombination Signal Sequence
s.c.	Subcutaneous
SLO	Secondary Lymphoid Organ
S1P	Sphingosine-1-Phosphate
S1P1	Sphingosine-1-Phosphate Receptor 1
TAP	Transporter associated with Antigen Processing
TCR	T Cell Receptor
tdLN	tumor-draining Lymph Node

TIL	Tumor-Infiltrating Lymphocyte
TNF-α	Tumor Necrosis Factor α

Acknowledgments

Thanks everybody for everything. It has been a time.

Firstly, I would like to thank my parents. Without their love and support through many years of chaos, I would not be here. Thanks to my brother, Matt, who is one of the most thoughtful and kind people around. Although it feels like it is not enough, all I can say to you guys is thank you, and I love you.

Secondly, I would like to thank my advisor, Dr. Justin Kline, who has been exactly the mentor I have needed for six long years. More than that he has been my friend through road trips, burritos, parking trouble, and happy hours. I would also like to thank the other members of the lab, especially Xiufen, who is the nicest person and most efficient scientist in Chicago; Sravya, who is my science sibling in every regard except we don't fight enough (we definitely would be the equivalent of the kind of siblings who non-ironically wear matching sweaters in a Christmas card); and James, whose positive outlook and drive changed the lab for the better at a time when we all needed a bit of help. RIP cool kid bay.

Next, I would like to thank my thesis committee: Dr. Barbara Kee, Dr. Andrew Koh, and Dr. Tom Gajewski. I am very grateful for the immeasurable help and advice that Dr. Kee gave me during my search for a post-doc position, and for all that I learned in Advanced Immunology II as a student and TA, and when I rotated in her lab. Thanks also to Dr. Koh for all of his help on ATAC-seq, and for teaching me everything I know about epigenetics (which, actually, is not that much).

I would also like to thank Dr. Peter Savage for always helping me when I needed advice, for feedback in lab meetings, and also for happy hours. Thanks also to all the members of the Savage Lab over the years. That time we got stuck in California after the Asilomar conference and went to Yosemite is easily a top ten moment of graduate school. Dave, please don't forget about me when you are famous for the Riot Theory of autoimmunity.

Thanks to all the students in the COI and beyond for making these past few years fun.

Special thanks to the members of all the intramural teams: Liz, Allen, Lydia, Shan, and Zach from our years as a juggernaut (and champion) broomball squad; the Co-stims softball champions; those fun soccer teams—never forget the Sangman slip game. Jordan, the teams are in good hands with you. Thanks also to the pickup soccer crew, George, AJ, French guy, *et al*. It has been a pleasure getting to know all of you. You know that you are spending time with good people when even some of the trips to the emergency room are fun. To my friends Shan, Zach, Chris, Ryan, Roy, Liana, Alex, and Dave, thank you for all the game nights, pub nights, cookouts at the point, and Sasquatch expeditions.

Finally, I would like to thank my pack. I would not be nearly as sane as I currently am without Curie the past couple of years. I would have included her as an author on my paper if listing dogs as authors was something you could still get away with. Last, but certainly not least, I would like to thank Lydia. Her love and presence has been the best part of my life these past few years. Through her I have gained another family and a whole bunch of Italian townie friends I never knew I needed. I cannot wait for our life together in Pasadena and beyond.

Abstract

Dendritic cells (DCs) act at the interface of the innate and adaptive arms of the immune system. Their primary function is to orchestrate adaptive immune responses by presenting antigens and providing costimulatory signals to T cells. For $CD8^+$ T cells, recognition of a cognate antigenic peptide bound to class I major histocompatibility complex (MHC-I) presented by a DC along with co-stimulation results in its activation—a proliferative burst and the acquisition of a potent cytotoxic effector program. In the context of a tumor, DCs are thought to activate $CD8^+$ T cells primarily through antigen cross-presentation, in which DCs generate antigenic peptides derived from exogenous proteins through proteasomal or lysosomal degradation and subsequently load these peptides onto MHC-I molecules for display. Here, using two murine tumor models lacking the MHC-I molecule H-$2K^b$ (K^b), we found that cancer cell-intrinsic MHC-I expression was required for optimal $CD8^+$ T cell priming. Furthermore, using genetically modified mouse strains lacking MHC-I or otherwise deficient in cross-presentation, we observed that DCs were capable of acquiring and presenting intact peptide/(p)MHC-I from cancer cells, and that this was sufficient for their ability to activate tumor antigen-specific $CD8^+$ T cells *ex vivo*. Finally, we confirmed that antigen presenting cells (APCs) were capable of presenting acquired, cancer cell-derived class I human leukocyte antigen (HLA-I; human MHC-I) molecules from human lymphoma cells, both *in vitro* and in xenograft experiments. Together, these results suggest that MHC-dressing, the presentation of exogenous pMHC-I complexes by DCs, makes a significant contribution to overall tumor antigen presentation.

Chapter 1: Introduction

1.1 Overview

Life has been flourishing, evolving, and diversifying on Earth for more than 3.5 billion years, resulting in an ecosystem of unimaginable complexity. Within this environment, species and individuals come into frequent contact, and survival often depends on an organism's ability to sense danger and to tell friend from foe. As such, species in all kingdoms of life have developed mechanisms of detecting and neutralizing threats[1–4], ranging from the expression of receptors recognizing broadly conserved molecular patterns associated with infections, cell stress, or damage[5,6], to the generation of proteins[7] or RNA oligonucleotides[3] tailored to a specific pathogen or toxin. Over time, species have layered many of these mechanisms in overlapping and complementary fashion[8]. The need for complex organisms to maintain homeostasis across sophisticated organ systems while constantly interacting with varied pathogens has led to the development of specialized cells tasked with ensuring the survival of the host amid these myriad challenges. In jawed vertebrates, an entire system of such cells—the immune system—monitors tissues for sign of damage and stress, communicates with commensal microorganisms, and wards off infections from pathogens.

The immune system is classically divided into two distinct parts: an innate immune system poised to rapidly detect and mitigate an array of defined threats, and an adaptive immune system which deliberately mounts a specific response to any given threat through the activation of lymphocytes from a preexisting repertoire. The innate immune system is comprised of specialized cells such as mononuclear phagocytes, granulocytes, and innate lymphoid cells, though epithelial and endothelial cells, stroma, and neurons are integral to innate immunity due to their roles in barrier integrity and stress response[9,10]. The adaptive immune system consists of

B and T cells. While the primary function of B cells is to generate antibodies[7], T cells play various roles in the immune response. Activated $CD4^+$ T cells can provide costimulation to B cells, produce effector cytokines, promote tissue repair, or exert regulatory activity on other immune cells[11,12]. Activated $CD8^+$ T cells target specific cells for lysis in order to remove infected and cancerous cells from the host[13].

In reality, the two arms of the immune system work synergistically to resolve any potential threats to the host, with cells typically associated with one aspect of the response fine-tuning or enhancing the functions of cells associated with the other. Dendritic cells (DCs), in particular, function at the interface of the innate and adaptive immune systems. Part of the mononuclear phagocyte system, DCs reside in tissues throughout the body, constitutively sampling their environment for antigens and danger- or pathogen-associated molecular patterns (DAMPs and PAMPs, respectively)[14]. DCs migrate from non-lymphoid tissues through afferent lymphatics to draining lymph nodes (LNs)[15]. There, migratory DCs and LN-resident DCs present peptide antigens on major histocompatibility complex (MHC) molecules to T cells[16]. In order to generate a productive T cell response, the DC must both present a peptide/MHC (pMHC) recognized by the T cell receptor (TCR) and provide costimulation through the expression of CD80 and/or CD86[16]. The DC can further instruct the nature of the T cell response by providing tertiary signals, such as the cytokines interleukin(IL)-12 and IL-23[17]. In this way, DCs are responsible for the initiation of adaptive immune responses.

1.2 $CD8^+$ T cell Development and Function

1.2.1 TCR Gene Recombination and Thymic Selection

T cells are adaptive immune cells which each express a unique cell-surface receptor (TCR) that recognizes a specific antigen or set of antigens with a high affinity. With a few

notable exceptions, they generally follow the rules of clonal selection theory, originally hypothesized by Frank Macfarlane Burnet in 1957 as the rules governing antibody generation[18]: 1) each lymphocyte bears a single receptor with a unique specificity; 2) antigen recognition through the receptor leads to activation; 3) all progeny of a lymphocyte bear the same receptor as the original cell; and 4) lymphocytes bearing receptors specific for a self antigen are removed from the repertoire. In reality, there are many cells in the body which share TCRs due to clonal expansion and bias in receptor generation[19]. Furthermore, each TCR can recognize a potentially large set of antigens[20], and a significant portion of the repertoire can recognize self antigens, necessitating mechanisms of dominant tolerance[21]. However, each T cell does express a single TCR and undergoes a proliferative burst following TCR engagement, exponentially increasing the number of T cell clones bearing the same TCR in a matter of days, before exerting effector functions to counter an infection or tumor, or becoming long-lived and self-renewing memory cells, capable of responding to the same threat months or years removed from the initial encounter with its antigen[13]. Clonal expansion upon antigen encounter allows each naive lymphocyte to exist in a very low frequency within the overall population, which contains an immense repertoire of TCRs, allowing the immune system to respond to diverse threats as they appear.

Rather than separately encode millions of individual TCR genes, diversity in the TCR repertoire is generated through site-specific somatic gene recombination. This process, known as V(D)J recombination after the variable (V), diversity (D), and joining (J) segments that comprise the TCR (and B cell receptor), can generate immense numbers of unique TCRs, with estimates ranging from 10^{15} to 10^{19} [22,23], through combinatorial diversity—the use of different combinations of V, D, and J genes—and junctional diversity—the removal and/or addition of base pairs at the junction of two segments resulting from imprecise DNA repair and the deliberate addition of

non-encoded bases[24]. V(D)J recombination is mediated by the RAG complex, whose core includes two proteins encoded by the recombination activating genes, *Rag1* and *Rag2*, which have structural and functional similarities to transposases found in invertebrates[25–28]. RAG1 and RAG2 form a heterodimer which recognizes recombination signal sequences (RSS)—a conserved heptamer and nonamer separated by a 12- or 23-bp spacer that resemble inverted repeats flanking transposable elements[29,30]—adjoining V, D, and J segments[31]. The RAG complex recombines the DNA by bringing a 12-RSS and a 23-RSS into close proximity in a DNA loop and creating double-stranded breaks at both RSSs. The DNA fragment between the two segments is fused into a circular fragment and discarded. Subsequent DNA repair and fusion of the two segments can lead to the insertion of palindromic (P)[32,33] and non-templated (N)[34–36] bases, the source of junctional diversity[37].

The stochastic nature of V(D)J recombination leads to the generation of TCRs which must be removed from the repertoire, either because they are incapable of recognizing antigens presented on host MHC molecules or because they bind too tightly to self antigens or the MHC itself[38].Because of this, V(D)J recombination is followed by a rigorous selection process[39]. While undergoing RAG-mediated recombination of the TCRα locus, thymocytes upregulate the coreceptors CD4 and CD8. The thymocytes then undergo the process of positive selection in the thymic cortex, where cortical thymic epithelial cells (cTECs) present an array of peptide antigens on class I (MHC-I) and class II (MHC-II) MHC that is distinct from those presented by all other cells in the body due to differential protease expression[40]. If the TCR is unable to bind to any MHC molecule, the thymocyte will undergo apoptosis having failed positive selection[38]. Most thymocytes fail to recognize MHC and die by neglect at this stage[41,42]. Successful engagement of the TCR with pMHC brings the TCR into close contact with the coreceptor, which binds to the side of the MHC molecule; CD4 binds MHC-II and CD8 binds MHC-I. The CD4/CD8 lineage

choice is determined by the interaction between the coreceptor and its partner MHC ligand[41].

Following positive selection, potentially dangerous TCRs are removed from the repertoire due to their intolerably high affinity for MHC, cross-reactivity to different MHC molecules, or particularly high avidity interactions with a given pMHC[43]. This process of negative selection can occur in either the thymic cortex or medulla, but appears to be more prominent in the former[42]. After migrating to the thymic medulla, regulatory T cells are selected from the $CD4^+$ population based on their avidity for self peptide antigens, the transcription of which occurs in medullary (m)TECs, primarily due to the expression of the transcription factor AIRE[44].

It must be noted that the developmental process described above pertains only to conventional $CD4^+$ and $CD8^+$ αβT cells. V(D)J recombination and thymic selection occur slightly differently for γδT cells[45]. Additionally, the selection events and developmental trajectories of alternative αβT cell lineages such as natural killer T cells and mucosal-associated invariant T cells are distinct[43]. The sum result of V(D)J recombination and thymic selection is a pool of T cells with a repertoire estimated to contain between 10^6 and 10^8 unique TCRs[46,47], each with the capacity to respond to a set of antigens, leaving the host with a well-stocked arsenal with which to ward off infections, eliminate cancerous cells, and maintain tissue homeostasis.

1.2.2 Activation and Function of $CD8^+$ T cells

Naive T cells circulate through the bloodstream, entering and exiting secondary lymphoid organs (SLOs), such as the spleen and LNs, in their constant quest to sense antigen. Naive T cells follow chemokine gradients, most notably CCL21, which binds to the receptor CCR7, and enter the LN through high endothelial venules. Entry to the spleen occurs through terminal arterioles which deposit the cells in the red pulp[48]. After entry, T cells migrate to the T cell zone of the LN

or splenic white pulp, again in a CCR7-dependent manner, following gradients of its ligands, CCL19 and CCL21, which are produced by DCs and radio-resistant stromal cells[48,49]. The T cells move along a random walk, transiently interacting with DCs until a T cell binds its cognate pMHC presented by a DC[50,51]. In the absence of TCR/pMHC engagement a single DC interacts with between 500 and 5,000 T cells per hour[51,52]; upon engagement the DC and T cell form a stable interaction which can last 48 hours[50].

This stable interaction, known as an immunological synapse, begins with the recognition of the pMHC by the TCR. Each TCR has six loops which interface with the pMHC, known as complementarity determining regions (CDRs). Each chain of the TCR dimer contributes three CDRs, two of which—CDR1 and CDR2—are germline-encoded and bind the surface of the MHC. The CDR3 loops interact directly with the peptide antigen and often contain residues encoded by P and N bases inserted during RAG recombination. The ability of T cells to recognize a wide array of peptides while maintaining a specific range of affinity for MHC molecules is due to the diversity of CDR3 sequences and relative lack of diversity in CDRs 1 and 2[53].

TCR/pMHC binding alone is insufficient for T cell activation. DCs must also provide costimulation in the form of CD80 and CD86 (also known as B7.1 and B7.2, respectively), two membrane-bound ligands recognized by their receptor, CD28, on the surface of T cells. Engagement of both the TCR and CD28 results in a burst of proliferation, with CD28 signaling crucial for IL-2 production and cell survival[54–57]. Other costimulatory receptor/ligand interactions such as 4-1BB/4-1BBL can compensate for the loss of CD28 signaling in $CD8^+$ T cells to a certain extent, though these receptors often work together with CD28 to maximize effector and memory responses[13]. Additionally, coinhibitory receptor/ligand interactions such as PD-1/PD-L1 dampen the effects of costimulation, rendering T cells dysfunctional[58,59]. The coinhibitory

receptor CTLA-4 binds CD80 and CD86 with greater affinity than CD28, thereby attenuating T cell activation directly by diminishing TCR signaling and indirectly through competition for ligands with CD28[60–62]. For $CD8^+$ T cells, optimal activation is also dependent on a third signal in the form of IL-12 or type I interferons (IFNs), as both of these signaling pathways promote cytotoxic effector function[13]. The primary source of IL-12 *in vivo* are type 1 conventional DCs (cDC1), while many innate immune cells are capable of producing type I IFNs in various circumstances[14]. Through the provision (or withholding) of three signals, TCR/pMHC binding, costimulation in the form of CD80 and/or CD86, and IL-12 or type I IFNs, DCs regulate $CD8^+$ T cell activation.

While engaged in the immunological synapse, T cells downregulate the sphingosine 1-phosphate receptor ($S1P_1$) and express its antagonist, CD69, to prevent lymph node egress and promote longer interactions with DCs[63,64]. After a few days, the now-activated $CD8^+$ effector cells re-express $S1P_1$ in order to follow the S1P gradient out of the LN and into the bloodstream, from there trafficking to the site of infection or tumor[48]. Upon arrival at their destination, effector $CD8^+$ T cells interact with other cells while moving through the tissue. Antigen recognition by the TCR prompts the $CD8^+$ T cell to kill the target cell presenting the cognate pMHC-I. The $CD8^+$ T cell releases perforin and granzymes into the extracellular matrix at the immunological synapse formed with the target cell. Perforin molecules oligomerize in the plasma membrane of the target cell, forming pores through which granzymes can enter the target cell[65]. Granzymes then trigger apoptosis in the target cell through various pathways, including caspase cleavage[66]. Secretion of tumor necrosis factor α (TNF-α) by $CD8^+$ T cells also promotes apoptosis by binding to the receptor TNFR1 on the target cell, leading to signaling through the receptor's death domain[67]. Additionally, effector $CD8^+$ T cells produce and secrete high levels of IFN-γ, which activates and polarizes macrophages and has profound effects on nearby cells, inducing

the expression of antiviral and antimicrobial proteins, chemokines, and many components of the MHC-I and MHC-II antigen presentation pathways[68].

1.2.3 The Role of CD8$^+$ T cells in Cancer

The immune system affects the development and progression of cancer by removing immunogenic cancer cells and altering the tumor microenvironment in various ways. This process, known as immunosurveillance or immunoediting, can lead to a spectrum of outcomes: at one end the outright clearance of cancerous cells, and at the other the selection of cancer cells better adapted to survive in the presence of an immune response and to manipulate it to their benefit[69]. The ability of the immune system to restrict tumor growth was hypothesized as early as 1909 by Paul Ehrlich[70], and the *in vivo* immunogenicity of transplantable and carcinogen-induced tumors was demonstrated using inbred mouse strains in the 1940s and '50s[71–73]. Further research demonstrated that a fraction of lymphocytes isolated from peripheral blood were able to specifically lyse cancer cells isolated from autologous tumor biopsies *in vitro*[74–78]. Following the discovery of MHC-restriction[79], CD8$^+$ T cell clones capable of lysing autologous cancer cells in a mechanism dependent on their ability to bind human leukocyte antigen (HLA) class I, the human equivalent of MHC-I, were isolated from patients with various tumors[80,81]. Shortly after the crystal structure of MHC-I was solved, informing that MHC-I molecules present peptide antigens to CD8$^+$ T cells[82,83], numerous groups identified HLA-I- and MHC-I-restricted tumor antigens capable of recognition by CD8$^+$ T cells[84–90].

The centrality of CD8$^+$ T cell effector function in the anti-tumor immune response is further evidenced by the fact that mice deficient in adaptive immune cells due to the absence of RAG1 or RAG2 are unable to reject transplanted syngeneic tumors and have increased susceptibility to both spontaneous and carcinogen-induced tumors; up to 40% of the latter are

rapidly rejected upon transplantation into immunocompetent hosts[91–93]. Furthermore, mice lacking IFN-γ (or its receptor, IFNGR1), perforin, and TNF-α all have increased susceptibility to spontaneous and carcinogen-induced tumors[91,94–98], though it must be stated that $CD8^+$ T cells are not the only source of these three proteins. Perhaps the greatest testament to the potency of $CD8^+$ T cells in selectively removing cancerous cells is the great lengths to which tumors go in order to subvert T cell immunity. It has taken decades to resolve presence of $CD8^+$ T cells capable of recognizing tumor antigens in patients with the continued cancer progression in those same patients, a paradox first observed by Hellstrom *et al.*, who proposed that one explanation could be that the immune reaction may destroy many cells while not being potent enough to completely eradicate the tumor[74]. We know now that these seemingly paradoxical observations are explained by an ever-escalating Darwinian dance between the immune system and the tumor[92].

Under the selective pressure of an ongoing immune response, cancer cells capable of subverting the immune response have a significant survival advantage. This was elegantly demonstrated by Wortzel *et al.* in 1984 using an experiment in which they exposed a murine ultraviolet light-induced fibrosarcoma tumor line—which is rejected in immunocompetent hosts—to antigen-specific $CD8^+$ T cell clones *in vitro*. The surviving cancer cells, which were selected for their ability to persist in the presence of $CD8^+$ T cells *in vitro,* then grew progressively *in vivo* upon engraftment into immunocompetent hosts[99]. In patients, the selection of cancer cells capable of subverting the adaptive immune response manifests itself in many ways: $CD8^+$ T cell-infiltrated tumors often express high levels of coinhibitory receptors and/or bear inactivating mutations in antigen presentation or IFN-γ signaling pathways[92,100–102]. Over time, the tumor microenvironment can become more hostile to $CD8^+$ T cells due to recurrent interactions with cancer cells, suppression from other immune cells in the tumor, or the limited

availability of key nutrients, all culminating in a T cell dysfunctional state[103]. Overcoming this dysfunction has been an area of intense research over the past two decades, leading to the development of immunotherapies that are now effectively deployed in the clinic[102,104]. Recently, significant progress has been made in defining the phenotypic heterogeneity of tumor-infiltrating $CD8^+$ T cells ($CD8^+$ TILs) in patients and in mouse models. $CD8^+$ TILs exhibit a spectrum of phenotypes, ranging from a TCF-1^+ population with high proliferative capacity and the ability to produce effector cytokines at one extreme, to a terminally dysfunctional TOX^+ population at the other[103,105]. In particular, the importance of the TCF-1^+ population in mediating the anti-tumor immune response following checkpoint blockade therapy has become clear despite persisting disagreement over their ontogeny and nomenclature[105].

In stark contrast to the advances in phenotypic characterization of $CD8^+$ TILs, the antigen specificity of the vast majority of these cells remains opaque, and remarkably little is understood of the priming events as they occur in humans. Prevailing models suggest that $CD8^+$ T cells specific for tumor neoantigens—tumor-specific antigens which are generated by somatic mutations within cancer cells—play a dominat role in restricting tumor growth[90], based on many studies demonstrating the presence of neoantigen-specific $CD8^+$ T cells in human and murine tumors[87,106], use of epitope prediction algorithms[107–110], and correlations between overall mutational burden and anti-tumor immunity[101,108,111,112]. However, a growing body of evidence suggests that T cells reactive to bona fide neoantigens are quite rare in the tumor[113,114]. An unbiased survey of TCR antigen specificities using yeast display identified tumor-infiltrating $CD8^+$ T cells which were reactive to unmutated self antigens in two patients[115]. Additionally, self-reactive memory phenotype $CD8^+$ T cells are enriched in the prostates of TRAMP mice[116], further suggesting that a significant population of tumor-infiltrating $CD8^+$ T cells recognize native self antigens rather than neoantigens. Tissue-resident memory $CD8^+$ T cells specific for

viral antigens from previously resolved or chronic infections are also found in the tumor and are reactivated following chockpoint blockade therapy[117–120].

Possibly the greatest mystery surrounding the anti-tumor $CD8^+$ T cell response is why some patients fail to ever develop one. Unsurprisingly, the best predictors of whether or not a patient will respond to checkpoint blockade therapy are a preexisting population of activated $CD8^+$ TILs and elevated expression of PD-L1 by cancer and stromal cells, either resulting from IFN-γ signaling or genetic mutation[121–128]. Gaining a greater understanding the priming events surrounding anti-tumor $CD8^+$ T cells—answering key questions in how these cells are activated —could yield new insights into why and in what circumstances they are activated, or not activated. These events remain opaque in human cancers largely beause priming of naive anti-tumor $CD8^+$ T cells cannot be observed in real time. By the time patients present with clinical disease manifestations, the tumor may have been growing and evolving for months or years. Then, the immune response would have either already have been ongoing and exerting its selective pressure on the tumor or failed to mount at all. To understand the requirements for anti-tumor $CD8^+$ T cell activation in humans, the best we can do is find correlates with $CD8^+$ T cell infiltration. However, murine tumor models can be used to study anti-tumor $CD8^+$ T cell priming as it occurs. DCs are generally the central regulators of T cell activation through antigen presentation and the provision of costimulation. As will be discuessed in the next section, DCs mediate $CD8^+$ T cell priming against tumors as well[129,130], and ongoing work continues to elucidate their various functions. This study, in investigating the mechanisms by which DCs present tumor antigens, addresses an outstanding question in how DCs mediate anti-tumor $CD8^+$ T cell priming.

1.3 DC Development and Function

1.3.1 DC Development

DCs, along with macrophages and monocytes, comprise the mononuclear phagocyte system. Monocytes are primarily found in circulation, spleen, and bone marrow, while DCs and macrophages exist in tissues throughout the body, including SLOs. All mononuclear phagocytes exert their function at least partially through phagocytosis, as their name suggests. Macrophages and monocytes remove dead or dying cells, clear pathogens, and integrate signals from their environment in order to maintain or restore tissue homeostasis, while DCs acquire antigens for processing and presentation to T cells[131].

In adult hematopoiesis, all lymphoid and myeloid lineages can be traced back to lymphomyeloid-primed progenitors (LMPPs)[132,133]. From there, models of the developmental trajectory of DCs have been somewhat convoluted, based on the obersved potential for various progenitor cells to develop into DCs *in vitro*[134]. LMPPs can differentiate into either common lymphoid progenitors (CLPs) or common myeloid progenitors (CMPs), committing the cells to one developmental trajectory or the other[135]. CLPs have been shown to retain DC potential when cultured *ex vivo*[134,136,137], however, fate mapping using *Il7r*^{Cre}-driven expression of YFP revealed that the vast majority of cDCs are not derived from CLPs[138], but rather from CMPs[136,139]. It is currently unknown whether there are any intermediate precursors with cDC potential between the CMP and the common DC progenitor (CDP), which is the earliest precursor committed to the DC lineage[14,133]. Models in which granulocyte-monocyte progenitors (GMP) give rise to DCs[135,140] have been contradicted by *in vivo* fate mapping experiments[133,141], and another population, the macrophage and DC progenitor (MDP)[131,142,143], was recently shown to be a mixed population of cells already committed to either the monocyte or cDC lineage using single-cell RNA-seq[141].

CDPs further differentiate into pre-DCs, the immediate precursors to cDCs, which exit the bone marrow into the blood, and from there seed SLOs and peripheral tissues[144–147], where they develop into cDCs over the course of a few days. As mentioned for virtually all the progenitor cells listed above, pre-DCs are a heterogeneous population of cells which are already committed to either the cDC1 or cDC2 lineage[148–150]. Throughout this developmental pathway, the most important signal cDCs and their progenitors receive comes from the fms-like receptor tyrosine kinase Flt3 interacting with its cytokine ligand, Flt3L. Flt3-deficient mice lack cDCs[151,152], while administration of Flt3L drastically increases cDC development and proliferation[153]. Other signals, such as granulocyte-monocyte colony-stmulating factor (GM-CSF) and NOTCH ligands, guide cDC differentiation, but are not strictly required for development. Here, it must be noted that in the past GM-CSF was widely used to generate bone marrow-derived DCs (BMDCs) *in vitro*. In reality, culturing BM cells in GM-CSF generates a heterogenous mixture of cells, including DCs and macrophages; current protocols use Flt3L for BMDC differentiation rather than, or in combination with, GM-CSF[154]. In non-lymphoid tissues, DCs acquire a migratory program after ~5-7 days and subsequently transit to draining LNs (dLNs) using CCR7 to follow a CCL21 gradient through afferent lymphatics into the LN via the sub-capsular sinus[15,155–158]. Various groups have characterized a transcriptional program associated with migratory DCs in homeostatic and inflammatory conditions[159–161], leading to these DCs being referred to "mature[162]," "activated[163]," or "mature immunoregulatory (mreg)[164]" in different contexts.

DCs which have not upregulated a migratory program: those resident to SLOs, as well as those in non-lymphoid tissues which will become migratory in the future but have not yet, have in the past been described as immature, due to their similar cell surface phenotype to that of resting DCs *in vitro*—they have intermediate and low expression of MHC-II and CD80/86,

respectively[165]. DCs are highly responsive to PAMP signaling through pattern-recognition receptors (PRRs) such as Toll-like receptors (TLRs), NOD-like receptors (NLRs), RIG-I-like receptors (RLRs), and cyclic GMP-AMP synthase (cGAS); DAMPs such as type 1 IFN; contact-dependent signals received through integrins and NOTCH receptors; and certain neurotransmitters[14,166–169]. Sensing one or a combination of these signals activates DCs, causing them to upregulate costimulatory molecules and components of the MHC-I and MHC-II presentation pathways, as well as cytokines such as type 1 IFN, IL-12, and IL-23, which can be context- and cDC lineage-sppecific. This activation process has previously been called "maturation," but the term is no longer widely used due to the fact that non-activated DCs are, in fact, developmentally mature and functional[14].

Numerous transcription factors are required for DC development, often interacting with each other[169]. PU.1 and BCL11A are required for DC development, at least partially due to their regulation of *Flt3* expression[170–172]. PU.1 is also crucial in promoting myeloid, rather than lymphoid differentiation by arresting cell cycle progression in early progenitor cells[173], as well as in regulating *Irf8* expression in early progenitors[148,174]. Meanwhile, the lineage-defining transcription factor for cDCs, ZBTB46, is a good marker for cDC lineage commitment, but is not required for cDC development[175–177]. Differentiation of the two cDC lineages is predominantly mediated by differential expression of IRF4 and IRF8[169].

IRF8 is required for the development of cDC1, acting at various stages of differentiation[169]. Interestingly, expression of *Irf8* is regulated by distinct transcription factors binding to unique enhancers at each stage of differentiation. Early *Irf8* transcription is controlled by PU.1 up to the CDP stage[174], while BATF3 maintains elevated *Irf8* expression in pre-cDC1 and mature cDC1[148]. Its role in the regulation of *Irf8* makes BATF3 essential for cDC1 development and function[178,179], and *Batf3*$^{-/-}$ mice have been widely utilized to study the impact of

cDC1 deficiency *in vivo*. BATF and BATF2 can partially compensate for the absence of BATF3[169,180]; however, removal of the *Irf8* enhancer which BATF3 binds results in the complete absence of cDC1[181]. The development of cDC1 is also dependent on NFIL3 and ID2[182,183], the latter of which is another important regulator of *Irf8* expression. NFIL3 acts upstream of ID2 by downregulating *Zeb2*[184–186]. ZEB2—an E-Box-binding protein—and ID2 are mutually repressive, with ID2 promoting a cDC1 fate and ZEB2 antagonizing it. While the absence of ID2 impairs cDC1 development, *Zeb2*$^{-/-}$ mice display a bias toward cDC1 differentiation at the expense of cDC2 and plasmacytoid DCs despite ZEB2 being dispensable for cDC2 development[184,185]. Interestingly, *Zeb2*$^{-/-}$*Id2*$^{-/-}$ mice display normal cDC1 and cDC2 development, though function of these cells has not been investigated[186].

The canonical transcriptional regulator of cDC2 is IRF4[169,187], though it mainly impacts the function of these cells rather than their development[14,188]. Conversely, the development of cDC2 is dependent on the transcription factors RelB and IRF2[189–191]. cDC2 can subdivided based on differential expression of KLF4 and NOTCH2[169]. KLF4 expression drives a Th2-promoting penotype in cDC2[192], while NOTCH2 expression promotes a Th17-polarizing phenotype[193–196] . Study of the interactions between these transcription factors has been complicated by the heterogeneity of cDC2 populations *in vivo*, and the molecular mechanisms of cDC2 differentiation are much less well understood than those of cDC1 differentiation. Furthermore, study of the development and function of cDC2, and to a lesser degree, cDC1, *in vivo* has been hindered by the fact that many cell surface molecules used to identify these cells by flow cytometry are differentially expressed by DC subsets across tissues and/or shared by other cell types, such as macrophages and monocytes[14,140]. Combining new fate mapping tools with modern technologies such as single-cell RNA-seq and ATAC-seq will be crucial in advancing the field of DC biology.

1.3.2 Function of cDC1

Murine cDC1 are typically identified by their expression of CD8α (for SLO-resident cDC1), CD103 (for migratory and non-lymphoid tissue cDC1), XCR1, DNGR-1, or a combination of these markers. In humans, the equivalent cells are marked by their expression of CD141, XCR1, and DNGR-1[14]. They express a unique array of PRRs, including TLR3, TLR11, and DNGR-1, as well as endocytic and scavenger receptors such as DEC-205 and CD36[140], which together dictate the role of cDC1 in activating $CD8^+$ T cells, Th1 polarization, and peripheral tolerance. $CD103^+$ cDC1 transport peripheral antigens from tissues to dLNs, while $CD8\alpha^+$ cDC1 capture antigens from lymphatics. Both migratory and SLO-resident cDC1 are capable of homing to the T cell zone of LNs and presenting antigens to T cells[140].

One of the hallmarks of cDC1 is their capacity for antigen cross-presentation. Splenic $CD8\alpha^+$ DCs were identified as the antigen-presenting cells (APCs) capable of cross-presentation in an experiment in which mice were pulsed intravenously with irradiated, ovalbumin (OVA)-loaded, $B2m^{-/-}$ splenocytes, and the ability of DC populations to present antigen to OVA-specific (OT-I) $CD8^+$ T cells was assessed *ex vivo* following FACS purification[197]. Simultaneously, splenic $CD8\alpha^+$ DCs were shown to preferentially acquire cell-associated antigens[198–202], leading many to speculate that their propensity for cross-presentation was the result of their heightened ability to acquire antigens. However, the main candidate for a cross-presentation-regulating scavenger receptor, CD36, was dispensable for cross-presentation[203,204]. Rather than the specialization of cDC1 cross-presentation being the result of increased antigen uptake, it is caused by differential intracellular antigen trafficking and processing[205,206]. Dudziak *et al.* demonstrated that the unique role of cDC1 in cross-presentation was the result of differential specialization in antigen processing and presentation by cDC1 and cDC2 by targeting OVA-

conjugated antibodies to one cDC subset or the other[207]. cDC1 more efficiently presented an OVA-derived peptide on MHC-I, while cDC2 more efficiently presented an OVA-derived peptide on MHC-II[207]. With the generation of *Batf3*$^{-/-}$ mice, Hildner *et al.* proved decisively that *in vivo* cross-presentation is cDC1-dependent shortly thereafter[178].

The heightened ability to cross-present antigens is the result of many intrinsic biological attributes of cDC1. Upon uptake via phagocytosis, pinocytosis, trogocytosis, or receptor-mediated endocytosis, an antigen arrives in an endosome or lysosome. Interestingly, antigen uptake via scavenger receptor-mediated endocytosis delivers antigens to lysosomes, while mannose receptor-mediated endocytosis delivers antigens to early endosomes in bone marrow-derived macrophages and GM-CSF-cultured BMDCs *in vitro*[208]. While murine cDCs do not express the mannose receptor *in vivo*, many similar endocytic C-type lectin receptors are expressed, most notably DEC-205 in cDC1 and DC-SIGN in cDC2[140,209]. DEC-205, in particular, is capable of delivering antigens to phagosomes promoting cross-presentation, and its ectopic expression confers elevated cross-presentation ability onto cDC2[210]. Ectopic expression of other endocytic receptors, such as Dectin-1 and FcγRIIA have been shown to promote cross-presentation in cells which are otherwise incapable, further indicating that the mechanism of antigen uptake is a crucial determinant of cross-presentation[206,211,212]. Additionally, cDCs do not express scavenger receptors to the same extent as macrophages, in which Mertk, Axl, and Tyro3 facilitate the silent clearance of dead cells[213].

One major caveat to the conclusions made by Dudziak *et al.* is that they targeted OVA to DEC-205 to deliver it to cDC1, so the heightened cross-presentation ability by cDC1 in this study may seem more pornounced based on the mechanism of antigen delivery[207]. However, the cDC1-specific factors promoting cross-presentation go beyond the surface receptor level. Direction of internalized antigens to proper cellular compartments is the hypothesized function

of WDFY4, a protein expressed by cDC1, but not cDC2 or macrophages, which has been implicated in the cross-presentation of cell-associated antigens. WDFY4 localizes near the plasma membrane, and is colocalized with both clathrin—which generates intracellular vesicles and is essential for receptor-mediated endocytosis—and the early/recycling endosome marker Rab11, but not with the lysosome marker Lamp1[214]. Exactly how specific receptors target antigens to different intracellular compartments *in vivo* is likely to be context-dependent. For example, DEC-205 was originally shown to target antigen to Lamp1$^+$ endosomes in (GM-CSF) BMDCs *in vitro*, and was postulated to promote antigen presentation on MHC-II rather than cross-presentation[215]. Indeed, B cells express high levels of DEC-205 on their surface, and targetting OVA to B cells using the same method as Dudziak *et al.* results in efficient antigen presentation on MHC-II and has been used extensively to study germinal center reactions[216,217]. While the authors did not specifically test for cross-presentation by B cells after targetting OVA to DEC-205, cross-presentation is a function that is not typically associated with B cells.

The properties of phagosomes within cDC1 further promote cross-presentation once the antigen arrives. Because peptides loaded onto MHC-I are largely generated by the proteasome in the cytoplasm, antigens must not be degraded in a phagosome before they can be transported to the cytoplasm[201]. In order to maintain intact antigens, cDCs express much lower levels of lysosomal proteases, such as cathepsins, than do macrophages, resulting in slower lysosomal degradation[218,219]. Phagosomes of cDC1 are maintained at a slightly alkaline pH through the expression of the NADPH oxidase NOX2, which generates reactive oxygen species[220–222], further inhibiting antigen degradation, as lysosomal proteases are generally most active in acidic conditions[220]. Finally, the cDC1-specific PRR DNGR-1, a C-type lectin receptor endoded by the gene *Clec9a*, recognizes filamentous actin, a DAMP associated with necrotic cell death[223–226]. DNGR-1 signaling via SYK leads to phagosomal rupture, exposing antigens to proteasomal

degradation in the cytoplasm[227].

In addition to their cross-presentation abilities, cDC1 promote effector Th1 and $CD8^+$ T cell responses through the production of IL-12 and IL-15[140,228–231]. Production of these two cytokines is often downstream of PRR signaling, and a few PRRs are expressed exclusively by cDC1. TLR3 is one such PRR which detects dsRNA within the debris of virally infected cells upon internalization[232]. Additionally, cDC1 express high levels of TLR11, which recognizes a profilin-like molecule that is made by *Toxoplasma gondii*[233]. Pattern recognition by either of these receptors leads to IL-12 production, and ligation of TLR3 also leads to production of IL-6 and type 1 IFN by cDC1[140,232,233].

1.3.3 Function of cDC2

Similarly to cDC1, cDC2 can be SLO-resident or migratory, and exist in tissues throughout the body. However, unlike cDC1, cDC2 specialize in antigen presentation on MHC-II and are relatively poor at cross-presentation of antigens on MHC-I[207]. This specialization is in part due to transcriptional regulation by IRF4, which controls the expression of cathepsin S, as well as the accessory proteins to MHC-II loading H-2M, H-2O, and CD74[188]. cDC2 also display much greater functional and transcriptional heterogeneity across tissues than do cDC1[159]. As such, cDC2 are important in orchestrating immunity to a wide array of threats.

cDC2 are very responsive to the cytokines thymic stromal lymphopoietin (TSLP), IL-4, IL-13, IL-25, and IL-33, all of which drive a Th2-promoting phenotype in cDC2[234–240], and cDC2 have a well-described role in allergic airway inflammation[241]. A subset of cDC2 expressing CD301b has been implicating in priming Th2 responses to papain and *Nippostrongylus brasiliensis* in cutaneous and mediastinal LNs, respectively[242]. Polarization of cDC2 to a Th2-promoting phenotype is dependent on IRF4 and KLF4[192,236–238]. Conversely, cDC2 can be

polarized to promote type 3 immunity by NOTCH2. These cDC2 are the primary source of IL-23 required by Th17, Tc17, and ILC3[193,194,243]. NOTCH2-dependent cDC2 express both CD11b and CD103 in the intestinal lamina propria, Peyer's patches, and mesenteric lymph nodes[194,243,244]. These cDC2 are also required for IL-17 production by $CD8^+$ T cells in the skin and cutaneous lymph nodes in response to the various *Staphylococcus* species[245,246], and their production of IL-23 promotes IL-17 and IL-22 production by T cells in murine models of dermal inflammation[247].

Both KLF4- and NOTCH2-dependent cDC2 are particularly sensitive to signals of tissue stress and damage. Interestingly, cDC2 have recently been shown to interact closely with neurons in the skin, and the two cell types probably interact in other tissues as well. Release of calcitonin gene-related peptide (CGRP) by $TRPV1^+$ afferent sensory neurons in response to topical imiquimod treatment or *Candida albicans* infection promotes IL-23 production by dermal $CD301b^+$ cDC2[166,248,249]. Release of Substance P by the same $TRPV1^+$ neurons, meanwhile, promotes the Th2-polarizing cDC2 response to topical papain treatment[250].

1.3.4 The Role of cDC1 in Cancer

The importance of cDC1 in anti-tumor immunity is well-documented[129,130]. The presence and activation of cDC1 in the tumor are strongly and positively correlated with $CD8^+$ T cell infiltration[251,252] and long-term patient survival[253] in many different cancers. The role of DCs in cancer is largely similar to their role in other immune responses; they internalize tumor antigens, integrate signals from their environment, and produce signals for other immune cells. A characterization of the different myeloid populations in the tumor demonstrated that neutrophils, monocytes, macrophages, and DCs are all capable of acquiring a fluorescent model tumor antigen[253]. However, follow-up studies highlighted the importance of migratory cDC1 in transporting tumor antigens to the tdLN. Despite the fact that all myeloid cells in the tumor can

internalize tumor antigens, and that these antigens can also, in theory, drain into the lymph node through the afferent lymphatics, the presence of fluorescent tumor antigens in the tdLN was dependent on CCR7-mediated DC trafficking[254,255]. Migratory cDC1 are then capable of transferring antigens, as well as MHC molecules, to other APC subsets via cell-cell contact-dependent synaptic vesicles[256].

Anti-tumor $CD8^+$ T cell responses are predominantly primed by cDC1[178,254,255], while anti-tumor $CD4^+$ T cell responses have been shown to be orchestrated by cDC2[257]. *Batf3*$^{-/-}$ mice are unable to mount $CD8^+$ T cell responses against tumor antigens, reject immunogenic tumors whose growth is typically checked in wild-type hosts, or respond to checkpoint blockade therapy[178,255,258]. The necessity of tumor antigen cross-presentation by cDC1 is further highlighted by the reduction in anti-tumor $CD8^+$ T cell priming in *Wdfy4*$^{-/-}$ mice, which have a defect in cross-presentation of cell-associated antigens[214], as well as in *Clec9a*$^{-/-}$ mice, which lack the cross-presentation-promoting f-actin receptor DNGR-1[259]. As in other immune contexts, $CD103^+$ cDC1 are also the primary source of IL-12 in the tumor and tdLN[253,260]. In addition to their requirement for anti-tumor $CD8^+$ T cell priming in the tdLN, cDC1 have important functions within the tumor environment. $CD103^+$ cDC1 recruit activated $CD8^+$ T cells to the tumor through their production of the chemokines CXCL9 and CXCL10, which attract $CD8^+$ T cells through the receptor CXCR3[252,261]. They can also reactivate T cells in the tumor through antigen presentation and the provision of secondary and tertiary signals[129,130].

As in normal, healthy tissues, pre-DCs can seed tumors, where they mature into functional cDC1 or cDC2[262]. Fully differentiated cDC1 can also be recruited into the tumor thanks to their expression of the chemokine receptors CCR5 and XCL1. The ligands for these receptors, CCL5 and XCL1, respectively, can be produced in the tumor by NK cells, as well as tissue resident memory and effector $CD8^+$ T cells[263]. By attracting cDC1 in this manner, $CD8^+$

TILs promote their own restimulation and ensure that cDC1 continue to infiltrate the tumor. Not all tumors are infiltrated by cDC1, however. Elevated tumor-intrinsic Wnt/β-catenin signaling leads to the exclusion of cDC1 from the tumor and a resulting absence of anti-tumor $CD8^+$ T cell priming[264]. Production of prostaglandin E_2 (PGE_2) by tumor cells can also suppress infiltration of the tumor by, and activation of, cDC1[265]. Activation of cDC1 in tumors occurs primarily in response to type 1 IFN. Bone marrow-chimeric mice in which all cDC1 are IFNAR-deficient are unable to mount antigen-specific $CD8^+$ T cell responses[251,266]. Type 1 IFN production in the tumor is the result of stimulator of interferon genes (STING) signaling following the recognition of internalized tumor DNA by cGAS in the cytoplasm of APCs[267]. Anti-tumor $CD8^+$ T cell priming has also been shown to be dependent on IKKβ expression by cDC1[268], though this defect may be due to impaired migration by cDC1 independent of any activation[160].

1.4 Antigen Presentation on MHC-I

1.4.1 The MHC-I Presentation Pathway

$CD8^+$ T cells survey cells for signs of transformation or infection by an intracellular pathogen through TCR/pMHC-I interactions. All nucleated cells present MHC-I loaded with peptides derived from proteins expressed by the cell. These peptides are generated through evolutionarily conserved degradation mechanisms which regulate protein turnover in homeostatic conditions and times of stress[269,270]. Protein degradation resulting in peptides bound for presentation on MHC-I is typically mediated in the cytoplasm by the proteasome[271], though peptides generated by cathepsins—most notably cathepsin S[272]—in lysosomes can also be loaded onto MHC-I. The proteasome is a large, multisubunit protease which unfolds and degrades ubiquitinated proteins in the cytoplasm[273,274]. While proteins are routinely ubiquitinated during normal turnover, defective or misfolded proteins are also ubiquitinated to mark them for

degradation by the proteasome. As a result, peptides generated by the proteasome include the products of alternative open reading frames of mRNAs[275], introns[276], and defective ribosomal products[277,278], as well as peptides from normal, functional proteins, including those with post-translational modifications[269,271,279]. The proteasome is also capable of fusing peptides from different proteins, creating non-coded peptide antigens[280,281]. Detection of misfolded or otherwise defective proteins in the endoplasmic reticulum (ER) results in their retrotranslocation to the cytoplasm via the ER-associated degradation (ERAD) pathway, subjecting these proteins to ubiquitination and proteasomal degradation as it would occur for cytoplasmic proteins[269,270].

Although proteolysis occurs in the cytoplasm, peptides are loaded onto MHC-I molecules in either the ER or vacuoles containing both ER-associated and endosome-associated proteins[270]. To access the lumen of these organelles, peptides generated by proteasomal degradation and bound for MHC-I presentation are translocated across the vacuolar membrane by the Transporter associated with Antigen Processing (TAP), a heterodimeric ATP-dependent transporter encoded by two genes within the MHC locus[282–285]. Because TAP can transport peptides which are much longer than those bound by MHC-I, further processing is required after translocation[286]. ER aminopeptidase associated with antigen processing (ERAAP; known as Eraminopeptidase-1, or ERAP1, in humans) preferentially trims long peptides down to a length suitable to accomodate MHC-I binding, typically 8-10 amino acids[287]. Resultant peptides are subsequently loaded by the aptly-named peptide loading complex (PLC), which consists of TAP, the MHC-I heavy chain, β_2-microglobulin, tapasin, ERp57, and calreticulin and facilitates peptide loading, as well as quality control[270]. Because empty MHC-I molecules are inherently unstable, if the peptide affinity for MHC-I is not sufficiently high, the complex dissociates and the empty MHC-I is either recruited into another PLC or degraded via ERAD[270]. This inherent instability also means that in the absence of functional TAP—either due to inhibition by pathogen virulence factors or

genetic deletion—almost no MHC-I reaches the plasma membrane[269]. Loss of tapasin[288,289], ERp57[290], and calreticulin[291] also decrease overall MHC-I presentation, though not as drastically.

Cells constitutively internalize surface receptors and other membrane components for essential processes such as nutrient uptake and signal transduction, necessitating mechanisms of recycling membrane-bound proteins to the cell surface[292]. APCs also internalize large parts of their plasma membrane in the acquisition of antigens via phagocytosis[269]. Endocytosis and recycling of MHC-I is regulated by a conserved tyrosine-based motif in its cytoplasmic domain, similar to canonical YXXϕ motifs associated with clathrin-mediated endocytosis expressed by many surface membrane-bound proteins[293,294]. Following endocytosis, MHC-I can be directed to an early endosome (also known as recycling endosome) or a late endosome[295]. MHC-I can be recycled to the plasma membrane within minutes upon arrival to an early endosome[296], while MHC-I targeted to a late endosome which then fuses with a lysosome are exposed to acidic conditions in which peptide binding is less stable. Dissociation of the peptide in a lysosome can lead to another peptide being loaded onto MHC-I in its place[297,298]; this new peptide can be derived from cathepsin-mediated pretoelysis, rather than proteasomal degradation[272]. Phagosomes within APCs also contain the Insulin Regulated Aminoprotease (IRAP), a close relative of ERAAP with similar functions in trimmung peptides that has been shown to colocalize with MHC-I[299]. Reloaded pMHC-I molecules can then be recycled to the plasma membrane from lysosomes, albeit not as efficiently as from early endosomes. Eventually, MHC-I, like other proteins, undergoes steady-state turnover, in this case regulated by ubiquitination of the cytoplasmic tail targeting MHC-I to lysosomes for degradation. Intracellular pathogens can also use MHC-I ubiquitination as a mechanism of immune evasion[300,301].

1.4.2 Antigen Cross-Presentation

Naive $CD8^+$ T cells must be activated before they can detect and remove infected or transformed cells. This usually involves activation in a SLO by an APC, frequently a cDC1, which is not itself infected or transformed[13]. The acquision of a foreign antigen and subsequent presentation of a derivative peptide on MHC-I is called cross-presentation. APCs such as cDC1 constantly sample their environment for antigens and signals through various mechanisms. Exogenous antigens can enter the cell through phagocytosis, macropinocytosis, receptor-mediated endocytosis, or trogocytosis[269]. Soluble antigens are typically acquired through macropinocytosis, which involves the uptake of large volumes of extracellular fluids[302–305], while large particles and dead cells are internalized via phagocytosis[306,307]. APCs can also sample antigens directly from live cells through trogocytosis, which involves tearing a small part of the plasma membrane and cytoplasm from the sampled cell[308]. Extracellular vesicles such as exosomes, another potential source of cell-derived antigen[309], can be acquired through macropinocytosis or receptor-mediated endocytosis[310]. The mechanism of uptake has been demonstrated to affect the subcellular localization of acquired antigens and the efficiency of cross-presentation[208]; however, exogenous proteins end up in endosomes or lysosomes—where they do not have immediate access to the proteasome—regardless of the mechanism of uptake[269].

Treatment of cells with proteasome inhibitors drastically reduces cross-presentation *in vitro*[311], indicating that many exogenous antigenic peptides are generated through proteasomal degradation in a similar manner to the generation of endogenous peptides in direct MHC-I presentation. Furthermore, TAP is required to transport exogenous antigens from the cytoplasm to the ER or MHC-I-loading vacuoles in many different systems[312,313]. Given that exogenous antigens arrive in vacuolar compartments of APCs but proteasomal degradation occurs in the cytoplasm, export of foreign antigens from endosomes or phagosomes to the cytoplasm is a

crucial step in cross-presentation[269]. The relatively slow phagosomal proteolysis of cDC1 is essential for their cross-presentation ability, as it preserves antigens so that they can be exported to the cytoplasm intact[221,222,312,314]. Transport of whole exogenous proteins from phagosomes to the cytoplasm has been shown to be mediated by ERAD[270,315]. Additionally, DNGR-1 signaling within cDC1 leads to phagosomal rupture and content release into the cytoplasm, where antigens are then subjected to proteasomal degradation[227]. Alternatively, cross-presentation can occur through a separate, vacuolar pathway[312]. In this mechanism, peptides are generated by cathepsins in a late endosome or lysosome, where they are loaded onto recycled MHC-I, newly-synthesized MHC-I chaperoned to the phagosome by CD74, or unstably-loaded MHC-I whose peptides become dissociated at low pH[272,294,297,298,316]. Vacuolar cross-presentation occurs independently of proteasomal degradation and TAP, though its contribution to overall *in vivo* cross-presentation is still undetermined[312,313].

1.4.3 MHC-Dressing in Antigen Presentation

In addition to processing internalized antigens and loading derivative peptides onto MHC-I, cells also have the ability to acquire intact pMHC-I from other cells in a process termed MHC-dressing, or MHC cross-dressing[309,317]. Intercellular transfer of MHC molecules and other surface proteins was first observed between T cells and APCs[318–322]. During the immunological synapse, TCR and CD28 signaling in the T cell can lead it to trogocytose pMHC molecules, CD80/86, and other membrane-bound proteins from the APC[323,324]. However, this does not seem to confer upon T cells any significant antigen presentation or costimulatory capacity, as these molecules are rapidly internalized and degraded[324]. The purpose and effects of pMHC internalization by T cells have not yet been fully elucidated and are probably context-dependent; various groups have proposed functions ranging from the promotion of tolerance by regulatory T

cells through the removal of self pMHC-II and CD80/86[325,326], to propagation TCR signaling from an endosome by internalized pMHC[327,328]. NK cells can similarly acquire pMHC-I molecules from traget cells, propagating inhibitory signals[329–332].

Many different cell types have been shown to acquire exogenous MHC molecules *in vitro* and *in vivo*; however, the capacity of cells to utilize MHC-dressing as a mechanism of antigen presentation varies[317]. Although exogenous pMHC complexes can be detected on the surface of T and NK cells, conferrance of antigen presentation function upon these cells is unlikely to be the primary effect of MHC-dressing[332]. Intercellular transfer of intact superantigens or prefabricated peptide antigens was first hypothesized to contribute to the induction of central tolerance in the thymus[333]. Indeed, transfer of MHC-I and MHC-II from thymic epithelial cells to DCs remains one of the best-characterized systems involving MHC-dressing in antigen presentation[334–337]. The observation that APCs can acquire intact MHC molecules was the result of an attempt to optimize viral transduction protocols for APCs *in vitro*. Russo *et al.* noticed that the large majority of human monocyte-derived DCs were positive for the virally-encoded surface protein δLNGFr, despite the transduction efficiency being quite low[338]. Further investigation demonstrated that monocyte-derived DCs acquired surface proteins, including HLA molecules, along with segments of the plasma membrane from human melanoma cells *in vitro*, and that monocyte-derived DCs were capable of presenting exogenous HLA-I to allo-specific T cells[338]. Shortly thereafter, Wolfers *et al.* demonstrated that tumor-derived exosomes contain both unprocessed antigens and pMHC complexes generated by the tumor cell, and that human monocyte-derived DCs and murine (GM-CSF + IL-4) BMDCs acquired exosome-derived MHC-I *in vitro*[339]. While injection of exosome-pulsed BMDCs promoted the rejection of autologous tumors in mice, it is unclear whether this was due to MHC-dressing, cross-presentation of exosome cargo, or a combination of the two[339]. In a subsequent study from

the same lab by André *et al.*, DCs were shown to be capable of presenting intact exosome-derived pMHC-I to antigen-specific $CD8^+$ T cells *in vitro* and *in vivo* in a TAP-independent manner, though it must be noted that *in vivo* MHC-dressing by DCs in this study involved the injection of superphysiological quantities of exosomes into the foot pad of mice[340].

In vivo acquisition of exogenous MHC-I derived from host cells was demonstrated by Herrera *et al.*, who separately transferred syngeneic *B2m*$^{-/-}$*I-A*$^{-/-}$ (GM-CSF) BMDCs and allogeneic BMDCs into C57BL/6 hosts and detected host MHC-I and MHC-II molecules on transferred BMDCs by antibody staining[341] . Interestingly, the authors also showed that MHC-dressing was temperature- and energy-dependent *in vitro*, suggesting that it was an active process within APCs. Dolan *et al.* later showed that MHC-dressing contributed to *in vivo* (OT-I) $CD8^+$ T cell priming in response to a subcutaneously (s.c.) injected mixture of live and dead fibroblasts which expressed ovalbumin[342]. Since these pioneering studies, MHC-dressing has been shown to occur and contribute to antigen presentation in various contexts. DCs in the thymus present substantial quantities of mTEC-derived MHC-I and MHC-II [334]. Interestingly, MHC-dressing by thymic DCs is correlated with acquisition of mTEC-derived cytoplasmic and membrane-bound proteins[335], suggesting that MHC-dressing is a consequence of DCs sampling their surroundings for antigens. *In vitro* studies suggest that the degree to which DCs acquire and present exogenous MHC is dependent on the lineage and environment—that cDC1 are better at presenting antigens through MHC-dressing than cDC2, and that thymic DCs are particularly adept compared to splenic DCs[336]. Hovewer, cDC2 which have been activated by type I IFN have recently been shown to present antigens to $CD8^+$ T cells via MHC-dressing[343]., so the use of MHC-dressing in antigen presentation is not stricly restricted to cDC1. DCs have also been shown to present intact pMHC-I derived from virally infected cells to $CD8^+$ T cells *in vivo*[344,345], though whether DCs can prime naive antiviral $CD8^+$ T cells or exclusively memory cells is a matter of debate, and may

depend on the infection and antigen load[346]. MHC-dressing has been observed using *in vivo* MHC-mismatched mouse models such as allogeneic transplantation and maternal microchimerism, and appears to have a prominent role in presentation of alloantigens[347–350].

The mechanism(s) by which MHC-dressing occur are incompletely defined, especially regarding *in vivo* MHC transfer. Several groups have found that *in vitro* incubation of APCs with purified exosomes is sufficient for MHC-dressing[339,340,348,349]. Furthermore, APCs can present exosome-derived MHC molecules *in vivo*[340]. These findings are contradicted by *in vitro* experiments conducted by numerous groups in which MHC-dressing is dependent on cell-cell contact, as transfer of MHC molecules and other membrane components between co-cultured cells is blocked when the cells are separated by a transwell membrane[256,337,341,344]. This has led to the assertion that MHC-dressing occurs through trogocytosis. Alternatively, Ruhland *et al.* proposed in a recent study that intercellular transfer of MHC molecules—as well as fluorescent protein antigens—occurs through the transfer of synaptic vesicles, but that this transfer requires direct cell-cell contact, perhaps reconciling the two models[256]. Regardless of the mechanism, acquisition of pMHC molecules appears to be an active process by APCs[337,341,344], and intercellular transfer is not unique to MHC molecules when MHC-dressing does occur. APCs which acquire and present exogenous MHC also incorporate lipids from the plasma membrane of the donor cell[338,344]. Furthermore, MHC-dressing is also correlated with the acquisition of cytoplasmic fluorescent protein *in vivo* in the thymus[335] and *in vitro*[256]. Taken together, these studies suggest the MHC-dressing can, and probably does, occur through more than one mechanism *in vivo*, and that the extent and mechanism(s) of MHC-dressing may be context-dependent.

1.5 Summary

For all the recent advances in the field of tumor immunology, the events surrounding anti-tumor $CD8^+$ T cell priming remain opaque, particularly the mechansims by which tumor antigens are presented by APCs in the tdLN. Migratory $CD103^+$ cDC1 acquire antigens in the tumor and transport them to the tdLN, where pMHC-I are presented to naive $CD8^+$ T cells. Antigen cross-presentation is a canonical function of cDC1; as such, that is the mechanism by which tumor antigens are presented in current models. MHC-dressing has not been rigorously studied in tumors for a variety of reasons, not least of which is that all cells in the host express the same MHC-I molecules, making it difficult to discern the effects of MHC-dressing from those of cross-presentation. Every *in vivo* demonstration of MHC-dressing has used a system involving mismatched MHC, such as allotransplantation or engraftment of parental bone marrow into F1 mice. Additionally, because cross-presentation has been so intensely studied and is operational *in vivo*, the potential of MHC-dressing in syngeneic systems has been overlooked or discounted. Its effect is understandable and quite visible in the presentation of alloantigens, but less comprehensible in situations when cross-presentation should be, in theory, sufficient.

In this study, we set out to contribute to the collective understanding of anti-tumor $CD8^+$ T cell priming. Specifically, we interrogated the mechanisms by which DCs present tumor antigens. In order to do this, we used two syngeneic murine tumor models, C1498 and B16-F10, in which the MHC-I molecule H-$2K^b$ was deleted using CRISPR/Cas9. When engrafting these tumors expressing K^b-restricted model antigens into wild-type syngeneic mice, we found that tumor-intrinsic MHC-I expression contributes to antigen-specific $CD8^+$ T cell priming. In isolation, this finding does not necessarily implicate MHC-dressing as a major mechanism of tumor antigen presentation. However, it was the impetus for all of the work that followed. From there, the two main questions we sought to answer were 1) Does MHC-dressing occur in the

tumor (if so, then how much)?; and 2) Is MHC-dressing sufficient for tumor antigen presentation in the absence of cross-presentation? In answering these questions in the affirmative, we believe that we have found a crucial mechanism underlying anti-tumor immunity.

Chapter 2: Materials and Methods

2.1 Mice

C57BL/6 (B6, H-2^{b}), B6.SJL (B6.SJL-*Ptprc*^{a}*Pepc*^{b}/BoyJ), OT-I (C57BL/6-Tg[TcraTcrb]1100Mjb/J), *Batf3*$^{-/-}$ (B6.129S(C)-*Batf3*^{tm1Kmm}/J), *Tap1*$^{-/-}$ (B6.129S2-*Tap1*^{tm1Arp}/J), and p40-IRES-eYFP (C.129S4(B6)-*Il12b*$^{tm1.1Lky}$/J) mice were purchased from Jackson Laboratories (Bar Harbor, ME) and bred in our facility. *K*$^{b-/-}$*D*$^{b-/-}$ (B6.129P2-*H-2K1*^{tm1Bpe} *H-2D1*^{tm1Bpe}/DcrJ) mice were provided by Dr. A. Bendelac, University of Chicago. 2C (B6.Cg-Cd8a<a> Tg(Tcra2C,Tcrb2C)1Dlo) mice were provided by Dr. T. Gajewski, University of Chicago. *Wdfy4*$^{-/-}$ mice were generated at the University of Chicago as described below. All mouse strains were bred and housed in a specific pathogen-free facility at the University of Chicago and used in accordance with protocols approved by the university's Institutional Animal Care and Use Committee following guidelines established by the National Institutes of Health. Six- to fourteen-week-old sex-matched littermate controls were used for all experiments unless specified otherwise.

Table 2.1: Mice

Mice	Strain full name	Source	Bred in our facility
C57BL/6	C57BL/6J	Jackson Laboratories, Bar Harbor, Maine	Yes
Ly5.1	B6.SJL-Ptprca Pepcb/BoyJ	Jackson Laboratories, Bar Harbor, Maine	Yes

Table 2.1, continued

		Gajewski Lab, University of	
Thy1.1	B6.PL-Thy1a/CyJ	Chicago	Yes
		Jackson Laboratories, Bar	
Tap1$^{-/-}$	B6.129S2-Tap1tm1Arp/J	Harbor, Maine	Yes
	B6.129P2-H2-K1tm1Bpe H2-	Bendelac Lab, University of	
K$^{b-/-}$*D*$^{b-/-}$	D1tm1Bpe/DcrJ	Chicago	Yes
Wdfy4$^{-/-}$		Made in this paper	Yes
		Gajewski Lab, University of	
OT-I	C57BL/6-Tg(TcraTcrb)1100Mjb/J	Chicago	Yes
		Gajewski Lab, University of	
2C	B6-Tg(Tcra2C,Tcrb2C)1Dlo	Chicago	Yes
		Jackson Laboratories, Bar	
NSG	NOD.Cg-Prkdcscid Il2rgtm1Wjl/SzJ	Harbor, Maine	No

2.2 Generation of *Wdfy4*$^{-/-}$ mice

Wdfy4$^{-/-}$ mice were generated using CRISPR/Cas9. Guide (g) RNAs flanking exon 4 of the *Wdfy4* gene were designed using the IDT design tool. Excising exon 4 results in a frame-shift in Wdfy4 after residue 116 (out of 3024) and a premature stop codon 30 amino acids later, as previously described[214]. Alt-R crRNA guides (sequences: ATGCATCACCAACGAGCTTT and AGCACCTGGGAACACCTTCG) and tracrRNA were purchased from IDT, and gRNA was assembled from the crRNA and tracrRNA according to the manufacturer's protocol. Embryo-grade water containing 20 ng/μL gRNA and 60 ng/μL Cas9 protein was injected into the nuclei of C57BL/6J embryos. Genotyping PCR primers (fwd: GCCTTGAGGTACATGGGCAA, rev:

GGTTACACACAGCTCGTCCAT) were designed up- and down-stream of predicted cut sites. A male *Wdfy4*$^{-/-}$ founder mouse was backcrossed with a C57BL/6 female. F1 offspring were genotyped by PCR, and the wild type and mutant bands were excised from the gel; DNA was purified using a QIAquick Gel Extraction Kit (Qiagen), according to the manufacturer's protocol. Finally, the PCR-amplified DNA was sequenced at the University of Chicago Comprehensive Cancer Center DNA Sequencing & Genotyping Facility. Sanger sequencing confirmed a 144 bp deletion containing the entirety of exon 4. F1 mice were backcrossed with C57BL/6J for two further generations. Subsequently, *Wdfy4*$^{+/-}$ heterozygous mice were bred in order to generate *Wdfy4*$^{+/+}$, *Wdfy4*$^{+/-}$, and *Wdfy4*$^{-/-}$ littermate mice that were used for experimentation.

Table 2.2: Key Reagents for generation of *Wdfy4*$^{-/-}$ mice

Guide RNA	Sequence	Platform	Manufacturer
Wdfy4 5' Sense	CATGTAGCCTTGAGGTACAT	Alt-R CRISPR-Cas9 crRNA	IDT
Wdfy4 5' Antisense	CTCCAGGGCTATTAACCTGG	Alt-R CRISPR-Cas9 crRNA	IDT
Wdfy4 3' Sense	CAGGCCTCGAAGGTGTTCCC	Alt-R CRISPR-Cas9 crRNA	IDT
Wdfy4 3' Antisense	GTCCCCTTTCCTCATAGACT	Alt-R CRISPR-Cas9 crRNA	IDT
tracrRNA		Alt-R CRISPR-Cas9 tracrRNA	IDT

2.3 RNA isolation and sequencing of PCR-amplified cDNA from splenocytes

Splenocytes from *Wdfy4*$^{+/+}$ and *Wdfy4*$^{-/-}$ littermate mice were suspended in Trizol, and RNA was purified via chloroform extraction. cDNA was generated from the RNA using the

High Capacity cDNA Reverse Transcription Kit (Applied Biosystems) according to the manufacturer's protocol. Partial *Wdfy4* cDNA was amplified by PCR (cycling conditions: 98°C for 3 minutes, followed by 34 cycles of 98°C for 10 seconds, 64°C for 30 seconds, and 72°C for 30 seconds, and a 10 minute final extension at 72°C) using four different combinations of primers; the two forward primers bound in exon 1 in the 5'-UTR and in exon 2 downstream of the ATG start codon, while the two reverse primers bound in exons 6 and 7 (primer sequences are listed in Table 2.3 below), such that all resulting bands spanned multiple exons — including the deleted exon 4, predicted frameshift mutation, and premature stop codon — while also removing the possibility of mistakenly amplifying potential genomic DNA contaminants. PCR products were purified from cut gel bands using a QIAquick Gel Extraction Kit (Qiagen) according to the manufacturer's protocol. Finally, the PCR-amplified DNA was sequenced at the University of Chicago Comprehensive Cancer Center DNA Sequencing & Genotyping Facility, and the sequences were aligned to the full-length *Wdfy4* transcript sequence using the NCBI's nucleotide BLAST alignment tool.

Table 2.3: PCR reagents for *Wdfy4* genotyping and mRNA sequence

PCR Reagents	Sequence	Manufacturer	Catalogue #
2X Taq RED Master Mix		Apex	42-138B
High Capacity cDNA Reverse Transcription Kit		Applied Biosystems	4368814

Table 2.3, continued

Phusion High-Fidelity DNA Polymerase		New England Biolabs	M0530S
Wdfy4 transcript ex1 fwd primer	CTGGTGTAGCTTGTGAAGGGT	IDT	
Wdfy4 transcript ex2 fwd primer	TTCACTAGAAGGGCAGTCGC	IDT	
Wdfy4 transcript ex6 rev primer	CCTCCAGACCCTGAGATTCG	IDT	
Wdfy4 transcript ex7 rev primer	CCCCGTTCTCAAACTCCAGG	IDT	
Wdfy4 genotyping fwd primer	GCCTTGAGGTACATGGGCAA	IDT	
Wdfy4 genotyping rev primer	GGTTACACACAGCTCGTCCAT	IDT	
Agarose LE		Denville	GR140-500
QIAquick Gel Extraction Kit		Qiagen	28704

2.4 Cell lines

The C1498 leukemia cell line was purchased from American Type Culture Collection, and the C1498.SIY cell line was generated in our laboratory as previously described[351]. The B16.OVA cell line was kindly provided by Dr. T. Schumacher (Netherlands Cancer Institute, Amsterdam, Netherlands). *H-2K^b* was deleted in C1498, C1498.SIY, and B16.OVA cells using

CRISPR/Cas9 targeting of exon 1 as we have previously described[202]. $K^{b-/-}$ cell lines were subsequently established following 3 rounds of FACS purification of K^b-negative cells. K^b was re-expressed with a C-terminal eGFP tag in C1498 $K^{b-/-}$ cells to generate C1498 K^{bAB} ($K^{b\ \text{Add-back}}$) cells using standard lentiviral transduction. The K^b-eGFP lentiviral construct[352] was kindly provided by Dr. S. Springer (Jacobs University Bremen, Germany). Surface expression of K^b protein was periodically assessed on all cell lines by flow cytometry. SIY antigen levels on cultured C1498.SIY and C1498.SIY $K^{b-/-}$ cell lines were periodically monitored by FACS to ensure equivalent eGFP fluorescence. The ability of BMDCs to cross-present C1498-derived SIY antigen and B16-derived OVA antigen was assessed as described below. 1969 sarcoma cells were a kindly provided by Dr. T. Gajewski (University of Chicago). C1498 and B16-F10 cell lines were grown in DMEM supplemented with 10% fetal bovine serum (FBS), 2-mercaptoethanol (2-ME), essential amino acids, and penicillin/streptomycin (complete DMEM). 1969 cells were grown in RPMI1640 supplemented with 10% fetal bovine serum (FBS), 2-mercaptoethanol (2-ME), essential amino acids, and penicillin/streptomycin (complete RPMI). Cells were cultured in a 37° C incubator with 5% CO_2. All cell lines used were routinely monitored for mycoplasma contamination using Venor GeM Mycoplasma PCR-Based Detection Kit.

Table 2.4: Cell Lines

Cell Lines	Source
C1498	ATCC
B16.OVA	Schumacher Lab, Netherlands Cancer Institute
OCI-Ly1	ATCC
OCI-Ly8	ATCC

2.5 Differentiation of BMDCs

Bone marrow was isolated from mice by flushing femurs, tibias, and pelvic bones with sterile PBS. Bone marrow cells were plated at 10^6 cells/mL in sterile complete RPMI media plus 100 ng/mL recombinant Flt3 ligand (Flt3L). Cells were cultured for 8 days, with media and Flt3L replacement at days 3 and 6. Differentiation of BMDCs was assessed on day 8 by flow cytometry following cell staining with fluorescent-conjugated antibodies directed against CD11c, MHC-II, CD24, and SIRP-α. BMDCs were considered to be differentiated if > 80% of the cells in culture were $CD11c^{hi}$ $MHC\text{-}II^{hi}$, and the ratio of cDC1-like ($CD24^+$ $SIRP\text{-}\alpha^{neg}$) to cDC2-like ($CD24^{neg}$ $SIRP\text{-}\alpha^+$) BMDCs was also noted.

2.6 $CD8^+$ T cell isolation for adoptive transfer experiments and *in vitro* cultures

Splenic TCR-tg 2C and OT-I $CD8^+$ T cells were isolated from TCR-tg mice by pressing harvested spleens through a 70 μm filter into sterile PBS containing 2mM EDTA and 0.5% bovine serum albumin (BSA). The cells were then labeled with anti-CD8α microbeads (Miltenyi) and positively selected by magnetic separation according to the manufacturer's protocol. Next, isolated cells were washed three times with sterile PBS, followed by labeling with CTV (Invitrogen) according to the manufacturer's protocol. For adoptive transfer experiments, CTV-labeled TCR-tg $CD8^+$ T cells were resuspended in sterile PBS at 10^7 cells/mL, and 10^6 cells were injected intravenously (i.v.) through the lateral tail vein of individual mice. For *in vitro* and *ex vivo* co-culture experiments, CTV-labeled TCR-tg $CD8^+$ T cells were resuspended to a concentration of 10^6 cells/mL in complete RPMI, and 10,000 cells were added to each culture well.

2.7 *In vitro* assessment of SIY and OVA antigen expression

BMDCs were resuspended in complete RPMI at 10^6 cells/mL, and 30,000 cells/well were plated in a 384-well plate following 8 days of differentiation, along with 10,000 CTV-labeled TRC-tg 2C or OT-I $CD8^+$ T cells. $K^{b+/+}$ and $K^{b-/-}$ C1498.SIY or B16.OVA cells were washed with sterile PBS and resuspended to a concentration of 3 x 10^7 cells/mL in microcentrifuge tubes. Cells were lysed by five cycles of rapid freezing and thawing, during which tubes were alternatively transferred between dry ice and a 37° C water bath. The cells were centrifuged at 10,000 x g for 5 min at 4o C, and 3 µL (equivalent lysate from 30,000 cells) of the supernatant was added to each well. TCR-tg $CD8^+$ T cell proliferation was assessed by flow cytometry to assess for CTV dilution following a 72-96 hour co-culture. TCR-tg $CD8^+$ T cells were identified by antibody staining for CD90, CD8β, and either the 2C TCR or Vα2 (the TCRα chain of OT-I).

2.8 Subcutaneous (s.c.) tumor inoculations

Cultured tumor cells were washed twice with PBS, counted, and resuspended in PBS at a concentration such that the injection volume was 100 µL (2 x 10^7 cells/mL for experiments directly investigating *in vivo* pMHC-I transfer, 4 x 10^7 cells/mL for *ex vivo* DC priming experiments, and 10^7 cells/mL for all other experiments). Mice were injected s.c. in the right flank (both flanks were injected for *ex vivo* DC priming experiments) with 100 µL of cells using a 27-gauge needle.

2.9 *In vivo* tumor growth experiments

10^6 tumor cells were inoculated s.c. into the right flank of each host mouse as described above. Tumor area was measured using a caliper every 2-3 days starting at day 5 by a lab

member who was blinded to the experimental setup. Mice were euthanized when they reached the humane endpoint established in the IACUC-approved protocol.

2.10 Lymph node (LN) sample preparation

Mice were euthanized, and the indicated LNs were harvested. For experiments involving analysis of DC populations, LNs were incubated in RPMI 1640 containing 2% FBS, 1 mg/mL collagenase IV, and 20 μg/mL DNase I for 30 min at 37°C. After DNase/collagenase digestion (for DC experiments) or immediately after isolation (all other experiments) LNs were pressed through 70 μm filters to create single-cell suspensions. For experiments in which cell counts of a population were required, 5,000 counting beads were spiked into each sample to normalize counts across samples and experiments. Samples were stained and analyzed by flow cytometry as described below.

2.11 Tumor sample preparation

Mice were euthanized; tumors were harvested, minced with either razor blades or dissection scissors, and incubated in RPMI 1640 containing 2% FBS, 1 mg/mL collagenase IV, and 20 μg/mL DNase I for 30 min at 37°C. Each tumor was then pressed through a 70 μm filter in order to generate a single cell suspension before proceeding with antibody staining and analysis as described below.

2.12 Antibody staining and flow cytometry

F_c receptors were blocked with an anti-FcγRII/FcγRIII (clone 2.4g2) antibody in FACS buffer (PBS containing 2% FBS, 0.02 mM EDTA, and 0.03% sodium azide) for 15 min on ice. Antibody staining was performed for 20-30 min on ice in FACS buffer. After washing,

secondary staining was performed for 20-30 min on ice if necessary. Samples were washed with FACS buffer and then with PBS. When possible, the cells were then stained with a Near-IR live-dead dye according to the manufacturer's protocol. Samples were fixed with 2% paraformaldehyde in PBS for 30 min at 4° C and subsequently washed. For the experiment in Supplemental Figure S7 in which MHC-dressing was assessed alongside tumor antigen uptake, the cells were permeabilized using 0.1% Triton X-100 in PBS for 30 min on ice, followed by one PBS wash, one wash with FACS buffer, and antibody staining in FACS buffer at room temperature for one hour in the dark. Finally, cells were washed, resuspended in FACS buffer and analyzed on an LSR Fortessa (4-15 or X-20 5-18) flow cytometer (BD) or Amnis Image Stream X cytometer at the University of Chicago Cytometry and Antibody Technology Core facility. See Table 2.5 for a comprehensive list of the antibodies used in this study.

Table 2.5: Flow cytometry antibodies and other reagents

Flow cytometry antibodies and reagents	Conjugate	Clone	Manufacturer	Catalogue #
CD16/32	unconjugated	2.4g2	Bio X Cell	BE0307
CD3	Biotin	17A2	Biolegend	100244
CD3	FITC	17A2	Biolegend	100204
CD4	Biotin	GK1.5	Biolegend	100404
CD4	PE/Cy7	GK1.5	Biolegend	100422
CD4	APC	GK1.5	Biolegend	100412
CD8a	Biotin	53-6.7	Biolegend	100704
CD8a	Pacific Blue	53-6.7	Biolegend	100725

Table 2.5, continued

CD8a	BV605	53-6.7	Biolegend	100744
CD8a	FITC	53-6.7	Biolegend	100706
CD8a	PerCP/Cy5.5	53-6.7	Biolegend	100734
CD8a	PE	53-6.7	Biolegend	100708
CD8a	PE/Cy7	53-6.7	Biolegend	100722
CD8a	APC	53-6.7	Biolegend	100712
CD8a	APC/Cy7	53-6.7	Biolegend	100714
CD8b	FITC	YTS156.7.7	Biolegend	126606
CD11b	Biotin	M1/70	Biolegend	101204
CD11b	BV510	M1/70	Biolegend	101263
CD11b	PerCP/Cy5.5	M1/70	Biolegend	101228
CD11c	Biotin	N418	Biolegend	117304
CD11c	PE/Cy7	N418	Biolegend	117318
CD11c	APC	N418	Biolegend	117310
CD19	Biotin	6D5	Biolegend	115504
CD24	FITC	M1/69	Biolegend	101806
CD44	Pacific Blue	IM7	Biolegend	103020
CD44	PE/Cy7	IM7	Biolegend	103030
CD45.1	Pacific Blue	A20	Biolegend	110722
CD45.1	FITC	A20	Biolegend	110706
CD45.1	PE	A20	Biolegend	110708
CD45.1	APC	A20	Biolegend	110714
CD45.2	Pacific Blue	104	Biolegend	109820

Table 2.5, continued

CD45.2	FITC	104	Biolegend	109806
CD45.2	PE/Cy7	104	Biolegend	109830
CD45.2	APC	104	Biolegend	109814
CD64	FITC	X54-5/7.1	Biolegend	139316
CD64	PE/Cy7	X54-5/7.1	Biolegend	139314
CD80	FITC	16-10A1	Biolegend	104706
CD80	PE	16-10A1	Biolegend	104708
CD86	BV605	GL-1	Biolegend	105037
CD86	FITC	GL-1	Biolegend	105006
CD86	PE	GL-1	Biolegend	105008
CD90.1	Pacific Blue	OX-7	Biolegend	202522
CD90.1	FITC	OX-7	Biolegend	202504
CD90.2	FITC	30-H12	Biolegend	105306
CD90.2	APC	30-H12	Biolegend	105312
CD90.2	PE/Cy7	30-H12	Biolegend	105314
CD103	BV421	2E7	Biolegend	121422
CD103	FITC	2E7	Biolegend	121420
CD103	PE	2E7	Biolegend	121406
B220	Biotin	RA3-6B2	Biolegend	103204
B220	FITC	RA3-6B2	Biolegend	103206
F4/80	BV421	BM8	Biolegend	123137
F4/80	PE/Cy7	BM8	Biolegend	123112

Table 2.5, continued

Gr-1	Biotin	RB6-8C5	Biolegend	108404
Granzyme B	PerCP/Cy5.5	QA16A02	Biolegend	372211
H-2Kb	PE	AF6-88.5	eBioscience	12-5958-82
H-2Kb	APC	AF6-88.5	Biolegend	116518
H-2Kb:SIINFEKL	APC	25-D1.16	Biolegend	141606
I-A/I-E	Biotin	M5/114.15.2	Biolegend	107604
I-A/I-E	Pacific Blue	M5/114.15.2	Biolegend	107619
I-A/I-E	FITC	M5/114.15.2	Biolegend	107606
I-A/I-E	PerCP/Cy5.5	M5/114.15.2	Biolegend	107626
IFN-γ	APC	XMG1.2	BD Pharmingen	554413
NK1.1	Biotin	PK136	Biolegend	108704
SIRP-α	PE	P84	Biolegend	144012
TCRβ	Biotin	H57-597	Biolegend	109204
TCRβ	FITC	H57-597	Biolegend	109205
TCRβ	PerCP/Cy5.5	H57-597	Biolegend	109228
TCR Vα2	PE	B20.1	Biolegend	127808
TCR Vα2	APC	B20.1	Biolegend	127810
TNF-α	PE	MP6-XT22	Invitrogen	12-7321-82
2C TCR	Biotin	1B2	University of Chicago Cytometry and Antibody	

Table 2.5, continued

			Technology Facility	
hCD14	PerCP/Cy5.5	63D3	Biolegend	367110
hCD19	APC	HIB19	Biolegend	302212
hCD19	FITC	HIB19	Biolegend	302206
hCD20	PerCP/Cy5.5	2H7	Biolegend	302326
HLA-A/B/C	PE	W6/32	Biolegend	311406
HLA-A*02	PE	BB7.2	Abcam	ab79523
Kb:SIY pentamer	PE		ProImmune	1803
Kb:SIINFEKL pentamer	PE		ProImmune	93
Streptavidin	FITC		Biolegend	405202
Streptavidin	PE		Biolegend	405204
Streptavidin	PerCP/Cy5.5		Biolegend	405214
Streptavidin	APC/Cy7		Biolegend	405208
LIVE/DEAD Fixable Near-IR Dead Cell Stain Kit			Invitrogen	L10119
Pacific Orange succinimidyl ester			Invitrogen	P30254
Golgi Plug			BD	555029
FOXP3/Transcription Factor Staining Buffer			Invitrogen	00-5523-00

2.13 Intracellular cytokine staining

tdLNs and analogous inguinal LNs from non-tumor-bearing mice were harvested and homogenized as described above. These samples were divided in three and the fractions were cultured in 200 µL complete RPMI containing anti-CD28 (1 µg/mL) and plate-bound anti-CD3 (1 µg/mL) antibodies, 100 nM SIY peptide, or media alone in a 96-well u-bottom plate for five hours at 37°C. Golgi Plug (BD) was added to each well one hour into the culture according to the manufacturer's protocol. Cells were then stained for cell surface markers as described above. Immediately after staining with a live/dead dye, the cells were fixed and permeabilized using a FOXP3/Transcription Factor staining kit (Invitrogen) according to the manufacturer's protocol, and stained overnight at 4°C with antibodies recognizing IFN-γ, TNF-α, and granzyme B.

2.14 *In vivo* TCR-tg $CD8^+$ T cell proliferation experiments

10^6 CTV-labeled TCR-tg $CD8^+$ T cells were adoptively transferred intravenously (i.v.) into congenic hosts at day -1 via the lateral tail vein. 10^6 tumor cells were injected s.c. into the right flank of each mouse at day 0. Mice were euthanized at day 6, and the right inguinal lymph node (LN)—which drains the tumor—of each mouse was harvested and processed as described above. The geometric mean fluorescence intensity (gMFI) of CTV in TCR-tg $CD8^+$ T cells was normalized across experiments by dividing the gMFI of each sample by the mean of the gMFIs of the non-tumor bearing control mice for each experiment, such that the group mean gMFI of TCR-tg $CD8^+$ T cells from non-tumor bearing mice = 1 for each experiment. Due to the large number of groups for experiments involving *Wdfy4*$^{-/-}$ mice, it was not possible to have sex-matched littermates in all groups. These experiments were designed such that every Wdfy4$^{-/-}$ mouse had sex-matched, co-housed, wild type and heterozygous littermates with the same tumor.

Multiple age-matched (within 3 weeks) litters were used in each experiment, and male and female mice were used in balanced numbers across groups.

2.15 Assessment of *in vivo* endogenous CD8$^+$ T cell response by pMHC-I pentamer stain

10^6 tumor cells were injected s.c. into the right flank of each mouse at day 0. Mice were euthanized at day 6, the right inguinal (tumor-draining) LN was harvested and homogenized as described above. In order to minimize scavenging of pMHC-I pentamers, all samples were labeled with anti-CD4, -CD19, -B220, and -Gr-1 biotin-conjugated antibodies in FACS buffer for 15 min on ice, followed by washing and incubation with biotin-binding Dynabeads (Invitrogen) for 10 min and subsequent magnetic depletion. Samples were then stained with 5 µL pMHC-I pentamer (SIY:K^b or $OVA_{257-264}$:K^b, both from Proimmune) in 50 µL of FACS buffer for 15 min in the dark at room temperature. Next, 50 µL FACS buffer containing antibodies recognizing CD90.2, CD8β, and CD44 was added to each sample, and the cells were incubated for a further 15 min in the dark at room temperature. The cells were then washed with FACS buffer, followed by PBS, fixed, and analyzed as described above.

2.16 Assessment of the endogenous anti-tumor CD8$^+$ T cell response by ELISpot

C57BL/6 mice were inoculated s.c. with 10^6 C1498.SIY $K^{b+/+}$ or $K^{b-/-}$ cells on day 0. Mice were euthanized at day 6 and tumor-draining LNs were isolated and homogenized. 10^6 cells from each sample were restimulated overnight with media alone or with 100 nM SIY peptide, and IFN-γ producing cells were identified using an IFN-γ ELISpot kit (BD Bio-sciences) according to the manufacturer's protocol. ELISpot plates were read using an ImmunoSpot Series 3 Analyzer, and data were analyzed with ImmunoSpot software.

2.17 Polyclonal CD8$^+$ T cell transfer

10^6 C1498.SIY $K^{b+/+}$ or $K^{b-/-}$ cells were injected s.c. into the right flank of each primary C57BL/6 mouse at day -7. Primary tumor-bearing and naïve mice were euthanized at day -1, the right inguinal lymph node (LN) was harvested and homogenized. LNs from 5 mice were pooled into each sample. CD8$^+$ cells were isolated by magnetic separation using anti-CD8α microbeads (Miltenyi) according to the manufacturer's protocol. The CD8$^+$-enriched cells were resuspended in sterile PBS, and 5 x 10^6 cells were adoptively transferred into naïve secondary C57BL/6 mice i.v. through the lateral tail vein. At day 0, all secondary mice were inoculated s.c. in the right flank with 10^6 C1498.SIY $K^{b+/+}$ cells. Tumors were then measured as described above for the duration of the experiment.

2.18 *In vivo* MHC-I transfer experiments

C57BL/6 and $K^{b-/-}D^{b-/-}$ mice were inoculated s.c. in the flank with 2 x 10^6 tumor cells at day 0. Mice were monitored for tumor growth and were euthanized when tumors became palpable in the majority of mice in the experiment (between days 6 and 10). Tumors were isolated (in some experiments tdLNs were isolated as well) and processed for analysis by flow cytometry or ImageStream cytometry as described above. B16.OVA $K^{b+/+}$ and $K^{b-/-}$ cells were treated with 100ng/mL recombinant IFN-γ in culture for 48 hours prior to s.c. inoculation.

2.19 *Ex vivo* DC priming assay

C57BL/6, *Tap1*$^{-/-}$, and $K^{b-/-}D^{b-/-}$ mice were inoculated s.c. with 4 x 10^6 C1498.SIY $K^{b+/+}$ or $K^{b-/-}$ cells in each flank on day 0 (3-5 mice per group). On day 6, tumor-draining inguinal, axillary, and brachial LNs were harvested and pooled by experimental group. These pooled LN samples were incubated with sterile RPMI 1640 containing 2% FBS, 1 mg/mL collagenase IV, and 20

μg/mL DNase I for 30 min at 37°C. Each sample was pressed through a 70 μm filter and washed with RPMI containing 10% FBS (R10). The samples were then washed with and resuspended in PBS supplemented with 0.5% bovine serum albumin and 2 mM EDTA. The samples were incubated with biotin-conjugated antibodies recognizing CD3, CD19, B220, Gr-1, and NK1.1 for 20 min on ice. After washing, the cells were incubated with biotin-binding Dynabeads (Invitrogen) for 10 min, and the bead-bound cells were depleted by magnetic separation. The cells were then stained with fluorescent-conjugated antibodies, as well as streptavidin-conjugated APC-Cy7 on ice for 20 min in the dark. The samples were washed with PBS and stained with a Near-IR live-dead dye for 10 min at room temperature in the dark. The samples were washed and resuspended in R10 media and $CD103^+$ migratory cDC1, $CD11b^+$ migratory cDC2, $CD8\alpha^+$ resident cDC1, and $CD11b^+$ resident cDC2 were FACS-purified on a BD FACSAria II sorter in the University of Chicago Cytometry and Antibody Technology Core facility using the gating strategy depicted in Figure 2.1. Sorted samples were then resuspended in complete R10 media containing gentamicin (50 μg/mL) and amphotericin B (2.5 μg/mL) at a concentration of of 10^6 cells/mL, and 30,000 cells were plated per well in a 384-well plate, along with 10,000 CTV-labeled TRC-tg 2C $CD8^+$ T cells which were isolated as described above. The cells were co-cultured for 72 hours and proliferation of 2C $CD8^+$ T cells was determined by flow cytometry. All buffers and media used in these experiments were sterile, passed through 0.2 μm filters.

2.20 MDM / OCI-Ly8 co-culture

Peripheral blood mononuclear cells (PBMCs) were extracted through Ficoll density gradient centrifugation using the peripheral blood of healthy HLA-A*02^{neg} human donors. Monocytes were isolated by adhering PBMCs to culture plates for two hours at 37°C. Non-

adherent cells were removed by washing. Monocyte-derived macrophages were then generated by culturing the adherent monocytes in complete RPMI media containing 50ng/mL M-CSF for 7 days. Following this process, monocyte-derived macrophages were then harvested by incubation in EDTA/Trypsin for 5 minutes followed by gentle scraping. 10^5 macrophages were then plated

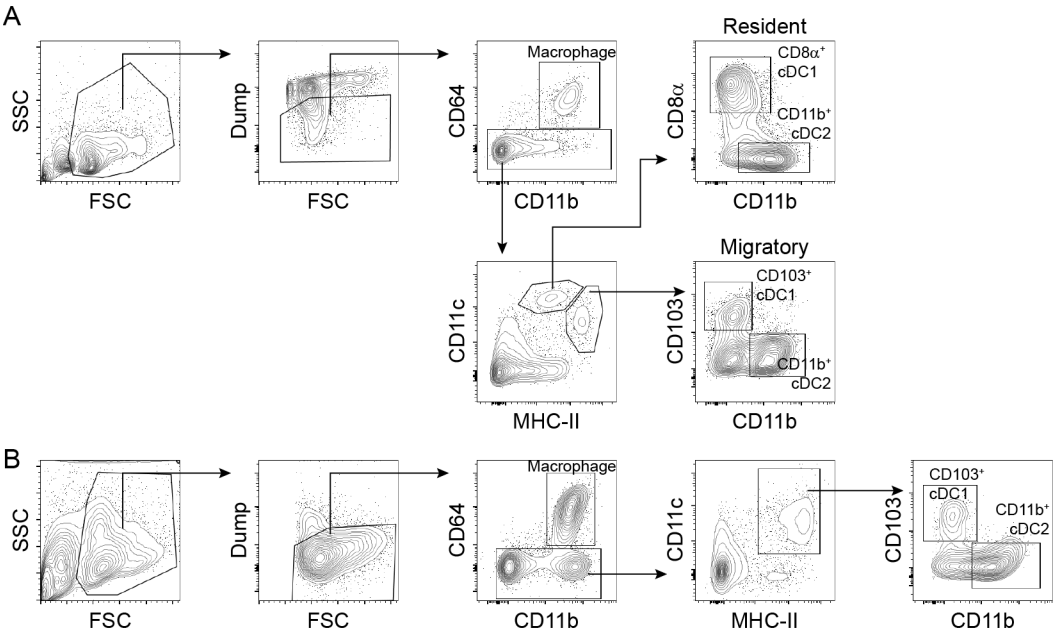

Figure 2.1: Gating strategy for the identification of DC subsets in the tumor and tdLN

Flow cytometry gating strategy for the tumor (**A**) and tdLN (**B**) used to identify DC subsets.

into each well of a 24-well plate, rested for 24 hours, and then co-cultured them with 10^5 CTV-labeled HLA-A*02^{pos} OCI-Ly8 lymphoma cells for 2 hours in the presence of 5ug/mL of an isotype (BE0083, Bioxcell) or anti-CD47 antibody (B6H12, Bioxcell). Macrophages were then collected from each well, identified by CD14 antibody staining and assessed for the expression of lymphoma cell-derived CTV, HLA-A*02, and CD19 as determined by flow cytometry.

2.21 Statistical Analysis

Statistical significance for tumor growth experiments was determined by two-way ANOVA with Sidak's post-hoc test using GraphPad Prism 7. For all other experiments, statistical significance was determined by ANOVA with a post-hoc Tukey HSD test using R version 3.6.3. The number of factors determined the type of ANOVA used in each specific case, and the type of ANOVA used is indicated in the figure legends. Rounded adjusted p-values are indicated when $10^{-4} \leq$ p-adj. < 0.1. When $10^{-8} <$ p-adj $< 10^{-4}$, it is indicated as being less than the next largest power of 10 (e.g. $p = 0.0000085$ would be displayed as $p < 10^{-5}$). Any p-adj $< 10^{-8}$ are indicated as $p < 10^{-8}$. Whenever a p value is not indicated, $p > 0.1$. Adjusted p values < 0.05 were considered to be statistically significant.

Table 2.6: Media, buffers, enzymes, and other key reagents

Media, buffers, and enzymes	Manufacturer	Catalogue #
1X DPBS	Gibco	14190-250
10X DPBS	Gibco	14200-166
RPMI 1640	Gibco	11875-119
DMEM	Gibco	11965-118
Fetal Bovine Serum	Gemini	100-106
MOPS	Sigma	M1254
2-Mercaptoethanol	Sigma	M3148
Penicillin/Streptimycin	Gibco	15140-122
Gentamicin	Sigma	G1272-10ML
Amphotericin B	Sigma	A2942-50ML
L-arginine	Sigma	A8094

Table 2.6, continued

L-glutamine	Sigma	G8540
Folic acid	Sigma	F8758
L-asparagine	Gibco	11013-026
0.05% Trypsin EDTA	Gibco	25300062
Venor GeM Mycoplasma Detection Kit, PCR-based	Sigma	MP0025-1KT
Dnase I	Roche	10104159001
Collgenase IV	Sigma	C5138
EDTA (0.5 M)	Alfa Aesar	60-00-4
Sodium azide	Sigma	S2002
Paraformaldehyde, 16% w/v	Alfa Aesar	43368
Triton X-100	Sigma	T8787
TRIzol Reagent	Ambion	15596018
Chloroform	Sigma-Aldrich	C2432-500ML
Isopropanol	Acros Organics	32727-0010
UltraPure DNA Typing Grade TAE (50X)	Invitrogen	24710030
CD8a Microbeads (mouse)	Miltenyi	130-117-044
LS Column	Miltenyi	130-042-401
Dynabeads biotin binder	Invitrogen	11047
50 mL Tube Top Filter (0.22-micron)	Corning	430320
Vacuum-Driven Filter Systems (0.22-	Olympus	25-227

Table 2.6, continued

micron)		
Cell strainer 70 micron	Fisher	22-363-548
CellTrace Violet Cell Proliferation Kit	Invitrogen	C34557
Recombinant mouse Flt3L (carrier-free)	Biolegend	550706
Recombinant human M-CSF	Peprotech	216-MC-025/CF
Anti-CD47 (clone: B6.H12)	Bio X Cell	BE0019-1
Mouse IgG1 Isotype control (clone MOPC-21)	Bio X Cell	BE0083

Chapter 3: Results

Dendritic cells can prime anti-tumor CD8$^+$ T cell responses through MHC-dressing

Brendan W. MacNabb[1], Sravya Tumuluru[2], Xiufen Chen[3], James Godfrey[3], Darshan N. Kasal[1], Jovian Yu[3], Marlieke L. M. Jongsma[4], Robbert M. Spaapen[4], Douglas E. Kline[1], and Justin Kline[1,2,3]

[1] Committee on Immunology, University of Chicago, Chicago, IL, USA, 60637

[2] Committee on Cancer Biology, University of Chicago, Chicago, IL, USA, 60637

[3] Department of Medicine, University of Chicago, Chicago, IL, USA, 60637

[4] Department of Immunopathology, Sanquin Research; Landsteiner Laboratory, Amsterdam UMC, University of Amsterdam; Cancer Center Amsterdam, Amsterdam, the Netherlands.

Primary contact: Justin Kline, jkline@medicine.bsd.uchicago.edu

3.1 Abstract

Antigen cross-presentation, wherein dendritic cells (DC) present exogenous antigen on MHC-I molecules, is considered the primary mechanism by which DCs initiate tumor-specific CD8$^+$ T cell responses. Here, we demonstrate that MHC-dressing, an antigen presentation pathway in which DCs acquire and display intact tumor-derived peptide:MHC-I molecules, also plays a critical role in orchestrating anti-tumor immunity. Cancer cell MHC-I expression was required for optimal CD8$^+$ T cell activation in two subcutaneous tumor models. *In vivo* acquisition of tumor-derived peptide:MHC-I molecules by DCs was sufficient to induce antigen-specific CD8$^+$ T cell priming. Transfer of human tumor-derived HLA molecules to myeloid cells was detected *in vitro* and in human tumor xenografts. In conclusion, MHC-I-dressing is crucial for anti-tumor CD8$^+$ T cell priming by DCs. In addition to quantitatively enhancing tumor

antigen presentation, MHC-dressing might also enable DCs to more faithfully and efficiently mirror the cancer cell peptidome.

3.2 Introduction

The immune response against tumors has been intensely studied over the past few decades[92], leading to the development and widespread administration of cancer immunotherapies in the clinic[102,104]. However, for all its success, cancer immunotherapy is not universally effective[353], and progress is hindered by persisting gaps in our collective understanding of the fundamental mechanisms required for the orchestration of effective anti-cancer immune responses, particularly at the level of early T cell priming. While the source, specificity, and priming mechanism of tumor-infiltrating $CD8^+$ T cells in human cancers remain largely unclear, murine cancer models have provided critical insights into these questions. Recently, the professional antigen presenting cells (APCs) involved in anti-tumor T cell priming have been identified[254,255]; however the specific pathways utilized by these APCs to acquire and present tumor-derived antigens *in vivo* remain incompletely defined.

Migratory $CD103^+$ and $CD11b^+$ dendritic cells (DCs) exist in tissues throughout the body, constitutively acquiring proteins from surrounding cells before trafficking to draining lymph nodes, where they present derivative peptide antigens to T cells in the context of major histocompatibility complex (MHC) molecules[15,140]. Migratory DCs within tumors similarly acquire and subsequently present cancer cell-derived antigens to T cells in tumor-draining lymph nodes (tdLNs)[130]. Recent evidence indicates that tumor antigens are exclusively transported to the tdLN by migratory $CD103^+$ DCs[255,256], and that these DCs are primarily responsible for antigen-specific $CD8^+$ T cell priming *in vivo*[254,255]. Migratory $CD103^+$ DCs, along with lymph node resident $CD8\alpha^+$ DCs, comprise the BATF3- and IRF8-dependent conventional type 1 DC (cDC1)

lineage[178,179,354]. Because antigen cross-presentation is a canonical function of cDC1[178,207] and numerous studies have demonstrated a requirement for cDC1 in the activation of anti-tumor $CD8^+$ T cell responses[130,178,251], prevailing thought is that tumor-specific $CD8^+$ T cells are primed exclusively through antigen cross-presentation[130,355,356].

However, an alternative antigen presentation mechanism has increasingly been recognized, in which DCs acquire and present intact peptide:MHC (pMHC) complexes captured directly from neighboring cells[317,338–342]. This phenomenon has been implicated in antigen presentation in various contexts ranging from viral infection[344] and vaccination[346] to thymic selection[335–337], graft rejection[348], and peripheral tolerance to maternal microchimerism[350]. By necessity, conclusions regarding the role of MHC-dressing in antigen presentation by DCs have largely come from *in vitro* studies and *in vivo* models involving MHC-mismatched bone marrow chimeric mice[335,342,344] or solid organ transplantation[348], due to difficulty in controlling for cross-presentation without altogether abrogating antigen presentation on MHC-I. Indeed, while MHC-dressing by DCs is sufficient to induce T cell priming in various contexts, the necessity of this antigen presentation pathway in mediating *in vivo* T cell activation has never been conclusively demonstrated in syngeneic hosts.

In this study, we utilized two syngeneic murine tumor models expressing distinct model antigens presented in the context of the MHC-I molecule, H-$2K^b$ (K^b), in order to determine the extent to which MHC-dressing was involved in tumor antigen-specific $CD8^+$ T cell priming. While the magnitude of the effect varied across models, $CD8^+$ T cell priming against K^b-restricted tumor antigens was significantly impaired in mice harboring $K^{b-/-}$ tumors, despite the cross-presentation pathway being fully intact. Furthermore, cancer cell-derived MHC-I molecules were readily observed within and on the surface of tumor-resident APCs, and MHC-I-deficient $CD103^+$ cDC1 isolated from tdLN of mice bearing K^b-sufficient tumors were capable

of stimulating antigen-specific $CD8^+$ T cells *ex vivo*. The importance of WDFY4-dependent antigen cross-presentation[214] in mediating anti-tumor $CD8^+$ T cell responses differed across experimental models, but in some cases was dispensable for *in vivo* $CD8^+$ T cell priming. Finally, we demonstrated that APCs become dressed with human MHC-I (human leukocyte antigen class I; HLA-I) molecules *in vitro* when co-cultured with HLA-mismatched tumor cells, and in tumors xenografted in immunodeficient mice. Acquisition of tumor cell-derived HLA-I molecules was strongly correlated with uptake of tumor antigens *in vitro*. Similarly, APCs isolated from murine tumors acquired both tumor-derived MHC-I and fluorescent antigen *in vivo*, suggesting that tumor cell phagocytosis and MHC-dressing may be linked processes. Taken together, our results demonstrate that MHC-dressing is central to the ability of cDC1 to orchestrate anti-tumor $CD8^+$ T cell responses.

3.3 Results

3.3.1 Development and validation of tumor models

In order to define the impact of cancer cell-derived MHC-I expression on subsequent anti-tumor $CD8^+$ T cell priming, two tumor models were utilized, C1498 leukemia and B16.F10 melanoma (both H-2^b). These models were selected due to differences in cell of origin and baseline MHC-I expression levels. The B16 and C1498 models have been extensively characterized, with well-established growth kinetics in syngeneic C57BL/6 mice[357,358]. Moreover, the timing and magnitude of endogenous antigen-specific $CD8^+$ T cell responses raised against these tumors have previously been defined[351,359]. To facilitate tracking of tumor antigen-specific $CD8^+$ T cell responses, C1498 cells expressing an H-$2K^b$ (K^b)-restricted model peptide antigen, SIYRYYGL (SIY)[202,351], and B16.F10 cells expressing the C-terminal domain (amino acids 161-385) of chicken ovalbumin (OVA), including its derivative K^b-restricted peptide antigen,

SIINFEKL ($OVA_{257-264}$)[360], were employed. K^b-deficient ($K^{b-/-}$) parental C1498, C1498.SIY and B16.OVA cell lines were generated using CRISPR/Cas9 (**Figure 3.1A-C**), which allowed for a direct comparison of antigen-specific $CD8^+$ T cell priming in mice bearing $K^{b+/+}$ versus $K^{b-/-}$ tumors. Additionally, K^b was re-expressed in C1498 $K^{b-/-}$ cells (C1498 $K^{bAdd\text{-}back}$; K^{bAB}) with a C-terminal eGFP tag[352], so that the localization of tumor-derived K^b molecules could be assessed within host APCs (**Figure 3.1A**).

In C1498.SIY cells, the SIY peptide was expressed in-frame at the C-terminus of eGFP, which allowed for monitoring of SIY antigen expression (eGFP fluorescence), and for assessing uptake of C1498.SIY-derived proteins by tumor-resident APC populations. Importantly, SIY-eGFP expression was identical in C1498.SIY $K^{b+/+}$ and C1498.SIY $K^{b-/-}$ cells, indicating that K^b deletion did not affect overall SIY antigen expression (**Figure 3.1B**). Additionally, bone marrow-derived dendritic cells (BMDCs) cultured with C1498.SIY $K^{b+/+}$ or C1498.SIY $K^{b-/-}$ cell lysates were similarly capable of presenting SIY to antigen-specific, T cell receptor transgenic (TCR-tg) 2C $CD8^+$ T cells *in vitro* (**Figure 3.1D**). As expected, subcutaneously (s.c.) implanted C1498.SIY $K^{b-/-}$ tumors progressed more rapidly than C1498.SIY $K^{b+/+}$ tumors in C57BL/6 mice (**Figure 3.1E**), as the former could not be directly targeted for lysis by $CD8^+$ T cells specific for K^b-restricted antigens. Conversely, C1498.SIY $K^{b+/+}$ and C1498.SIY $K^{b-/-}$ tumors exhibited similar growth in $Rag2^{-/-}$ mice lacking mature B and T cells (**Figure 3.1F**), indicating that growth rate differences between $K^{b-/-}$ and $K^{b+/+}$ C1498.SIY tumors in C57BL/6 mice was due to impaired effector responses by adaptive immune cells in the absence of cancer cell K^b expression.

Consistent with observations in C1498 cells, K^b deficiency did not affect OVA antigen expression in B16.F10 cells, as evidenced by equivalent *in vitro* activation of $OVA_{257-264}$-specific TCR-tg OT-I $CD8^+$ T cells by BMDCs cultured with lysates from B16.OVA $K^{b+/+}$ versus

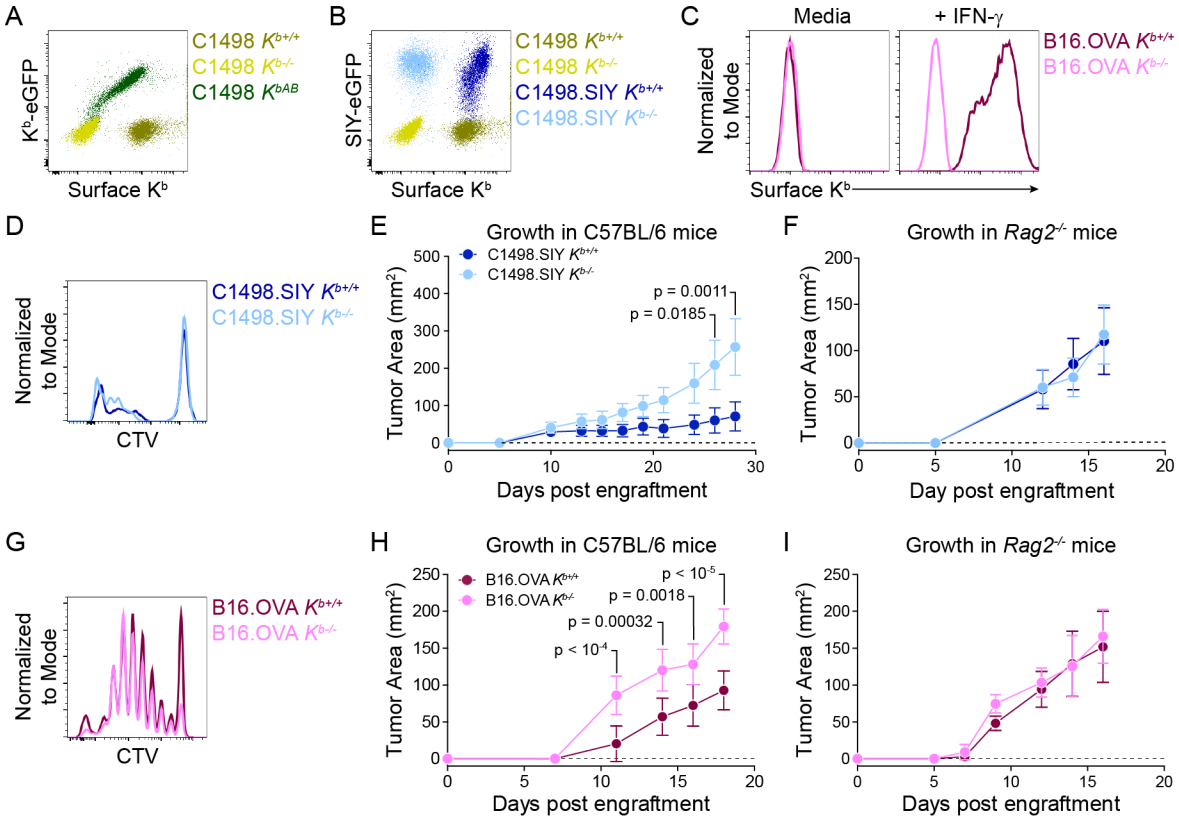

Figure 3.1: Validation of $K^{b-/-}$ cell lines.

A) Surface anti-K^b antibody staining and K^b-eGFP expression in C1498 $K^{b+/+}$, $K^{b-/-}$, and K^{bAB} cell lines *in vitro*.

B) Surface anti-K^b antibody staining and SIY-eGFP expression in C1498.SIY $K^{b+/+}$ and $K^{b-/-}$ cell lines *in vitro*.

C) Surface anti-K^b antibody staining on B16.OVA $K^{b+/+}$ and $K^{b-/-}$ cell lines *in vitro* with and without IFN-γ treatment (100ng/mL for 48 hours).

D) Histogram showing CTV dilution by TCR-tg 2C $CD8^+$ T cells following 72-hour co-culture with BMDCs and lysate from C1498.SIY $K^{b+/+}$ or $K^{b-/-}$ cells.

E and F) Growth kinetics of s.c. C1498.SIY $K^{b+/+}$ and $K^{b-/-}$ tumors in C57BL/6 (E) and $Rag2^{-/-}$ mice (F).

G) Histogram showing CTV dilution by TCR-tg OT-I $CD8^+$ T cells following 72-hour co-culture with BMDCs and lysate from B16.OVA $K^{b+/+}$ or $K^{b-/-}$ cells.

H and I) Growth kinetics of s.c. B16.OVA $K^{b+/+}$ and $K^{b-/-}$ tumors in C57BL/6 (H) and $Rag2^{-/-}$ (I) mice.

Statistical significance for tumor growth experiments was determined by two-way ANOVA with Sidak's post-hoc test for multiple comparisons. Tumor growth data are depicted as mean ± s.d. and were pooled from two independent experiments (n = 10 mice per group in E and H; n = 5 mice per group in F) or from one experiment (I, n = 5 mice per group).

B16.OVA $K^{b-/-}$ cells (**Figure 3.1G**). Furthermore, as observed in the C1498.SIY model, B16.OVA $K^{b-/-}$ tumors grew significantly faster than B16.OVA $K^{b+/+}$ tumors in C57BL/6 mice (**Figure 3.1H**), while the two tumors grew similarly in *Rag2*$^{-/-}$ mice (**Figure 3.1I**). Thus, we generated two tumor models—featuring different baseline MHC-I levels and expression of distinct K^b-restricted antigens—in which to assess the role of cancer cell-derived MHC-I in anti-tumor $CD8^+$ T cell priming.

3.3.2 Anti-tumor $CD8^+$ T cell priming against C1498.SIY tumors is largely dependent on cancer cell MHC-I expression

Once the necessary tumor cell lines were validated, the degree to which MHC-I expression by cancer cells affected antigen-specific $CD8^+$ T cell priming in tdLNs was determined by assessing the expansion of CellTrace violet (CTV)-labeled, adoptively transferred 2C $CD8^+$ T cells six days following subcutaneous (s.c.) inoculation of C1498.SIY $K^{b+/+}$ or C1498.SIY $K^{b-/-}$ cells in congenic C57BL/6 hosts (**Figure 3.2A**). In tdLNs of mice bearing C1498.SIY $K^{b+/+}$ tumors, 2C $CD8^+$ T cells proliferated extensively, as measured by dilution of their CTV fluorescent signal, and had accumulated both in terms of overall number and as a proportion of all tdLN $CD8^+$ T cells (**Figure 3.2B-E**). Strikingly, 2C $CD8^+$ T cell priming was almost completely abrogated in tdLNs of mice with C1498.SIY $K^{b-/-}$ tumors; very few 2C $CD8^+$ T cells had divided, and 2C T cell frequencies and numbers were similar to those observed in analogous cutaneous lymph nodes (cLN) of tumor-free control mice (**Figure 3.2B-E**). Additionally, 2C $CD8^+$ T cells which had proliferated in response to C1498.SIY $K^{b+/+}$ tumors produced the effector cytokines IFN-γ and TNF-α, as well as the cytolytic protein, granzyme B (**Figure 3.3**). Thus, expression of K^b by C1498.SIY cells is required for the priming of functional effector 2C $CD8^+$ T cells.

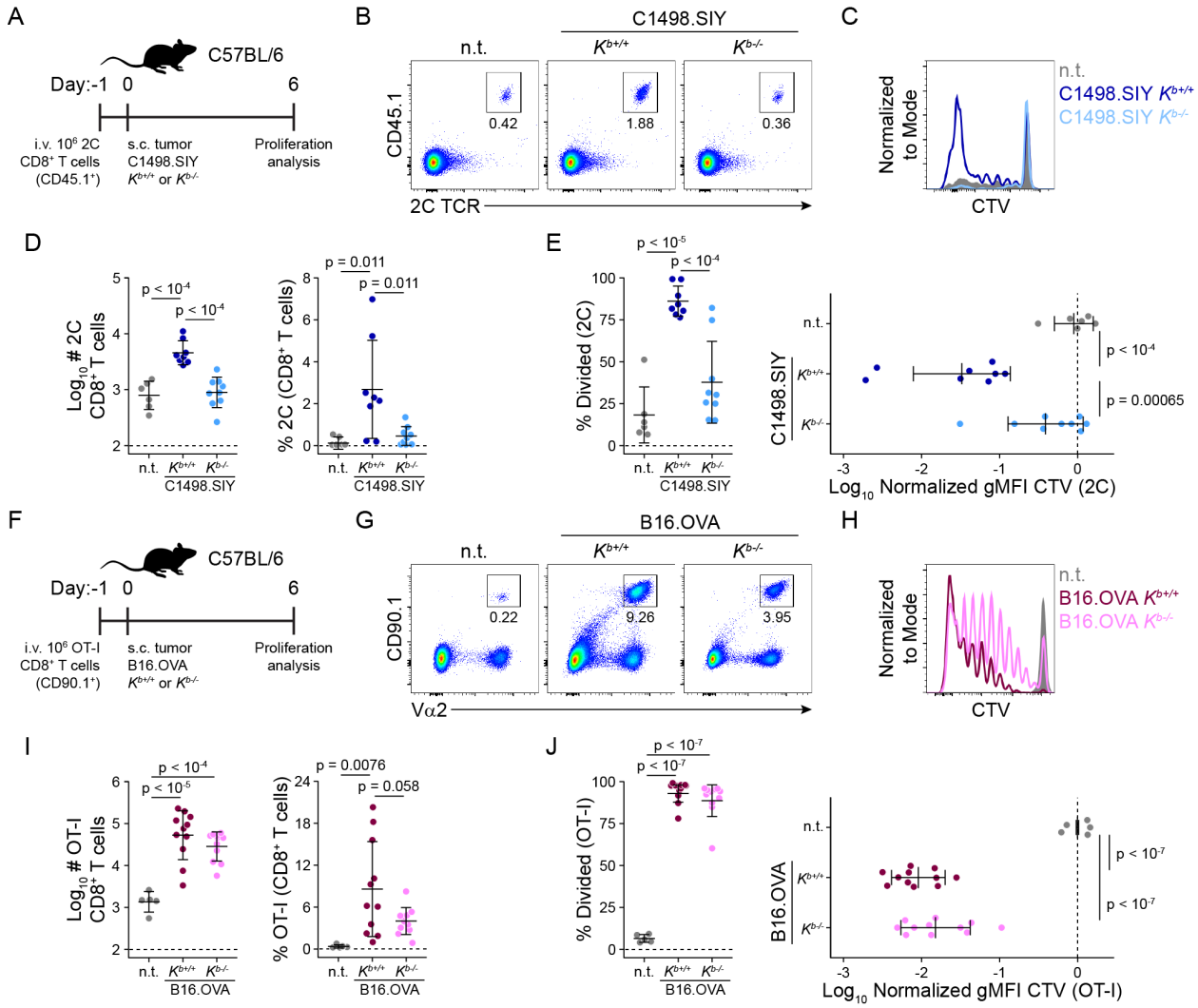

Figure 3.2: Cancer cell intrinsic K^b expression is required for optimum in vivo activation of K^b-restricted antigen-specific TCR-tg $CD8^+$ T cells.

A) Experimental design for analysis of *in vivo* TCR-tg 2C $CD8^+$ T cell priming. 10^6 CTV-labeled $CD45.1^+$ 2C $CD8^+$ T cells were adoptively transferred into C57BL/6 mice ($CD45.2^+$) on day -1. Recipient mice were inoculated with 10^6 C1498.SIY $K^{b+/+}$ or $K^{b-/-}$ cells on day 0. 2C proliferation was assessed on day 6.

B and C) Representative flow cytometry plots depicting the identification of (B) and CTV dilution within (C) 2C $CD8^+$ T cells in the tdLN.

D) Number (left) and frequency (right) of 2C $CD8^+$ T cells in the tdLN.

E) Proliferation of 2C $CD8^+$ T cells, quantified as percent divided (left), and the geometric mean fluorescence intensity of CTV within the population (right).

F) Experimental design for analysis of *in vivo* TCR-tg OT-I $CD8^+$ T cell priming. 10^6 CTV-labeled $CD90.1^+$ OT-I $CD8^+$ T cells were adoptively transferred into C57BL/6 mice ($CD90.2^+$) on day -1. Recipient mice were inoculated with 10^6 B16.OVA $K^{b+/+}$ or $K^{b-/-}$ cells on day 0. OT-I proliferation was assessed on day 6.

G and H) Representative flow cytometry plots depicting the identification of (G) and CTV dilution by (H) OT-I $CD8^+$ T cells in the tdLN.

I) Number (left) and frequency (right) of OT-I $CD8^+$ T cells in the tdLN.

Figure 3.2, continued
J) Proliferation of OT-I CD8$^+$ T cells, quantified as percent divided (left), and the geometric mean fluorescence intensity of CTV within the population (right).
Statistical significance was determined by one-way ANOVA with post-hoc Tukey's HSD for multiple comparisons. $p < 0.05$ was considered statistically significant. All summary plots are depicted is mean ± s.d. Data are pooled from three independent experiments. n.t. = no tumor.

A similar experiment was performed in which CTV-labeled OT-I CD8$^+$ T cells were adoptively transferred into congenic C57BL/6 host mice challenged s.c. with B16.OVA $K^{b+/+}$ or $K^{b-/-}$ cells the following day (**Figure 3.2F**). By day 6, OT-I CD8$^+$ T cells proliferated extensively and expanded markedly in tdLNs of mice with B16.OVA tumors regardless of K^b expression, although there was a non-statistically significant reduction in priming in mice bearing B16.OVA $K^{b-/-}$ tumors (**Figure 3.2G-J**).

We next sought to determine the impact of cancer cell-intrinsic MHC-I expression on endogenous anti-tumor CD8$^+$ T cell activation. C57BL/6 mice were inoculated s.c. with C1498.SIY $K^{b+/+}$ or $K^{b-/-}$ cells, and numbers of endogenous antigen-specific CD8$^+$ T cells were measured in the tdLN by K^b:SIY pentamer staining and flow cytometry six days later. Consistent with observations in TCR-tg adoptive transfer experiments, endogenous SIY-specific CD8$^+$ T cells expanded considerably in response to C1498.SIY $K^{b+/+}$ tumors, while the numbers of SIY-specific CD8$^+$ T cells recovered from tdLNs of mice bearing C1498.SIY $K^{b-/-}$ tumors were comparable to the analogous cLNs from tumor-free control mice (**Figure 3.4A and B**). Furthermore, numbers of functional, SIY antigen-specific T cells, as measured by IFN-γ ELISpot, were significantly reduced in tdLNs of mice with C1498.SIY $K^{b-/-}$ tumors (**Figure 3.4C**). In order to verify that tumor-derived K^b molecules were required specifically at the level of CD8$^+$ T cell priming, and that diminished CD8$^+$ T cell activation against $K^{b-/-}$ tumors had functional consequences with regard to the control of tumor growth, we performed an experiment in which the priming and effector phases of the anti-tumor CD8$^+$ T cell response

were uncoupled. CD8$^+$ T cells were isolated from tdLNs of mice six days post injection (d.p.i.) of C1498.SIY $K^{b+/+}$ or $K^{b-/-}$ cells, such that initial priming occurred either against a K^b-sufficient or -deficient tumor. CD8$^+$ T cells were also isolated from analogous cLNs of tumor-free control mice. Equal numbers of isolated CD8$^+$ T cells were then adoptively transferred into cohorts of naive C57BL/6 mice that were subsequently challenged with C1498.SIY $K^{b+/+}$ cells (**Figure**

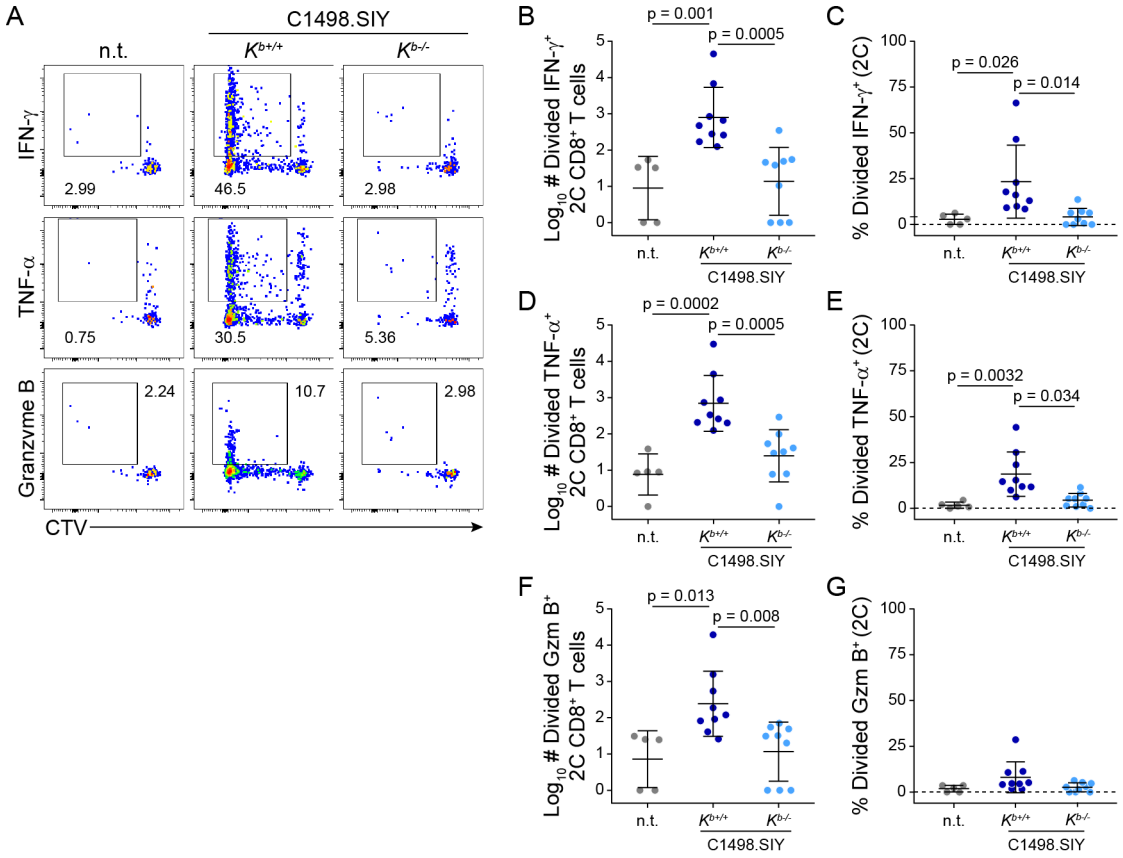

Figure 3.3: 2C TCR-tg CD8$^+$ T cells produce effector cytokines in response to C1498.SIY $K^{b+/+}$ tumors.

10^6 CTV-labeled CD45.1$^+$ 2C CD8$^+$ T cells were adoptively transferred into C57BL/6 mice (CD45.2$^+$) on day -1. Recipient mice were inoculated with 10^6 C1498.SIY $K^{b+/+}$ or $K^{b-/-}$ cells on day 0. 2C cells were re-stimulated *ex vivo* with SIY peptide for 5 hours on day 6 and assessed for production of IFN-γ, TNF-α, and granzyme B.

A) Representative flow cytometry plots from intracellular cytokine staining.

B-G) Number (B, D, and F) and frequency (C, E, and G) of proliferated 2C CD8$^+$ T cells producing IFN-γ (B and C), TNF-α (D and E), and granzyme B (F and G). Data are pooled from two independent experiments and depicted as mean ± s.d.

Statistical significance was determined by one-way ANOVA with post-hoc Tukey's HSD for multiple comparisons.

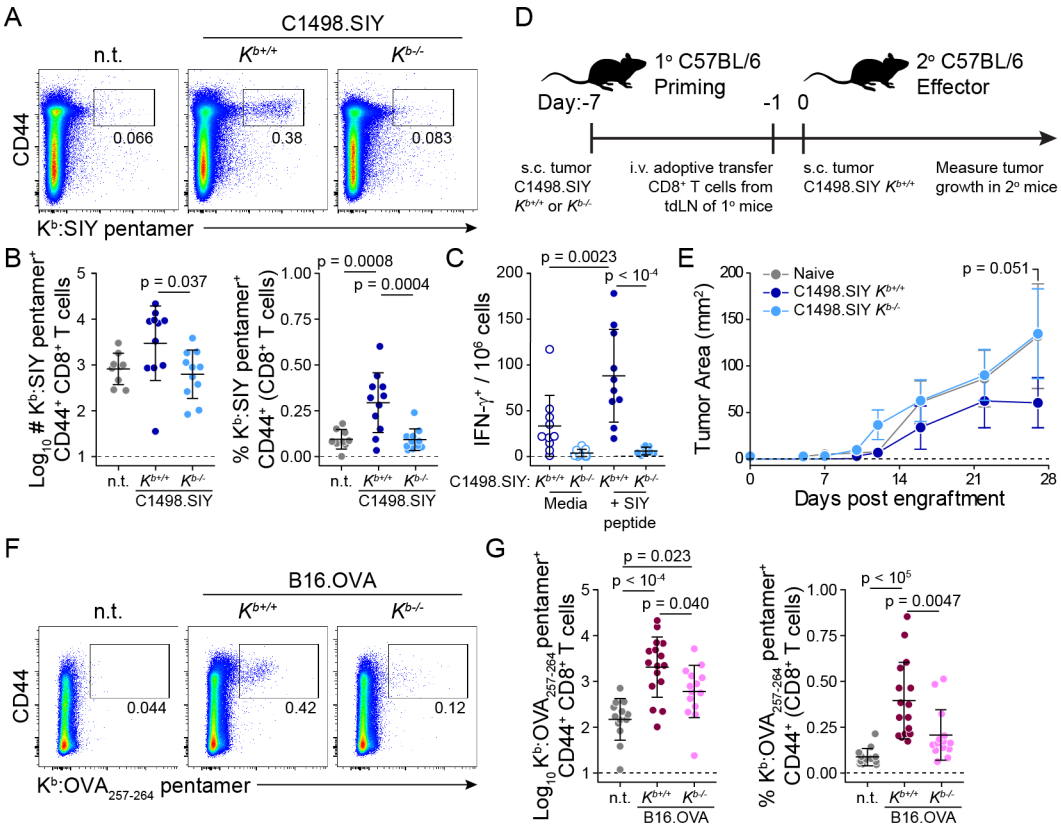

Figure 3.4: Endogenous antigen-specific $CD8^+$ T cell responses against K^b-restricted tumor antigens are reduced against K^b-deficient tumors.

A and B) K^b:SIY pentamer stain of endogenous $CD8^+$ T cells from the tdLN of C57BL/6 mice bearing C1498.SIY $K^{b+/+}$ or $K^{b-/-}$ tumors at day 6. Representative flow cytometry plots are shown in A and data are quantified in B.

C) ELISpot of IFN-γ production in the tdLN of C57BL/6 mice bearing s.c. C1498.SIY $K^{b+/+}$ or $K^{b-/-}$ tumors at day 6.

D and E) Primary C57BL/6 mice received s.c. C1498.SIY $K^{b+/+}$ or $K^{b-/-}$ tumors at day –7. On day –1, 5 x10^6 MACS-enriched $CD8^+$ T cells from the tdLN of primary mice were adoptively transferred into naïve secondary C57BL/6 mice. At day 0, secondary mice were challenged with s.c. C1498.SIY $K^{b+/+}$ tumors. Tumor growth was measured in secondary mice to compare functional control by $CD8^+$ T cells transferred from primary mice. Experimental design is shown in (D) and the growth of s.c. C1498.SIY $K^{b+/+}$ tumors in secondary (recipient) mice is depicted in (E).

F and G) Identification (F) and quantification (G) of endogenous $OVA_{257-264}$-specific $CD8^+$ T cells in the tdLN of C57BL/6 mice bearing B16.OVA $K^{b+/+}$ or $K^{b-/-}$ tumors at day 6 by K^b:$OVA_{257-264}$ pentamer stain.

Statistical significance for tumor growth in (E) was determined by two-way ANOVA with Sidak's post-hoc test for multiple comparisons. For all other comparisons, statistical significance was determined by one-way ANOVA with post-hoc Tukey's HSD. $p < 0.05$ was considered statistically significant. Tumor growth in (E) is shown as mean ± s.e.m.; other plots are depicted is mean ± s.d. Data are pooled from two (E), three (B and C), or four (G) independent experiments. n.t. = no tumor.

3.4D). Adoptive transfer of $CD8^+$ T cells initially primed against a K^b-sufficient tumor provided superior control of C1498.SIY $K^{b+/+}$ tumors in secondary recipients compared with $CD8^+$ T cells initially primed against a K^b-deficient tumor, which provided no greater protection against tumor growth than did $CD8^+$ T cells transferred from cLN of tumor-free mice (**Figure 3.4E**). Thus, K^b expression by C1498.SIY tumor cells is required for early priming of functional antigen-specific $CD8^+$ T cell responses.

To determine the role of tumor-derived MHC-I in endogenous $CD8^+$ T cell priming in a second model, C57BL/6 mice were inoculated s.c. with B16.OVA $K^{b+/+}$ or B16.OVA $K^{b-/-}$ cells, and $OVA_{257-264}$-specific $CD8^+$ T cell responses were analyzed in tdLNs at 6 d.p.i. Staining with K^b:$OVA_{257-264}$ pentamer revealed robust expansion of endogenous antigen-specific $CD8^+$ T cells in tdLNs of mice bearing B16.OVA $K^{b+/+}$ tumors, and that this expansion was significantly reduced in mice bearing B16.OVA $K^{b-/-}$ tumors (**Figure 3.4F and G**). This result contrasts with those in **Figure 3.2F-J**, in which OT-I $CD8^+$ T cell priming occurred independently of K^b expression by B16.OVA. We speculate that OT-I $CD8^+$ T cell priming was not representative of the overall pool of endogenous $OVA_{257-264}$-specific $CD8^+$ T cells, which would have varying affinities for the K^b:$OVA_{257-264}$ complex[361]. Additionally, while endogenous $OVA_{257-264}$-specific $CD8^+$ T cell priming was reduced when B16.OVA cells lacked K^b expression, it was not completely abrogated as was SIY-specific $CD8^+$ T cell priming against C1498.SIY $K^{b-/-}$ tumors. Together, these results highlight the differential impact of tumor-intrinsic K^b expression on anti-tumor $CD8^+$ T cell responses mounted against K^b-restricted antigens in distinct tumor models. Nevertheless, K^b expression by cancer cells is clearly required for optimal endogenous $CD8^+$ T cell priming against K^b-restricted antigens in both tumor models.

3.3.3 MHC-I expression by the tumor does not affect antigen uptake or provision of costimulatory signals by DCs

The demonstrated importance of K^b expression by cancer cells in tumor antigen-specific $CD8^+$ T cell priming, coupled with the established role of cDC1 in mediating this process, strongly suggested that MHC-I-dressing by DCs was involved. However, it was formally possible that this effect occurred independently of MHC-dressing, because a lack of tumor K^b expression might have affected antigen uptake or DC activation. To determine whether K^b expression by cancer cells affected uptake of tumor antigens, we analyzed different APC populations in C1498.SIY $K^{b+/+}$ or $K^{b-/-}$ tumors for acquisition of SIY-eGFP by flow cytometry. Gating strategies utilized to identify tumor-resident APC populations, and to identify unique DC subsets in tdLNs are depicted in **Figure 2.1**. APCs in both C1498.SIY $K^{b+/+}$ and $K^{b-/-}$ tumors were equally capable of acquiring tumor-derived SIY-eGFP fluorescence at 6 d.p.i. (**Figure 3.5**), consistent with published results demonstrating tumor antigen uptake by all myeloid populations in the tumor environment[253].

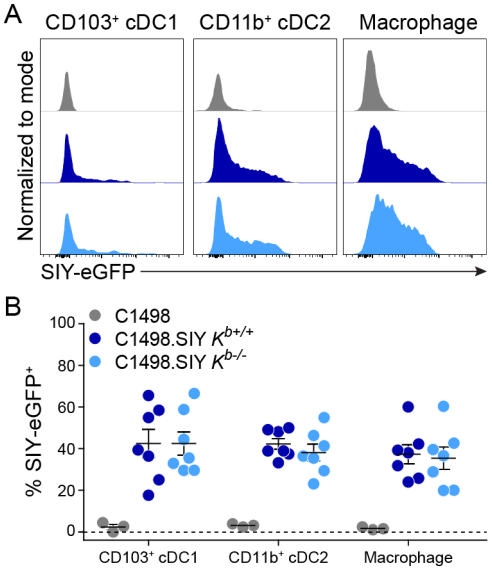

Figure 3.5: Similar SIY-eGFP uptake by DCs in C1498.SIY $K^{b+/+}$ and $K^{b-/-}$ tumors. Flow cytometry analysis of DCs isolated from the tumors of C57BL/6 mice bearing C1498.SIY $K^{b+/+}$ or $K^{b-/-}$ tumors at day 6, shown with representative histograms (A) and quantification (B). Statistical significance was determined by two-way ANOVA with post-hoc Tukey's HSD. Summary plots are depicted as mean ± s.e.m.

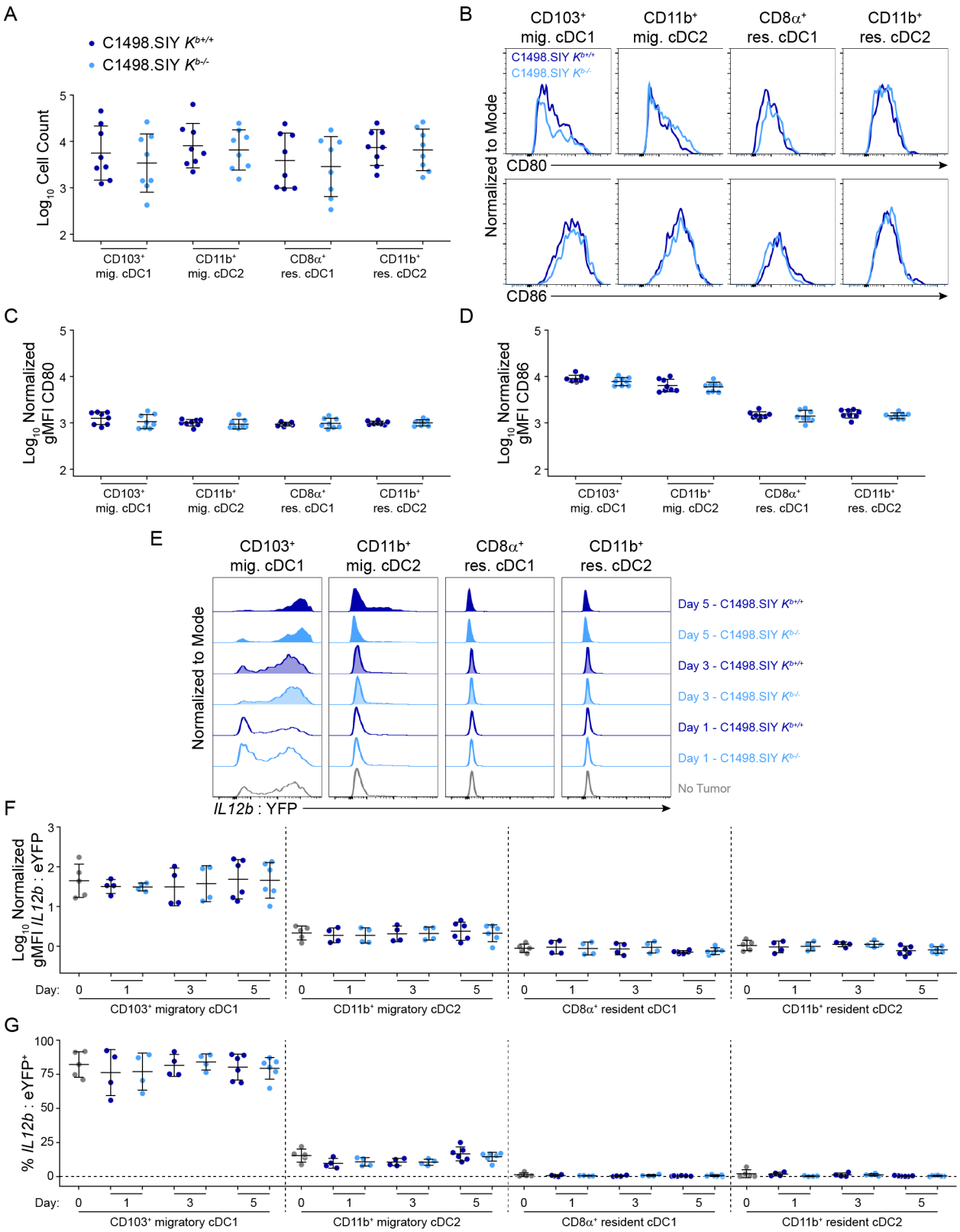

Figure 3.6: Similar DC counts and costimulatory signals in tdLNs of C1498.SIY $K^{b+/+}$ and $K^{b-/-}$ tumor-bearing mice.

Figure 3.6, continued
A) Cell number for the cDC populations in the tdLN of C57BL/6 mice bearing C1498.SIY $K^{b+/+}$ or $K^{b-/-}$ tumors at day 6.
B-D) CD80 and CD86 levels on cDC populations in the tdLN of C57BL/6 mice bearing C1498.SIY $K^{b+/+}$ or $K^{b-/-}$ tumors at day 6. Representative flow cytometry histograms are shown in B, and geometric mean fluorescence intensity data are shown in C (CD80) and D (CD86).
E-G) *IL-12b* expression by cDC subsets in the tdLN of $IL12b^{Ires\text{-}YFP}$ reporter mice bearing s.c. C1498.SIY $K^{b+/+}$ or $K^{b-/-}$ tumors. Representative histograms are shown in E, and the data are quantified as geometric mean fluorescence intensity (F) and percent IL-12b$^+$ cells (G).
Statistical significance was determined by two-way ANOVA (C and D) or three-way ANOVA (F and G), with post-hoc Tukey's HSD. Summary plots are depicted as mean ± s.d. Data are pooled from two independent experiments.

Next, we considered the possibility that K^b expression by cancer cells may impact DC maturation and provision of costimulation—an essential step in T cell activation. Expression of costimulatory molecules was assessed by flow cytometry on DCs isolated from the tdLNs of C57BL/6 mice bearing C1498.SIY $K^{b+/+}$ or $K^{b-/-}$ tumors at 6 d.p.i. No differences in DC number or frequency were observed (**Figure 3.6A**), nor were there differences in CD80 or CD86 cell surface expression levels on DC populations in the tdLN of mice bearing C1498.SIY $K^{b+/+}$ or $K^{b-/-}$ tumors (**Figure 3.6B-D**). Additionally, no differences in IL-12p40 expression were observed within DCs isolated from tdLNs of $IL12b^{IRES\text{-}YFP}$ mice bearing C1498.SIY $K^{b+/+}$ or $K^{b-/-}$ tumors. (**Figure 3.6E-G**). Thus, the reduction in CD8$^+$ T cell priming observed against K^b-deficient tumors is not due to a defect in the acquisition of tumor antigens or provision of necessary secondary or tertiary signals by DCs.

3.3.4 Tumor-resident DCs acquire and present cancer cell-derived MHC-I

DCs have been shown to present exogenous MHC-I molecules in MHC-mismatched *in vivo* transplantation[341,348] and maternal microchimerism[350], as well as *in vitro* co-culture models[336,338,339,342]. The data presented above suggest that MHC-I transfer between cancer cells and APCs occurs in the syngeneic tumor context as well. To determine the extent to which

cancer cell-derived MHC-I molecules were acquired by tumor-resident APCs, C1498 $K^{b+/+}$, $K^{b-/-}$, or K^{bAB} cells were inoculated s.c. into MHC-I-deficient $K^{b-/-}D^{b-/-}$ mice. At 6-10 d.p.i., anti-K^b cell surface antibody staining revealed that DC and macrophage populations isolated from C1498 $K^{b+/+}$ and K^{bAB} tumors had broadly acquired cancer cell-derived K^b molecules to a similar degree (**Figure 3.7A-E**). Further, no presentation of K^b molecules by $K^{b-/-}D^{b-/-}$ tumor-infiltrating T cell populations was observed (**Figure 3.7C**), indicating that acquisition of tumor-derived MHC-I molecules was a unique property of phagocytic cells. However, presentation of C1498-derived K^b molecules was not detectable on migratory or resident APC populations in tdLNs (**Figure 3.8**), likely due to limited sensitivity of detection by conventional flow cytometric analysis.

To assess the localization of C1498-derived K^b molecules on or within APCs, and to verify that the presentation of C1498-derived K^b molecules by APCs observed in Figure 3.7A-C was not an artifact resulting from the complete absence of endogenous MHC-I in $K^{b-/-}D^{b-/-}$ mice, over 4,000 $CD11c^+$ MHC-II^+ cells from C1498 K^{bAB} tumors engrafted in 12 wild type C57BL/6 hosts were visualized using ImageStream cytometry (**Figure 3.7F**). Surprisingly, the majority of APCs isolated from C1498 K^{bAB} tumors had internalized K^b-eGFP molecules, and only a small subset of the imaged APCs displayed K^b-eGFP exclusively at the cell membrane (**Figure 3.7G**), suggesting that MHC-dressing may be associated with tumor antigen uptake. Importantly, eGFP fluorescence was absent in $CD11c^+$ MHC-II^+ cells isolated from control C1498 $K^{b+/+}$ tumors lacking eGFP expression, and eGFP fluorescence in $CD11c^+$ MHC-II^+ cells isolated from a control C1498.SIY $K^{b+/+}$ tumor was almost exclusively classified as internal in a system in which any acquired eGFP fluorescence must be internal (**Figure 3.7G**).

To test the hypothesis that MHC-dressing and tumor antigen phagocytosis may be linked processes *in vivo*, C1498.SIY $K^{b+/+}$ or $K^{b-/-}$ tumors were raised in $K^{b-/-}D^{b-/-}$ mice, and tumor-resident APCs were analyzed by imaging flow cytometry for acquisition of tumor antigen (SIY-

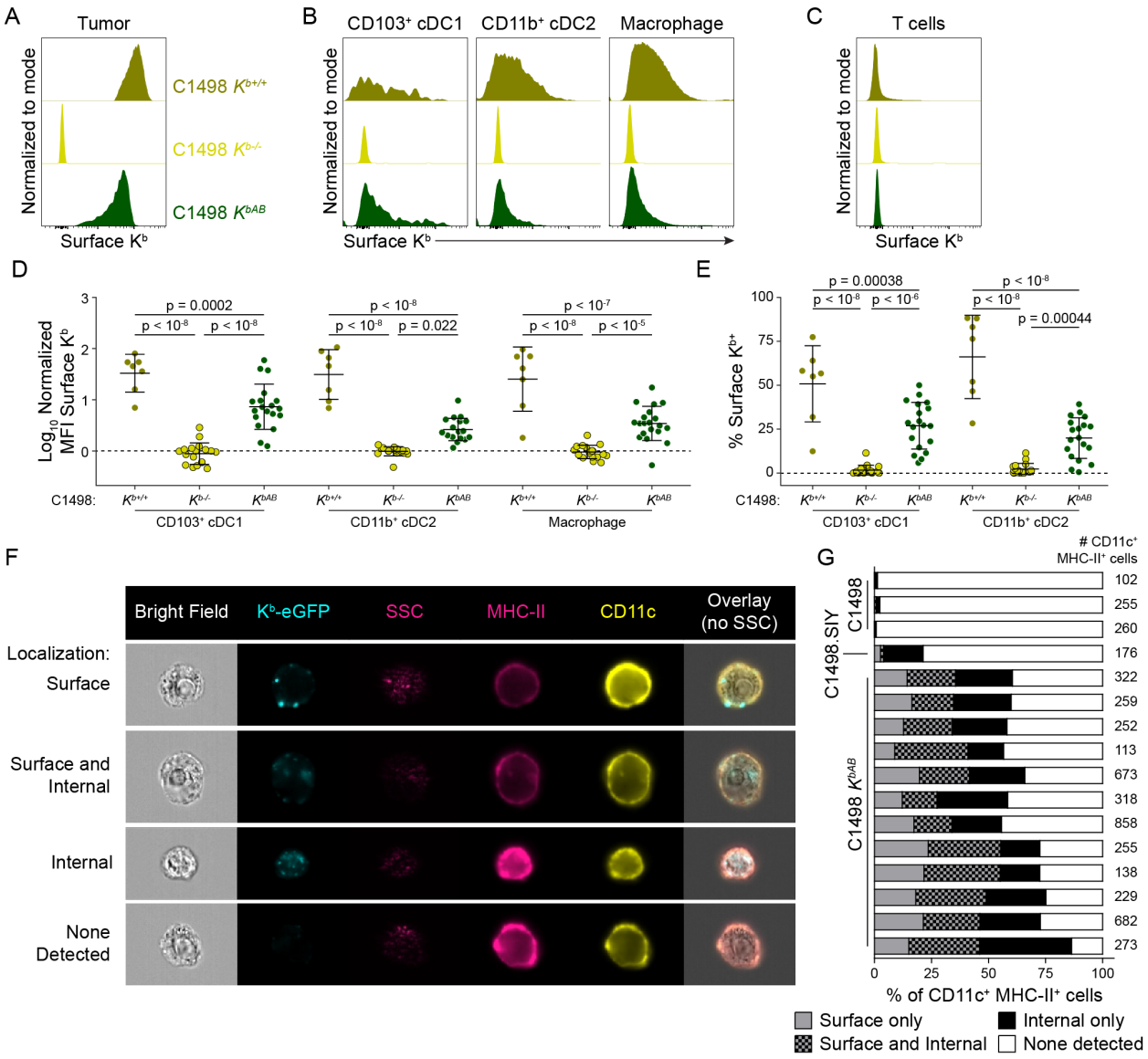

Figure 3.7: Acquisition of C1498-derived K^b molecules by APC populations in the tumor.
A-C) Representative flow cytometry histograms for surface K^b staining of cancer cells (A), APCs (B), and T cells (C) isolated from the tumor of C57BL/6 and *K$^{b-/-}$D$^{b-/-}$* mice bearing s.c. C1498 *K$^{b+/+}$*, *K$^{b-/-}$*, or *K^{bAB}* tumors at day 6-10.
D and E) Quantification of surface K^b staining of APC populations shown in B, as either mean fluorescence intensity (D) or percent K^{b+} (E).
F and G) ImageStream cytometry of CD11c$^+$ MHC-II$^+$ APCs isolated from C1498 K$^{b-/-}$ or K^{bAB} s.c. tumors in C57BL/6 hosts at day 6-10. Representative images are shown in F, and quantification of intracellular versus surface K^b localization is shown in G, with each bar representing one mouse.
Statistical significance for D and E was determined by two-way ANOVA with post-hoc Tukey's HSD test. Graphs are depicted as mean ± s.d. Data are pooled from five (D and E) or three (G) independent experiments.

eGFP) and cancer cell-derived K^b using an intracellular anti-K^b antibody stain. Imaging revealed that the APCs which acquired cancer cell-derived MHC-I molecules had also internalized the model tumor antigen SIY-eGFP (**Figure 3.9**), often with at least some colocalization in fluorescent signal between SIY-eGFP and internalized K^b molecules. These results demonstrate the ability of APCs to acquire C1498-derived MHC-I molecules in the tumor environment and suggest that this MHC-dressing is highly correlated with—and might occur through—internalization of tumor material, including antigens.

Attempts to replicate these results in the B16.OVA model were hindered by the fact that B16.OVA cells express very low levels of K^b *in vitro*[93,362,363], and while K^b is rapidly upregulated on B16.OVA cells *in vivo* in wild type hosts in response to IFN-γ[93], this did not occur in $K^{b-/-}D^{b-/-}$ mice, presumably due to their significantly reduced pool of endogenous $CD8^+$ T cells

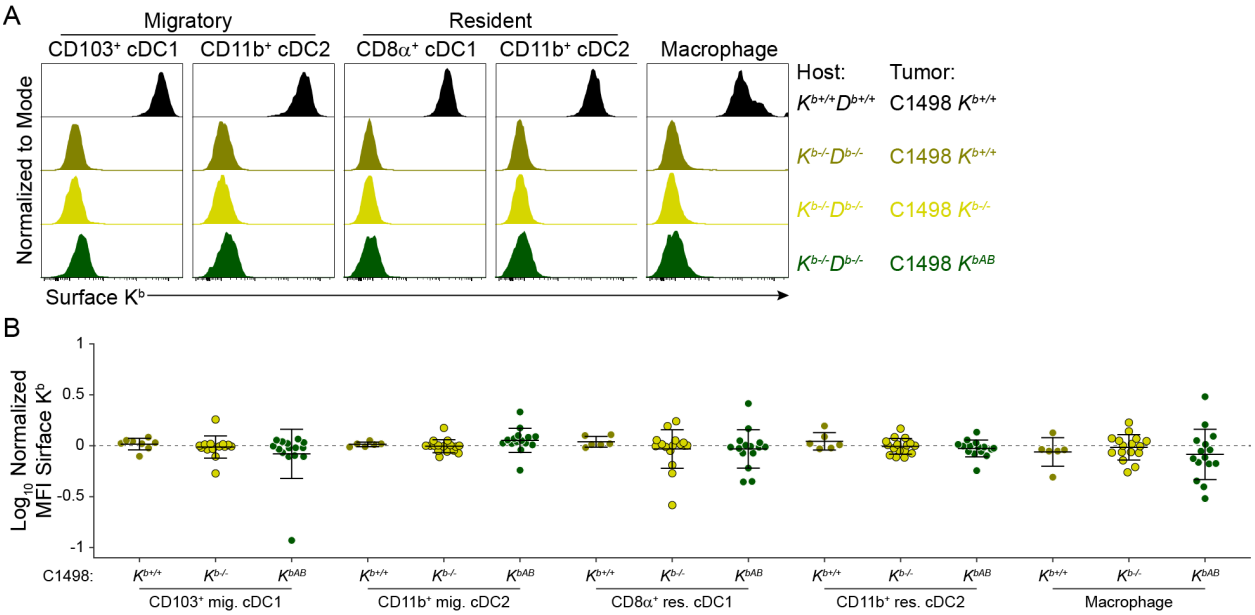

Figure 3.8: C1498-derived K^b molecules are not detected on the surface of APCs in the tdLN by flow cytometry.
Surface staining for K^b on APCs isolated from the tdLN of $K^{b-/-}D^{b-/-}$ mice bearing s.c. C1498 $K^{b+/+}$, $K^{b-/-}$, and K^{bAB} tumors at day 6-10. Representative flow cytometry histograms (A) and quantification of the data (B) are shown. Data are pooled from four independent experiments and depicted as mean ± s.d. Statistical significance was determined by two-way ANOVA with post-hoc Tukey's HSD test.

(**Figure 3.10A-C**). To overcome this obstacle, B16.OVA $K^{b+/+}$ and B16.OVA $K^{b-/-}$ cells were pre-treated with IFN-γ *in vitro* for 48 hours prior to s.c. inoculation into $K^{b-/-}D^{b-/-}$ mice. IFN-γ treatment induced K^b upregulation on B16.OVA $K^{b+/+}$ cells, but not on B16.OVA $K^{b-/-}$ cells (**Figure 3.1C**). Analysis of tumors at 6-10 d.p.i. revealed that K^b-sufficient B16.OVA cells retained IFN-γ-induced K^b expression *in vivo*, and as in the C1498 system, APCs isolated form B16.OVA tumors were broadly capable of acquiring and presenting tumor cell-derived K^b molecules (**Figure 3.10D-F**). Thus, the ability of APCs to become dressed with cancer-derived MHC-I is not restricted to a single tumor model.

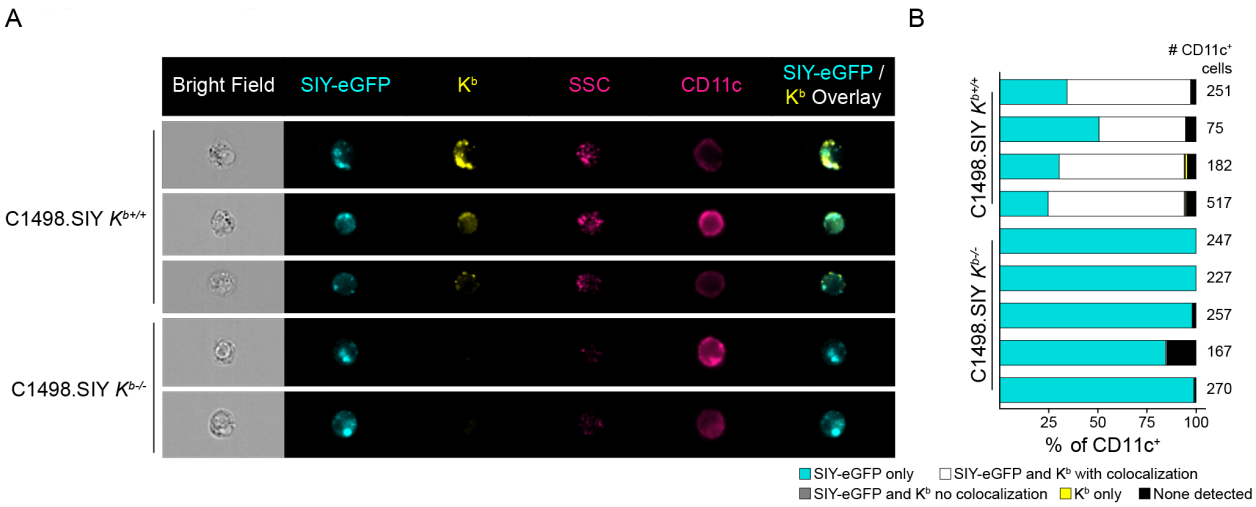

Figure 3.9: Correlation between acquisition of tumor-derived K^b molecules and internalization of a fluorescent tumor antigen.
$CD11c^+$ APCs isolated from C1498.SIY $K^{b+/+}$ or $K^{b-/-}$ tumors in $K^{b-/-}D^{b-/-}$ mice at day 7 were analyzed by imaging flow cytometry.
A) Representative images of $CD11c^+$ APCs showing phagocytosis of a model tumor antigen (SIY-eGFP) and the acquisition of tumor-derived K^b molecules by intracellular antibody stain.
B) Summary bar graph of the data. Each bar represents one mouse, and the number of $CD11c^+$ APCs imaged is indicated to the right. Three samples were excluded from the quantification because fewer than 50 $CD11c^+$ APCs were imaged in focus.

3.3.5 Presentation of tumor-derived pMHC complexes by CD103$^+$ DCs is sufficient for antigen-specific CD8$^+$ T cell priming *ex vivo*

Considering the necessity for tumor derived K^b molecules in optimal tumor antigen-specific CD8$^+$ T cell priming, the known requirement of cDC1 in this process, and the ability of APCs to acquire and present tumor-derived MHC-I, we next assessed the sufficiency of MHC-I-dressing by DCs as a means of tumor antigen presentation. Accordingly, C1498.SIY $K^{b+/+}$ and C1498.SIY $K^{b-/-}$ tumors were inoculated s.c. in wild type, $K^{b-/-}D^{b-/-}$, and $Tap1^{-/-}$ mice. Due to

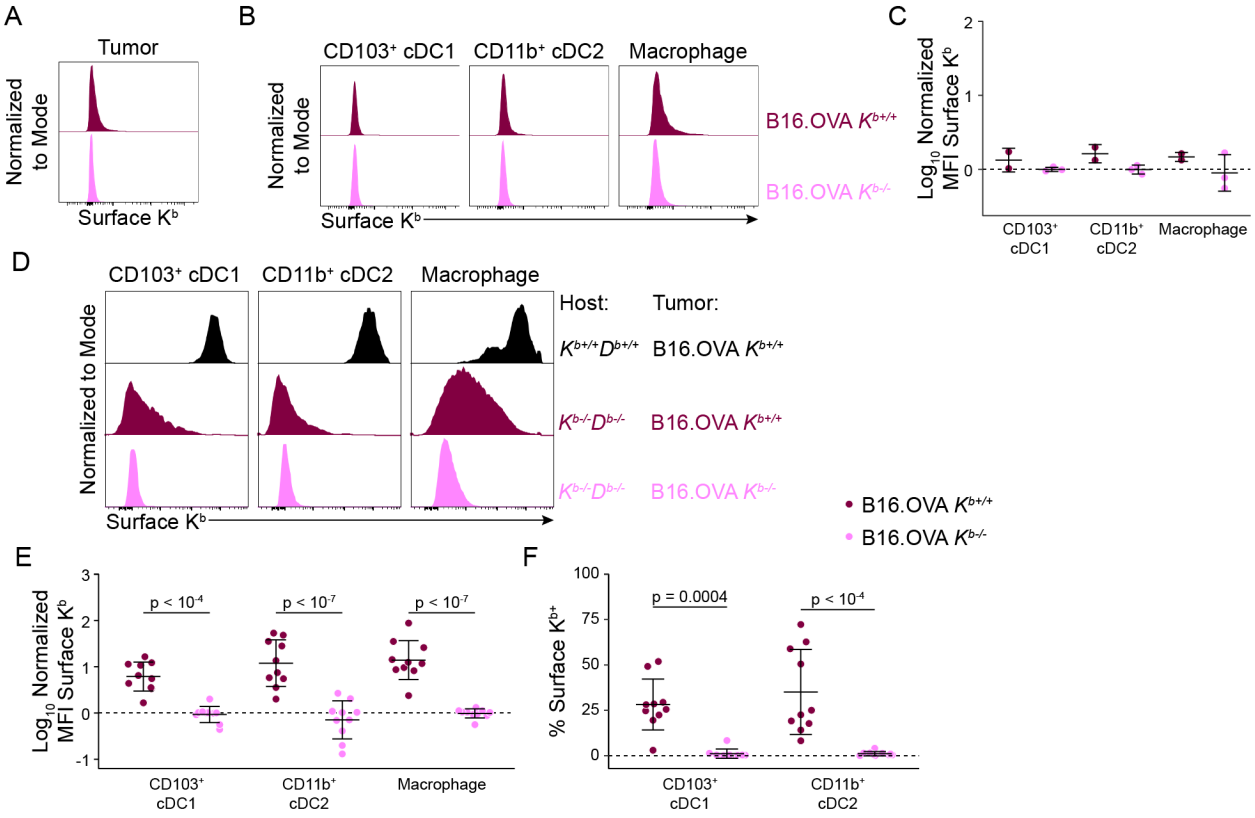

Figure 3.10: Acquisition of B16.OVA-derived K^b molecules by APC populations in the tumor.
A-C) $K^{b-/-}D^{b-/-}$ mice received s.c. B16.OVA $K^{b+/+}$ or $K^{b-/-}$ tumors, which were analyzed at day 6-10. Surface staining for K^b is shown for tumor cells (A) and APCs (B) in the tumor, and the data are quantified (C).
D-F) B16.OVA $K^{b+/+}$ and $K^{b-/-}$ cells were pre-treated with IFN-γ for 48 hr *in vitro* prior to s.c. inoculation into C57BL/6 or $K^{b-/-}D^{b-/-}$ hosts. Representative flow cytometry histograms of K^b surface staining are shown APCs (D), and the APC data are quantified as mean fluorescence intensity (E) and percent K^{b+} (F). Data in E and F are pooled from three independent experiments, and all summary plots are depicted as mean ± s.d.
Statistical significance was determined by two-way ANOVA with post-hoc Tukey's HSD.

defective peptide transport from the cytoplasm into the endoplasmic reticulum where MHC-I loading occurs, *Tap1*$^{-/-}$ mice are largely incapable of classical antigen cross-presentation[282,364]. Six days later, tdLN-resident and migratory cDC1 and cDC2 populations were separately FACS-purified and co-cultured directly *ex vivo* with CTV-labeled 2C CD8^{+} T cells (**Figure 3.11A**). The

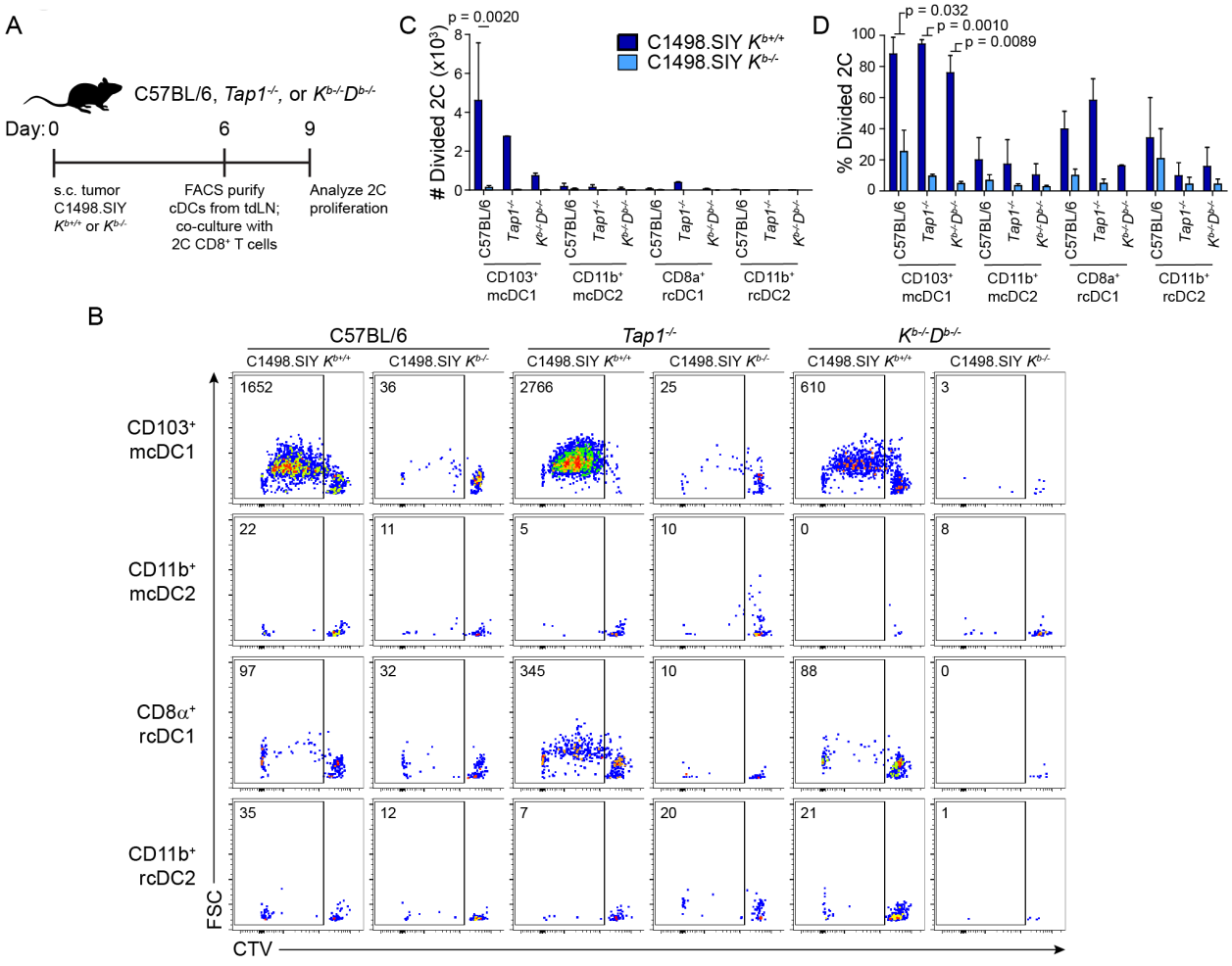

Figure 3.11: Presentation of C1498.SIY-derived pMHC complexes by CD103^{+} cDC1 is sufficient for TCR-tg 2C CD8^{+} T cell priming *ex vivo*.
A) Experimental design. cDC populations were sorted from the tdLN of C57BL/6, *Tap1*$^{-/-}$, and *K*$^{b-/-}$*D*$^{b-/-}$ mice bearing C1498.SIY *K*$^{b+/+}$ or *K*$^{b-/-}$ tumors at day 6 and co-cultured with CTV-labeled TCR-tg 2C CD8^{+} T cells for 72 hours.
B) Representative flow cytometry plots showing proliferation of 2C CD8^{+} T cells.
C and D) Bar graphs quantifying the data from B as number (C) and frequency (D) of divided 2C CD8+ T cells. Bar graphs are depicted as mean + s.d.
Data are pooled from two independent experiments and statistical significance was determine by three-way ANOVA with post-hoc Tukey's HSD test.

ability to mediate 2C CD8$^+$ T cell activation was restricted almost exclusively to migratory CD103$^+$ cDC1 from mice bearing C1498.SIY $K^{b+/+}$ tumors, which was expected given the previously reported role of CD103$^+$ cDC1 in presenting tumor antigens to CD8$^+$ T cells[254,255]. Remarkably, cross-presentation of the SIY antigen in this context was dispensable for 2C CD8$^+$ T cell activation *ex vivo*, as evidenced by the fact that priming was mediated similarly by *Tap1*$^{-/-}$, $K^{b-/-}D^{b-/-}$, and wild type CD103$^+$ cDC1 (**Figure 3.11B-D**). Further, migratory CD103$^+$ cDC1 from tdLNs of wild type mice bearing C1498.SIY $K^{b-/-}$ tumors were incapable of stimulating 2C CD8$^+$ T cells (**Figure 3.11B-D**), which is consistent with data presented in **Figures 1 and 2**, further emphasizing the requirement for cancer cell-derived MHC-I in anti-tumor CD8$^+$ T cell priming. This result demonstrates that acquisition and presentation of C1498 cell-derived K^b:SIY molecules by CD103$^+$ cDC1 is both necessary and sufficient for tumor-specific CD8$^+$ T cell priming in this model.

3.3.6 Generation and characterization of *Wdfy4*$^{-/-}$ mice

After establishing the role of MHC-I-dressing as a means of antigen presentation by migratory CD103$^+$ cDC1, we sought to determine the extent to which *in vivo* anti-tumor CD8$^+$ T cell priming occurred independently of classical cross-presentation in the C1498.SIY model. Here, we utilized *Wdfy4*$^{-/-}$ mice, in which the cross-presentation of cell-derived antigens is defective in cDC1[214]. We generated *Wdfy4*$^{-/-}$ mice by deleting exon 4 using CRISPR/Cas9, resulting in a frameshift and premature stop codon after only 146 amino acids (aa; compared to the 3,184 aa full-length protein; see Materials and Methods for full details, scheme depicted in **Figure 3.12**). Deletion of exon 4 from *Wdfy4* was confirmed by PCR amplification of genomic DNA and subsequent Sanger sequencing (**Figure 3.12B**). Furthermore, cDNA was generated from RNA isolated from *Wdfy4*$^{+/+}$ and *Wdfy4*$^{-/-}$ splenocytes. Regions of the *Wdfy4* transcript were

PCR amplified using four different primer pairs spanning multiple exons, including exon 4. The removal of exon 4 and resulting frameshift mutation were also confirmed by Sanger sequencing, and depicted with the corresponding amino acid sequence from the mutation through the premature stop codon (**Figure 3.12C-E**). Thus, although there is no validated antibody available to measure the murine WDFY4 protein levels, these results indicate that there is no

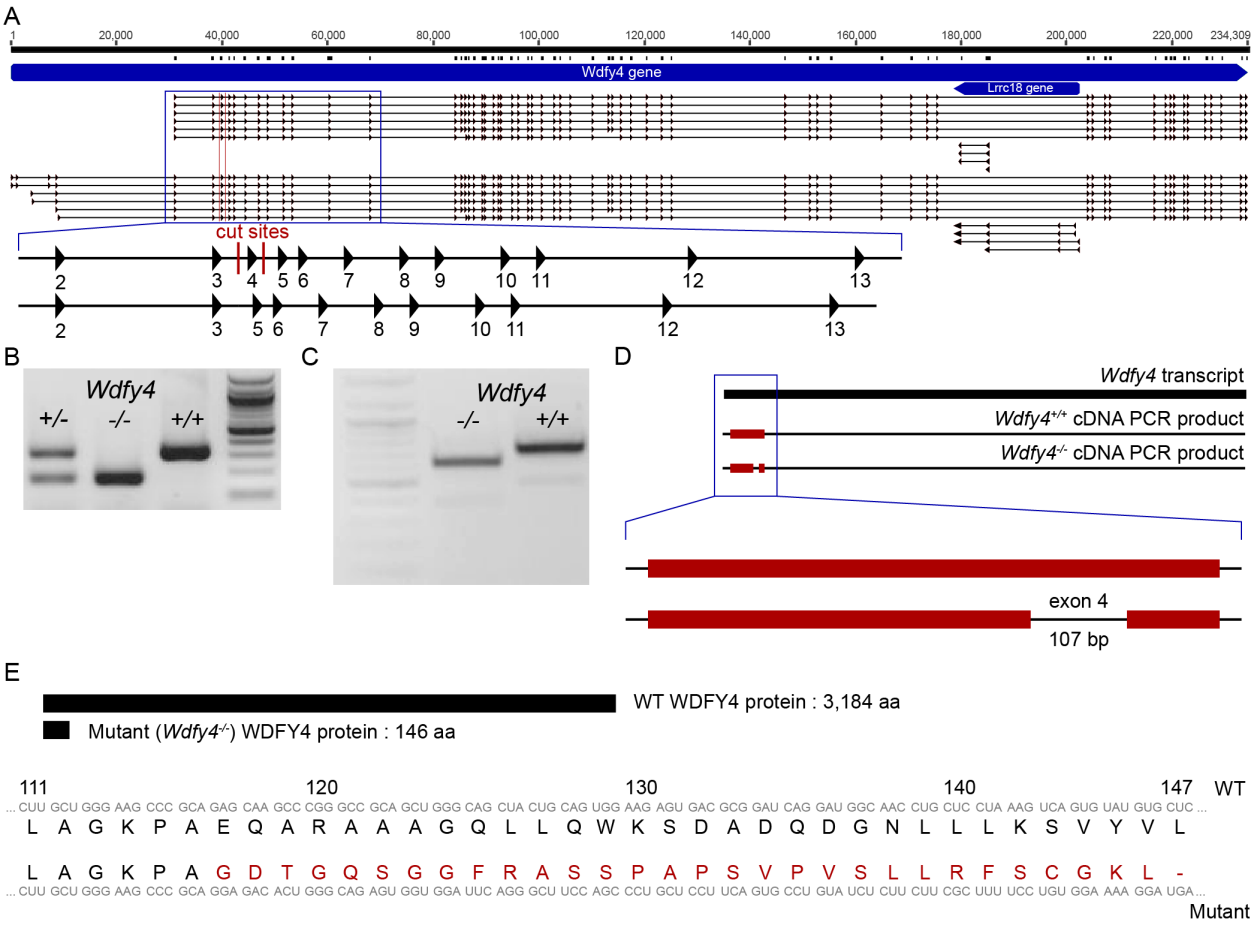

Figure 3.12: Generation of *Wdfy4*$^{-/-}$ mice.
A) Illustration of the *Wdfy4* gene depicting the exons in different splice variants, with gRNA target sites indicated flanking exon 4.
B) PCR amplification of the genomic DNA surrounding exon 4, with a 144 bp excision in the mutant (knockout) allele.
C and D) PCR amplification of a segment of the *Wdfy4* transcript containing exon 4 from *Wdfy4*$^{+/+}$ and *Wdfy4*$^{-/-}$ splenocytes, with a 107 bp deletion in the mutant (knockout) allele. Alignment of the amplified cDNA fragments are shown in red.
E) Illustration showing the length of *Wdfy4* wild type and mutant (knockout) proteins (to scale), along with the RNA (grey) and translated amino acid sequences (wild-type and consensus sequences shown in black and the mutated region depicted in red) in the region containing the frameshift mutation and stop codon.

functional WDFY4 protein in the *Wdfy4*$^{-/-}$ mice.

No defects were observed in T cell numbers in secondary lymphoid organs in *Wdfy4*$^{-/-}$ animals (**Figure 3.13**). Importantly, WDFY4 deficiency did not affect the numbers, proportions, or expression of costimulatory molecules by DC populations in cLNs (**Figure 3.14**), where anti-tumor CD8^{+} T cell responses are mounted against s.c. tumors. Further, DC numbers and phenotype were broadly similar in various organs in *Wdfy4*$^{+/+}$ and *Wdfy4*$^{-/-}$ mice, with the exception of mesenteric LNs, where a reduction in CD103^{+} CD11b^{neg} migratory cDC1 was observed in *Wdfy4*$^{-/-}$ mice (**Figure 3.15**); however, no other significant differences in DC populations were observed.

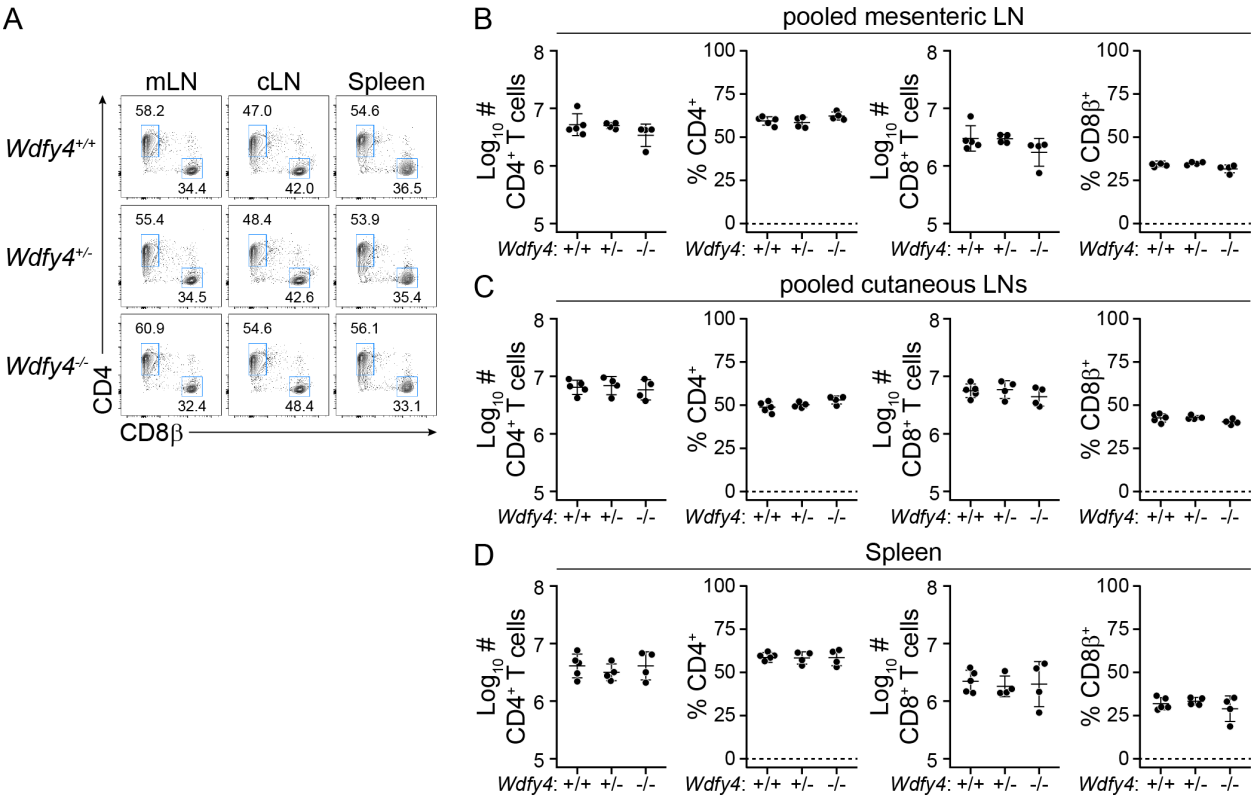

Figure 3.13: Normal T cell populations in secondary lymphoid organs of *Wdfy4*$^{-/-}$ mice.
A) Flow cytometry plots identifying CD4^{+} and CD8^{+} T cells in mesenteric (mLN) and cutaneous (cLN) LNs as well as spleens from *Wdfy4*$^{+/+}$, *Wdfy4*$^{+/-}$, and *Wdfy4*$^{-/-}$ mice.
B-D) Quantification of (A) by number and frequency in the mLNs (B), cLNs (C), and spleen (D).
Statistical significance was determined by one-way ANOVA with post-hoc Tukey's HSD test.

In order to validate our *Wdfy4*$^{-/-}$ mice in a tumor system in which they have a previously described phenotype[214], *Wdfy4*$^{-/-}$ and *Wdfy4*^{WT} littermate mice were inoculated s.c. with 10^6 1969

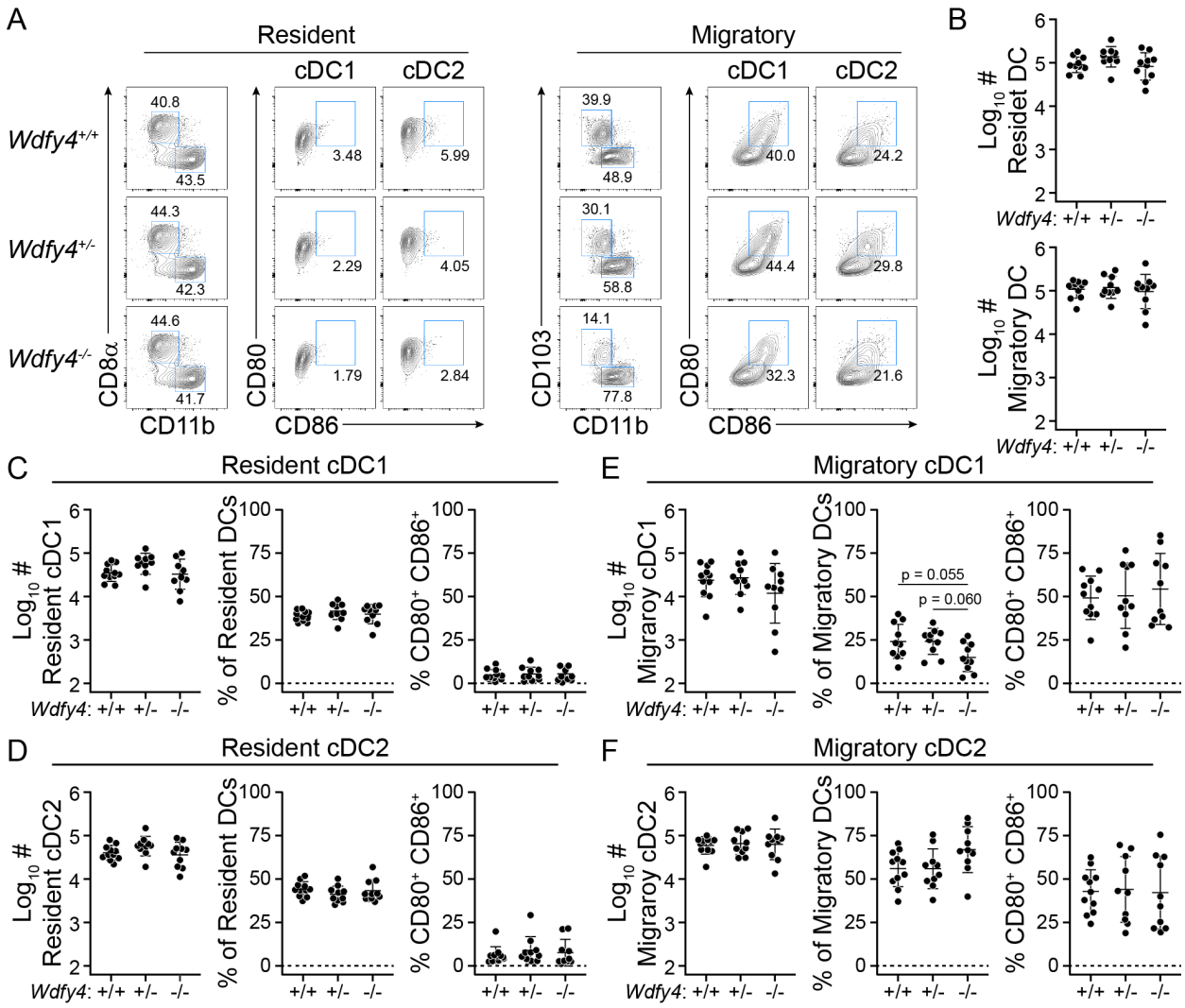

Figure 3.14: Normal cDC development and costimulatory molecule expression in cutaneous LNs of *Wdfy4*$^{-/-}$ mice.

A) Representative flow cytometry plots of cDC populations in pooled cLNs of *Wdfy4*$^{+/+}$, *Wdfy4*$^{+/-}$, and *Wdfy4*$^{-/-}$ mice.

B) Counts of resident and migratory cDCs in pooled cLNs of *Wdfy4*$^{+/+}$, *Wdfy4*$^{+/-}$, and *Wdfy4*$^{-/-}$ mice.

C-F) Quantification of count, frequency, and CD80/CD86 expression data for resident CD8α$^+$ cDC1 (C), resident CD11b$^+$ cDC2 (D), migratory CD103$^+$ cDC1 (E), and migratory CD11b$^+$ cDC2 (F) in pooled cLNs.

Statistical significance was determined by one-way ANOVA with post-hoc Tukey's HSD test, and $p < 0.05$ was considered to be statistically significant. Data are pooled from three independent experiments.

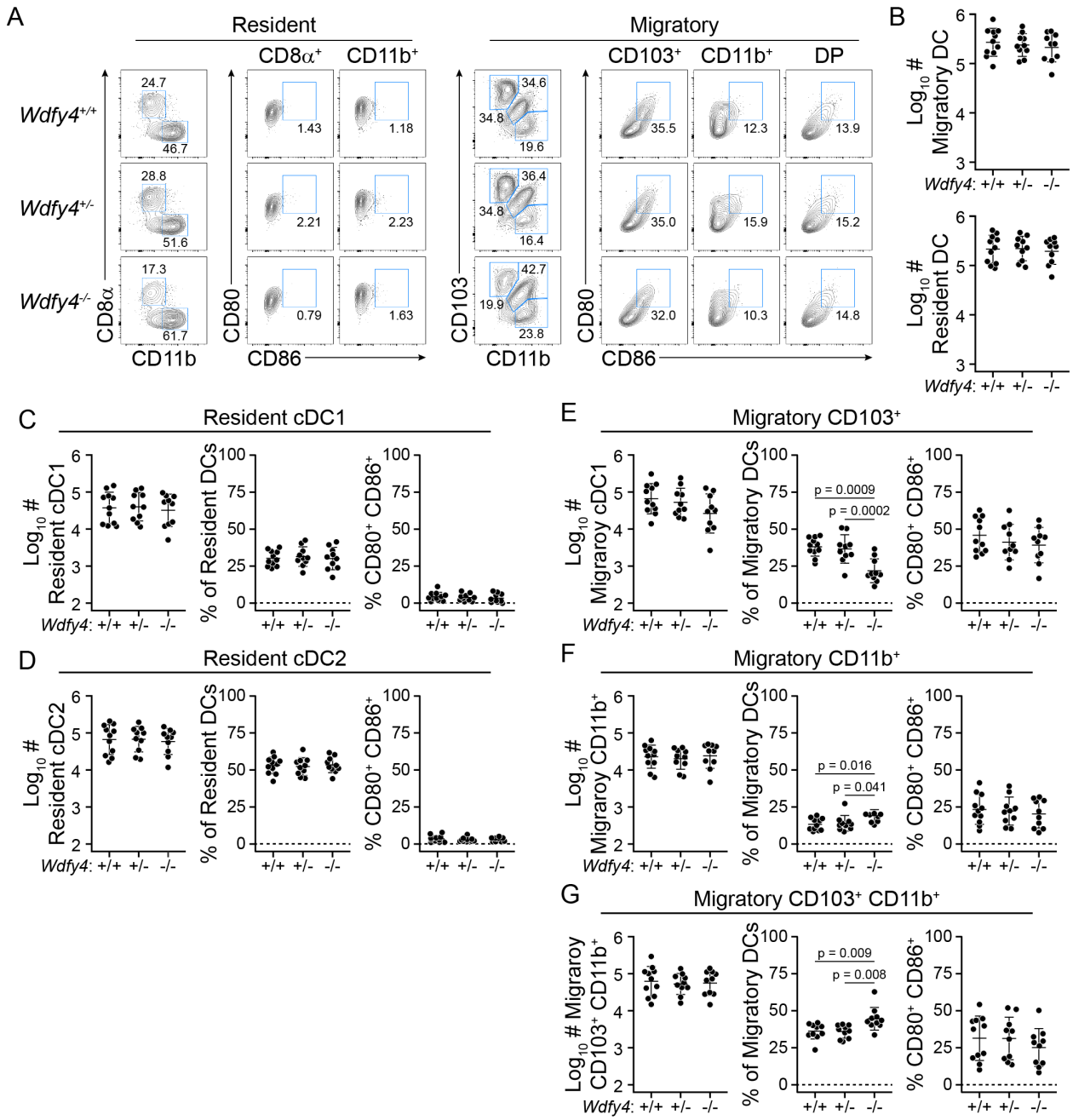

Figure 3.15: Reduced CD103$^+$ cDC1 populations in mesenteric LNs of *Wdfy4*$^{-/-}$ mice.
A) Representative flow cytometry plots of cDC populations in pooled mesenteric LNs (mLNs) of *Wdfy4*$^{+/+}$, *Wdfy4*$^{+/-}$, and *Wdfy4*$^{-/-}$ mice.
B) Counts of resident and migratory cDCs in pooled mLNs of *Wdfy4*$^{+/+}$, *Wdfy4*$^{+/-}$, and *Wdfy4*$^{-/-}$ mice.
C-G) Quantification of count, frequency, and CD80/CD86 expression data for resident CD8α$^+$ cDC1 (C), resident CD11b$^+$ cDC2 (D), migratory CD103$^+$ cDC1 (E), and migratory CD11b$^+$ cDC2 (F), and migratory CD103$^+$ CD11b$^+$ cDC2 in pooled mLNs (G).
Statistical significance was determined by one-way ANOVA with post-hoc Tukey's HSD. Data are pooled from three independent experiments.

sarcoma cells, a tumor which is typically rejected by wild-type mice in a $CD8^+$ T cell-dependent manner[214]. As previously observed[214], 1969 tumors were uniformly rejected by wild-type mice, but grew progressively in *Wdfy4*$^{-/-}$ mice (**Figure 3.16**). In fact, 1969 tumor growth in *Wdfy4*$^{-/-}$ mice tended to be more rapid than in *Batf3*$^{-/-}$ mice which are largely devoid of cDC1 (**Figure 3.16**). This result confirms the requirement for WDFY4-dependent cross-presentation in mounting a productive $CD8^+$ T cell response against 1969 sarcoma, while also highlighting that although MHC-dressing contributes to anti-tumor $CD8^+$ T cell priming in certain systems, there is clearly still a role for classical cross-presentation in this process.

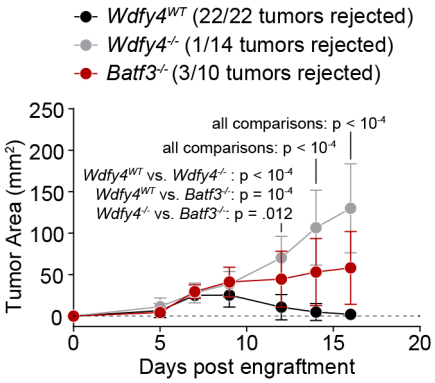

Figure 3.16: *Wdfy4*$^{-/-}$ mice fail to reject an immunogenic tumor. Growth curves of s.c. 1969 tumors in littermate *Wdfy4*^{WT} and *Wdfy4*$^{-/-}$ mice, as well as in *Batf3*$^{-/-}$ mice. Statistical significance was determined by two-way ANOVA with Sidak's post-hoc test for multiple comparisons. Data are depicted as mean ± s.d. and pooled from two independent experiments.

3.3.7 WDFY4-dependent cross-presentation is dispensable for anti-tumor $CD8^+$ T cell priming against C1498.SIY tumors *in vivo*

To test the sufficiency of MHC-dressing in anti-tumor antigen-specific $CD8^+$ T cell priming in mice unable to cross-present cell-associated antigens, CTV-labeled $CD45.1^+$ 2C $CD8^+$ T cells were adoptively transferred into $CD45.2^+$ *Wdfy4*$^{+/+}$, *Wdfy4*$^{+/-}$, and *Wdfy4*$^{-/-}$ mice. One day later, these mice were inoculated s.c. with 10^6 C1498.SIY $K^{b+/+}$ or $K^{b-/-}$ cells. Six days after tumor inoculation, tdLNs were isolated along with analogous cLNs from non-tumor-bearing mice and analyzed for the activation and expansion of 2C $CD8^+$ T cells. As expected, minimal

2C T cell proliferation occurred in non-tumor bearing control mice and in mice bearing C1498.SIY $K^{b-/-}$ tumors, regardless of *Wdfy4* genotype (**Figure 3.17A and B**). For mice bearing C1498.SIY $K^{b+/+}$ tumors, 2C proliferation was robust in tdLNs of both $Wdfy4^{+/+}$ and $Wdfy4^{+/-}$ mice, and only slightly reduced in $Wdfy4^{-/-}$ mice (**Figure 3.17C-F**) with statistical significance reached when analyzing CTV dilution, but not by 2C cell number or frequency. At the same time, 2C $CD8^+$ T cell proliferation was significantly greater in $Wdfy4^{-/-}$ mice bearing C1498.SIY $K^{b+/+}$ tumors than in any mice bearing C1498.SIY $K^{b-/-}$ tumors and in tumor-free control mice by the same measures (**Figure 3.17C-F**), demonstrating that WDFY4-dependent cross-presentation is dispensable for *in vivo* $CD8^+$ T cell priming in response to s.c. C1498.SIY tumors. This result also suggests that classical cross-presentation contributes minimally to overall presentation of tumor-derived SIY by cDC1, or alternatively that WDFY4 plays a role in antigen presentation via MHC-I-dressing by cDC1.

To determine the extent to which WDFY4 might be directly involved in MHC-I-dressing, $Wdfy4^{-/-}$ mice were crossed with $K^{b-/-}D^{b-/-}$ mice. C1498 $K^{b+/+}$ or $K^{b-/-}$ tumors were raised in $Wdfy4^{WT}\,K^{b-/-}D^{b-/-}$ and littermate $Wdfy4^{-/-}\,K^{b-/-}D^{b-/-}$ mice, and the ability of APCs to present C1498-derived K^b molecules was assessed by flow cytometry as in **Figure 3.7**. Both $Wdfy4^{+/+}\,K^{b-/-}D^{b-/-}$ and $Wdfy4^{+/-}\,K^{b-/-}D^{b-/-}$ mice were included in the $Wdfy4^{WT}\,K^{b-/-}D^{b-/-}$ group, as heterozygotes were phenotypically identical to homozygous wild type mice in **Supplemental Figures S10-S12**, and were equally capable of mounting anti-tumor T cell responses in **Figure 3.17**. APCs isolated from $K^{b-/-}D^{b-/-}$ mice harboring C1498 $K^{b+/+}$ tumors were clearly capable of acquiring and presenting C1498-derived K^b molecules regardless of whether or not they expressed WDFY4 (**Figure 3.18**), indicating that MHC-I-dressing is a WDFY4-independent process.

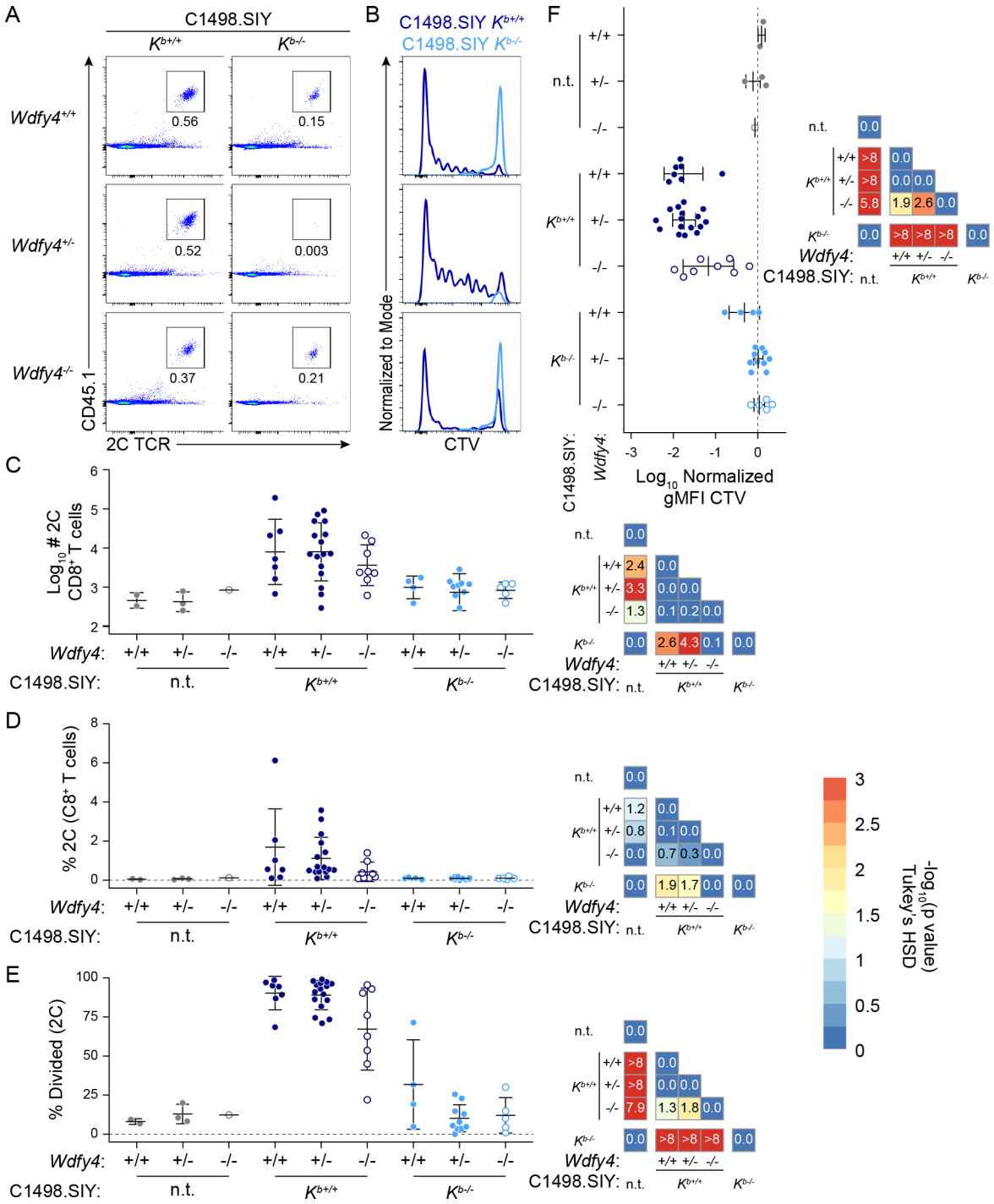

Figure 3.17: *In vivo* TCR-tg 2C CD8$^+$ T cell priming occurs in the tdLN of *Wdfy4*$^{-/-}$ mice bearing C1498.SIY *K*$^{b+/+}$ tumors.

In vivo TCR-tg 2C CD8$^+$ T cell priming was assessed in the tdLN of *Wdfy4*$^{+/+}$, *Wdfy4*$^{+/-}$, and *Wdfy4*$^{-/-}$ mice bearing s.c. C1498.SIY *K*$^{b+/+}$ or *K*$^{b-/-}$ tumors at day 6.

A) Representative flow cytometry plots showing frequency of 2C among CD8$^+$ T cells.

B) Representative histograms of CTV dilution by 2C CD8$^+$ T cells.

C) Summary plot of the number of 2C CD8$^+$ T cells in the tdLN (left) and heatmap depicting the p values for pairwise comparisons (right).

Figure 3.17, continued
D) Summary plot of the frequency of 2C among $CD8^+$ T cells in the tdLN (left) and heatmap depicting the p values for pairwise comparisons.
E) Plot of the percent of 2C $CD8^+$ T cells which had proliferated in the tdLN (left) and heatmap depicting the p values for pairwise comparisons (right).
F) Summary plot of the geometric mean fluorescence intensity of CTV within 2C $CD8^+$ T cells in the tdLN (left) and heatmap depicting the p values for pairwise comparisons (right).
Statistical significance was determined by one-way ANOVA with a Tukey's post-hoc HSD test. The $-\log_{10}$ of the adjusted p value is indicated in each tile of the heatmap. $p < 0.05$ ($-\log_{10}(p) > 1.30$) was considered to be statistically significant. The data are pooled from three independent experiments. n.t. = no tumor.

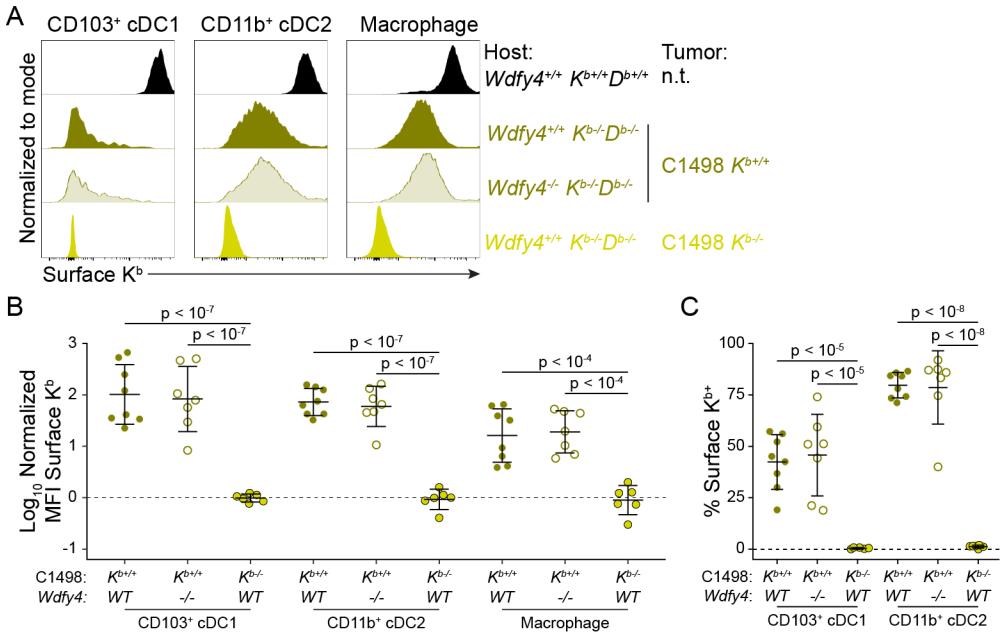

Figure 3.18: MHC-dressing occurs independently of WDFY4.
Wdfy4$^{-/-}$ $K^{b-/-}D^{b-/-}$ and *Wdfy4*^{WT} $K^{b-/-}D^{b-/-}$ mice were inoculated with s.c. C1498 $K^{b+/+}$ or $K^{b-/-}$ tumors. APCs were analyzed for the presence of C1498-derived K^b molecules by surface antibody staining and flow cytometry.
A) Representative flow cytometry histograms.
B) Summary plot of normalized mean fluorescence intensity.
C) Summary plot of percent K^{b+} DCs. The *Wdfy4*^{WT} group includes four *Wdfy4*$^{+/+}$ and four *Wdfy4*$^{+/-}$ mice.
Data are pooled from two independent experiments. Statistical significance was determined by two-way ANOVA with post-hoc Tukey's HSD.

3.3.8 APCs acquire and present HLA-I molecules derived from human cancer cells

The above data indicate that MHC-dressed DCs have a critical, non-redundant role in mediating the activation of tumor antigen-specific $CD8^+$ T cell responses in murine cancer models. Given the obvious challenges associated with investigating transfer of HLA molecules from cancer cells to APCs *in vivo*, in which all cells express the same HLA molecules, we sought to ascertain the extent to which human HLA-I-dressing occurred in the context of *in vitro* assays and xenograft models. First, HLA-A*02^{neg} monocyte-derived macrophages (MDM) from a healthy donor were co-cultured with CTV-labeled HLA-A*02^{pos} $CD19^+$ OCI-Ly8 diffuse large B cell lymphoma cells (**Figure 3.19A**). MDM were utilized due to ease of acquisition and culture, as well as our observation that, like DCs, macrophages acquire and present cancer cell-derived MHC-I molecules in murine tumors (**Figure 3.7**). OCI-Ly8 lymphoma cells were chosen due to their high baseline expression of HLA-I, and because they express HLA-A*02, a common HLA-A allele for which a specific antibody exists. Following a 4-hour co-culture, MDMs failed to acquire detectable OCI-Ly8 cell-derived CTV fluorescence and remained HLA-A*02^{neg}.

Based on data presented in **Figure 3.7**, which suggest that MHC-dressing and phagocytosis of tumor antigens are linked processes, a CD47-blocking antibody (α-CD47) was included in the MDM/OCI-Ly8 culture to induce phagocytosis by blocking CD47-SIRPα interactions. MDMs treated with an isotype control antibody acquired neither lymphoma cell-derived CTV fluorescence nor captured HLA-A*02 molecules from OCI-Ly8 lymphoma cells, while MDMs treated with α-CD47 acquired an abundance of both (**Figure 3.19A**, **top**), and displayed acquired HLA-A*02 on the cell surface. Consistent with our observations in murine models (**Figure 3.7**), MDMs that acquired the most CTV fluorescence also presented the highest levels of OCI-Ly8 cell-derived HLA-A*02 (**Figure 3.19A**). Thus, human APCs are capable of acquiring and presenting HLA molecules derived from human cancer cells. Also notable was the

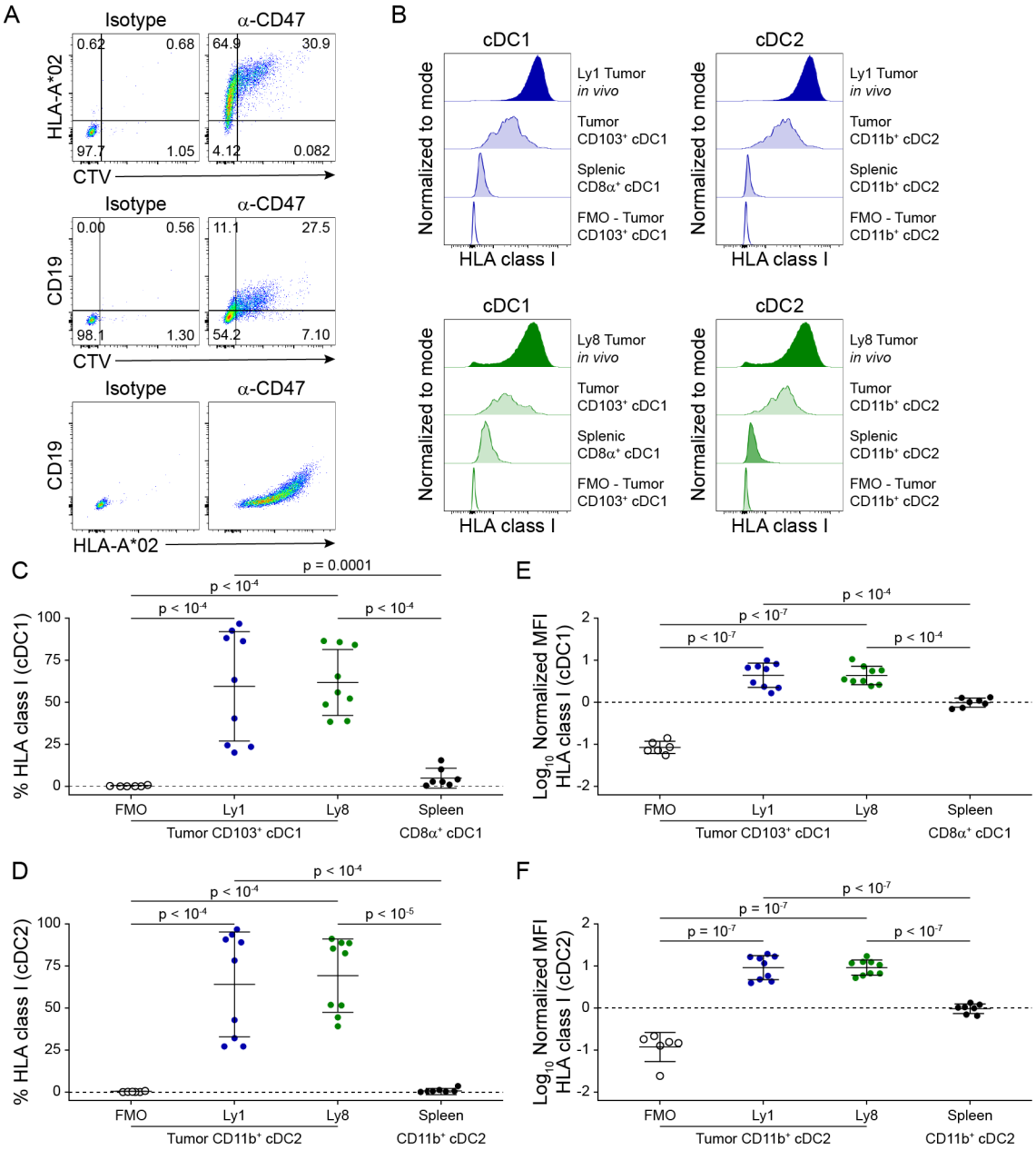

Figure 3.19: APCs are capable of MHC-dressing with human HLA molecules.
A) Monocyte-derived macrophages (MDMs) were differentiated from the blood of a healthy HLA-A*02^{neg} donor and subsequently co-cultured with CTV-labeled HLA-A*02^{+} OCI-Ly8 lymphoma cells for 4 hours *in vitro* with or without an α-CD47 blocking antibody. Representative flow cytometry plots of MDM for acquired OCI-Ly8-derived HLA-A*02 versus CTV (top), CD19 versus CTV (middle), and CD19 versus HLA-A*02 (bottom).
B-F) OCI-Ly1 (blue) and OCI-Ly8 (green) tumors were xenografted s.c. into NOD.*Prkdc*^{scid}*Il2rg*^{null} (NSG) mice. Representative histograms showing cell surface staining for tumor-derived HLA-I molecules on DCs are shown in B. Data are quantified as % HLA class I^{+} among cDC1 (C) and cDC2 (D), as well as normalized MFI of HLA class I for cDC1 (E) and cDC2 (F). Flow cytometry plots in A are from one experiment, representative of three independent experiments.

Figure 3.19, continued
Data in A are from one experiment, representative of three independent experiments. Data in C-F are pooled from two independent experiments, and statistical significance was determined by one-way ANOVA with post-hoc Tukey's HSD test.

fact that the MDM that acquired the highest OCI-Ly8-derived CTV and HLA-A*02 also displayed low levels of lymphoma-derived CD19 on their cell surface (**Figure 3.19A**, **middle and bottom**)**,** suggesting that the ability of a surface protein to transfer from one cell to another is not unique to MHC/HLA molecules, and potentially is a broader phenomenon.

To determine whether HLA molecules from human tumor cells are also transferred to APCs *in vivo*, lymphoma xenograft models were utilized. Here, human OCI-Ly1 and OCI-Ly8 lymphoma cells were inoculated s.c. into immune-deficient NOD.*Prkdc*^{scid}*Il2rg*^{null} (NSG) mice, devoid of B, T, and NK cells. Tumor resident DCs isolated from lymphoma xenografts displayed high levels of lymphoma-derived HLA-I molecules on their cell surface (**Figure 3.19B-F**). Comparatively, HLA-I was not detected on splenic DCs in NSG mice bearing lymphoma xenografts (**Figure 3.19B-F**). Together, these data indicate that *in vivo* MHC/HLA-I-dressing by tumor APCs is conserved in mice and humans.

3.4 Acknowledgments

We would like to thank Drs. T. Gajewski, A. Bendelac, T. Schumacher, and S. Springer for their generosity in sharing mice, cell lines, and constructs which were central to this research. Special thanks to L. Degenstein of the University of Chicago Transgenics/ES Cell Technology Mouse Core Facility for her help with microinjections. Thanks also to Dr. P. Savage for careful review of the manuscript and insightful conversations during the project. The authors have no financial interests to disclose. This work was funded by R01 CA16670 to J.K. and used common resources managed by the University of Chicago Cytometry and Antibody Technology core

facility, which is supported by P30 CA014599 to the University of Chicago Comprehensive Cancer Center. B.W.M., D.S.K., and D.E.K. were supported by the Immunology Training Grant at the University of Chicago (T32 AI007090). B.W.M. was also supported by the Careers in Immunology Fellowship from the American Association of Immunologists.

Chapter 4: Discussion

4.1 Summary

In this study, we have determined that MHC-dressing contributes to anti-tumor $CD8^+$ T cell priming *in vivo* based on four key experimental observations: 1) K^b-restricted tumor antigen-specific $CD8^+$ T cell responses are reduced, and in some cases completely absent, against cancers lacking K^b expression (**Figures 3.2 - 3.4**); 2) APCs acquire cancer cell-derived K^b in the tumor, and this is likely associated with internalization of tumor antigens (**Figures 3.7 - 3.10**); 3) presentation of C1498-derived SIY by migratory $CD103^+$ cDC1 isolated from the tdLN was dependent on K^b expression by the tumor, while DC-intrinsic expression of MHC-I and TAP were dispensable (**Figure 3.11**); 4) *in vivo* 2C T cell priming against C1498.SIY was WDFY4-independent (**Figure 3.17**).

The finding that MHC-I-dressing by migratory $CD103^+$ cDC1 is a critical antigen presentation pathway for mounting anti-tumor $CD8^+$ T cell responses challenges our current understanding of the mechanisms by which cancer antigens are presented by DCs. At the same time, our observations raise a profound, yet simple question: Why does MHC-I-dressing appear to play such an important role in tumor antigen presentation when cross-presentation is the hallmark function of cDC1? Any definitive answer will require significant additional investigation; however, we can say at this time that the contribution of MHC-dressing to antigen presentation varies across antigens and systems. Although our results highlight a key role of MHC-I-dressing in anti-tumor immunity, they certainly do not diminish the importance of classical cross-presentation. For example, whereas MHC-dressing was absolutely required for antigen-specific $CD8^+$ T cell priming against C1498.SIY tumors, both MHC-dressing and classical cross-presentation were operational in the priming of $CD8^+$ T cells in the B16.OVA

model. Although not directly addressed, the fact that immunogenic 1969 regressor tumors grew progressively in *Wdfy4*$^{-/-}$ mice (**Figure 3.15**), coupled with the data indicating that MHC-dressing occurred independently of WDFY4 (**Figure 3.16**), suggests that cross-presentation of 1969 tumor-derived antigens is necessary for immune mediated rejection in this model system. Although MHC-dressing occurred in the C1498 and B16 tumor environments, its subsequent contribution to CD8$^+$ T cell priming in the tdLN differed, opening avenues for future study into questions regarding specific contexts in which MHC-dressing contributes to antigen presentation.

Another recent study by Duong *et al.* likewise found MHC-dressing to be important for tumor antigen presentation in the transplantable MC57 regressor tumor model[343]. In that study, the authors concluded that a population of cDC2 activated by type I IFN signaling mediated anti-tumor CD8$^+$ T cell priming via MHC-dressing. That study differs from ours in a few key aspects. First, the demonstration of MHC-dressing in the tumor by Duong *et al.* involved the engraftment of MC57 tumors—originally derived from C57BL/6 mice (H-2^b)—into Balb/c (H-2^d) hosts. While this models a tumor in theory, it bears more similarity to MHC-mismatched transplantation models, in which MHC-dressing has been studied previously[335,337,341,348,349]—due to the complete mismatch in MHC alleles—than a true tumor, in which cancer cells are syngeneic with the host. In contrast, all experiments in this study were performed with syngeneic tumor models, and the acquisition of MHC-I molecules by APCs was observed using MHC-deficient hosts or tumors expressing eGFP-tagged MHC-I (**Figures 3.7 - 3.11**). Second, we showed that DCs in tdLNs were capable of priming CD8$^+$ T cells via MHC-dressing, while Duong, *et al.* focused exclusively on MHC-dressing by tumor-resident APCs. This distinction is important, because while antigen presentation in the tumor is crucial for sustained T cell immunity, CD8$^+$ T cells must first be activated in the tdLN before they gain the ability to traffic to the tumor[13].

Finally, the two studies identify different APC populations presenting tumor antigens via MHC-dressing. This could be a result of the two studies investigating antigen presentation from different sites. Data presented in **Figures 3.7, 3.10, 3.18, and 3.19** show that both cDC populations and macrophages are all similarly dressed with MHC-I molecules in the tumor. That these cells are capable of presenting tumor antigens via MHC-dressing *in situ* is highly likely. Likewise, Duong *et al.* show that both cDC1 and type I IFN-activated cDC2 isolated from the tumor are capable of presenting tumor antigen via MHC-dressing, despite their focus being on the latter[343]. That our study and that of Duong *et al.* both found that MHC-dressing contributes to tumor antigen presentation, but to different degrees and through distinct APCs further suggests that the relative contribution of MHC-dressing to anti-tumor $CD8^+$ T cell priming is contextual.

4.2 MHC-dressing in antigen presentation

A number of factors likely determine the extent to which MHC-I-dressing occurs, as well as its impact on $CD8^+$ T cell activation. Intuitively, the abundance of donor cell MHC-I must be a decisive factor, as MHC-dressing did not occur in B16.OVA tumors *in vivo* in the absence of MHC-I expression on tumor cells (**Figure 3.10A-C**) — DCs cannot be dressed with non-existent MHC-I molecules. Beyond the tumor context, reports of MHC-dressing have primarily focused on MHC-mismatched transplantation models[341,348] and thymic tolerance[335–337], environments with high levels of MHC expression and abundant cell death, the latter of which has been shown to promote MHC-dressing *in vitro*[342]. We cannot comment on the impact of cell death on MHC-dressing in the tumor based on the experiments performed herein, but tumors are commonly enriched in cells undergoing various forms of cell death. Given that exosomes are a well-characterized source of MHC-I[339,340,348,349], exosome production by the tumor may be another factor that contributes to MHC-I dressing in the tumor environment. However, any requirement

for *in vivo* exosome secretion in MHC-dressing is currently undetermined. Furthermore, redundancies in potential mechanisms of MHC acquisition may obscure the importance of any one source. As described in greater detail in the next section, MHC-dressing appears to be linked with tumor antigen uptake by APCs. If this is the case, and MHC-dressing is a byproduct of antigen uptake, then any mechanism by which a cell inhibits phagocytosis or trogocytosis would likewise diminish MHC-dressing. One example could be the upregulation of "don't eat me" signals that facilitate the evasion of phagocytosis by tumor cells, such as CD47. The inverse of this scenario is demonstrated in **Figure 3.19A**, in which we showed that blockade of CD47/SIRP-α interactions resulted in both enhanced internalization of OCI-Ly8 lymphoma cell antigens and HLA-dressing by MDMs *in vitro*.

It is also possible that the nature of the antigen itself is an important factor in determining whether its presentation occurs primarily through MHC-dressing or classical cross-presentation. Immune cells express unique proteases compared to non-immune cells, and expression of different proteasomal subunits leads to the generation of distinct peptidomes presented on MHC molecules by different cell types[40]. It is therefore possible that certain peptide antigens displayed on MHC-I in a tumor cell are not efficiently generated in professional APCs. While this may be the case, specific antigens presented exclusively through MHC-dressing have yet to be identified in syngeneic models. This explanation also does not account for the fact that both SIY and SIINFEKL antigens can be presented by DCs through cross-presentation[214,365], despite the demonstrated importance of MHC-dressing for their presentation in the tumor context. For a majority of antigens, a more likely explanation is that MHC-dressing simply increases the density and overall number of MHC-I molecules loaded with donor cell-derived peptide antigens. Thus, the contribution of MHC-dressing to antigen presentation would be the result of the quantity, rather than the quality, of antigens presented in this manner. Resolving this issue

could reveal key insights for the identification of neo-antigens in patients, as the preferred mechanism of antigen presentation for a given peptide could be a confounding factor in current prediction algorithms.

Given the varied nature of the models in which MHC-dressing has been implicated in antigen presentation, a particularly appealing hypothesis is that MHC-I-dressing is a default mechanism by which DCs present the antigens acquired in tissues. Direct transfer of pMHC-I molecules from surrounding cells through phagocytosis, trogocytosis, or exosome capture represents a rich source of intact pMHC-I, all of which would contain a peptide that is necessarily generated from a donor cell-derived protein. We envisage that MHC-I-dressing occurs constitutively and silently under steady-state conditions, unobserved because all host cells express the same MHC-I molecules. Importantly, the occurrence of MHC-dressing would not preclude classical cross-presentation functioning as the dominant antigen presentation pathway in response to external stimuli, such as the detection of necrotic cell death via DNGR-1[223,225–227] or pathogen-associated molecular patterns via TLRs[366]—both of which would generate a bias toward classical cross-presentation necessitated by the release of cellular antigens into the extracellular matrix upon lytic or necrotic cell death, or the need to present pathogen-derived antigens. Again, here we can only speculate that the contributions of MHC-dressing and cross-presentation to overall presentation of a given antigen are a matter of degrees, and that MHC-dressing is dependent on the density of pMHC molecules present on the donor cell surface.

4.3 Stochastic recycling as a proposed mechanism for MHC-dressing

The mechanism by which MHC-dressing occurs is still disputed. Super-physiological concentrations of purified exosomes are a sufficient source of MHC-I complexes to facilitate MHC-dressing *in vivo*[340,348,350]. Conversely, *in vitro* experiments have demonstrated that MHC-

dressing requires direct cell-cell contact[256,341,344], leading to speculation that MHC-dressing requires trogocytosis or contact-mediated transfer of synaptic vesicles. It is possible that the mechanism by which MHC-dressing occurs is context dependent, especially *in vivo*, where there are many more variables than in simple *in vitro* co-culture experiments. Our data strongly suggest that MHC-dressing is linked with tumor antigen uptake; this association between MHC-dressing and acquisition of donor cell-derived fluorescent proteins is not without precedent[256,335]. We hypothesize that APCs internalize exogenous pMHC-I complexes, and that these complexes are subsequently recycled to the plasma membrane from an endosome via the endogenous MHC-I recycling pathway (**Figure 4.1**). This mechanism would account for the observed correlation between MHC-dressing and tumor antigen uptake, as MHC-dressing would be a useful byproduct of the DC's habitual sampling of its surroundings. Indeed, should a DC internalize tumor cargo which maintained its original membrane topology, subsequent membrane fusion between this cargo and the endosome containing it would result in exposure of the cytoplasmic face of acquired MHC-I molecules to its trafficking chaperones, as well as the release of antigenic proteins to the cytoplasm, simultaneously promoting antigen presentation through both MHC-dressing and canonical cross-presentation (**Figure 4.1**). Unless acquired MHC-I molecules were routinely ubiquitinated[295], there is no reason they would not be presented by an APC after export to the plasma membrane from an early/recycling endosome; APCs are capable of MHC-I recycling[296,367,368] and are likely not able to discriminate between endogenous and exogenous MHC-I molecules. Our data and this proposed model neither discriminate between receptor-mediated endocytosis, phagocytosis, and trogocytosis as the mechanism of MHC-dressing, nor discount extracellular vesicles as a source of tumor antigens, be they intact pMHC-I complexes or whole proteins.

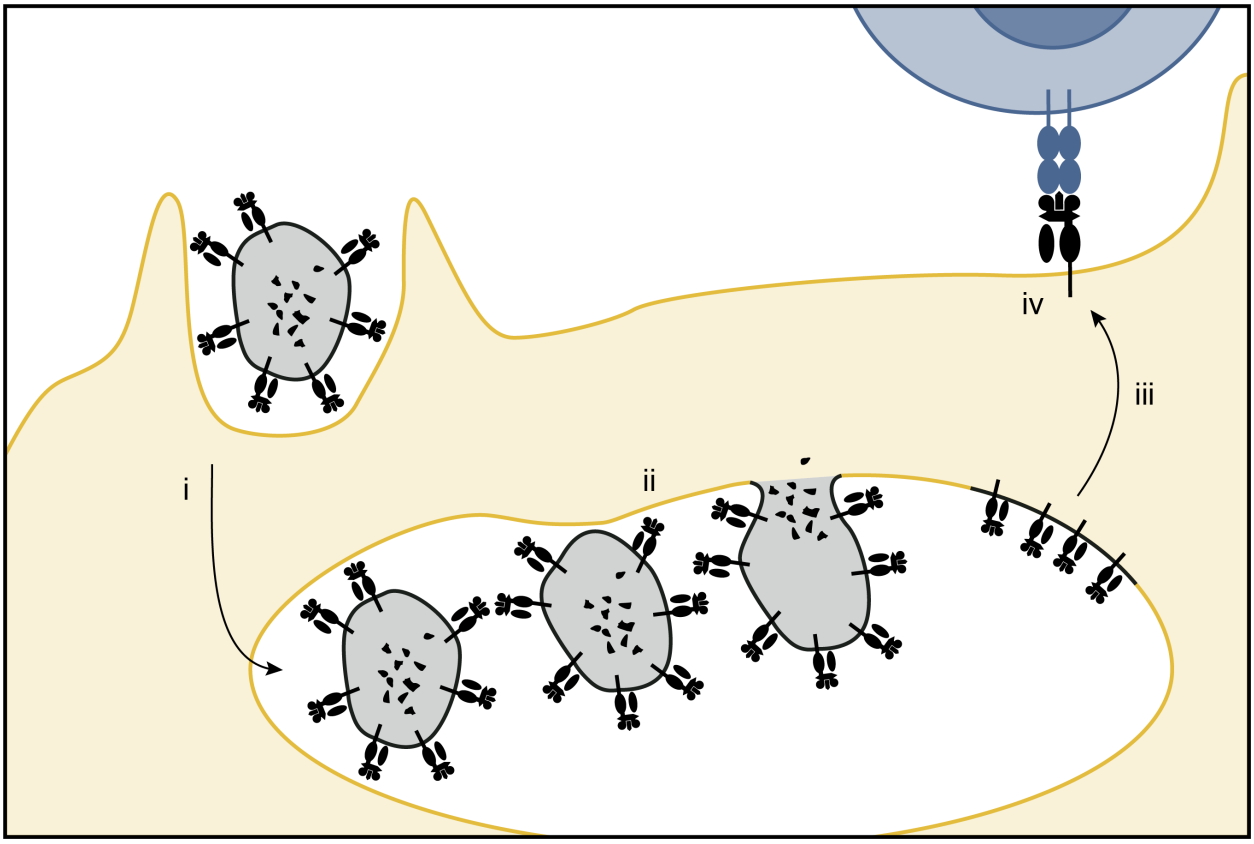

Figure 4.1: Endosomal recycling as a potential mechanism of MHC-I-dressing. Proposed mechanism of MHC-dressing. i) DCs first acquire tumor cargo (or cargo from any donor cell) containing pMHC-I complexes; ii) membrane fusion in an endosome releases the contents of the internalized cargo into the cytoplasm while incorporating membrane-bound proteins into the endosomal membrane with their original topology preserved; iii) pMHC-I molecules traffic to the plasma membrane of the DC via the endogenous MHC-I recycling pathway; iv) acquired pMHC-I molecules are displayed to $CD8^+$ T cells.

If MHC-dressing results from stochastic recycling of MHC-I acquired during antigen uptake, defining one mechanism or cell surface receptor as the master regulator of MHC-dressing seems unlikely. Here, cross-presentation may serve as a useful precedent. The specific endocytic/phagocytic receptor involved in antigen uptake determines the destination of internalized antigen and its propensity for cross-presentation[208,210]. However, there is no one endocytic receptor specific for cross-presentation; internalization through DEC-205[207,210,369], Dectin-1[211], Fcγ receptors[212], and DC-SIGN[370]—to name a few—have all been shown to facilitate cross-presentation. The commonality is that when these receptors promote cross-presentation,

their cargo is generally delivered to an endosome that is not especially proteolytic[206,371]. Even among these receptors, the ultimate destination of the internalized cargo can vary; despite their ability to promote cross-presentation, DEC-205[215] and DC-SIGN[372] have also been shown to direct cargo to lysosomes. Additionally, the functional importance of DNGR-1, another receptor which promotes cross-presentation, appears to be in its ability to facilitate phagosomal rupture and exposure of antigens to the proteasome, rather than being strictly limited to endocytosis[227]. Furthermore, DNGR-1 is not strictly required for cross-presentation[202]. In our model, any endocytic/phagocytic receptor could theoretically promote MHC-dressing, so long as it directs its cargo to an endosome from which MHC-I can be recycled.

Due to the expression of a wide array of endocytic/phagocytic receptors by APCs, the loss of any one receptor is unlikely to eliminate MHC-dressing in all circumstances. However, it is possible that certain receptors will be important for MHC-dressing in a situational basis. For instance, CD36 has been shown to contribute to MHC-dressing *in vitro* and is required for internalization of mTEC-derived fluorescent antigen by cDC1 in the thymus. Moreover, interruption of SIRP-α/CD47 signaling was required for *in vitro* HLA-dressing by MDMs in **Figure 3.19**, but this receptor/ligand interaction cannot regulate *in vivo* MHC-dressing by cDC1, which do not express SIRP-α. To again use cross-presentation as an example, the intrinsic ability of individual receptors to facilitate cross-presentation of internalized antigens has largely been determined through gain-of-function experiments. Ectopic expression of DEC-205[210], Dectin-1[211], and FcγRIIA[212] conferred cross-presentation ability onto cells which were otherwise incapable. Similar gain-of-function experiments could be useful in identifying receptors that can promote MHC-dressing by cell lines such as HEK-293 *in vitro*.

A related conundrum from our work stems from the finding that migratory $CD103^+$ cDC1 were exclusively able to prime anti-tumor $CD8^+$ T cell responses via MHC-dressing despite all

APC subsets being equivalently dressed with MHC-I molecules in the tumor. In contrast, Duong *et al.* found that cDC2 activated by type I IFN signaling in the tumor were capable of presenting tumor antigens via MHC-dressing[343]. This discrepancy may result from the two studies relying on DCs from different sites, the tumor versus the tdLN. As the focus of this study was on anti-tumor $CD8^+$ T cell priming, antigen presentation capacity was assessed by DCs isolated from the tdLN. It is possible that cDC2 are also capable of presenting tumor antigens by MHC-dressing in the tumor models we employed, but not in the tdLN, due to differences in migration or ability to effectively transport intact pMHC-I molecules to the tdLN for presentation. This explanation would be consistent with studies from the laboratory of Max Krummel, which demonstrated that all myeloid cells in the tumor internalize tumor antigens, and both tumor-resident cDC1 and, to a lesser extent, cDC2 can prime $CD8^+$ T cells *ex vivo*[253]. Despite this, only migratory $CD103^+$ cDC1 transport tumor antigens to the tdLN, and this cDC population are the most potent mediators of $CD8^+$ T cell activation by a wide margin[254,256]. Another distinction between our study and that of Duong *et al.* is that the tumor model used in their study, MC57, is typically rejected in wild-type hosts, while our two modes, C1498 and B16-F10, grow progressively. The activation of cDC2 by type I IFN was required for their ability to present antigens via MHC-dressing in that study, and their presence in MC57 tumors was proposed as the primary reason why those tumors are rejected[343]. It could be the case that we observed no $CD8^+$ T cell priming by cDC2 in the tdLN because this type I IFN-stimulated cDC2 population is unique to MC57 tumors and may not exist in tumors that fail to be spontaneously rejected.

Another possible answer for why only migratory $CD103^+$ cDC1 present tumor antigens through MHC-dressing in the tdLN despite all APCs being MHC-dressed in the tumor may be inferred from the underlying cell biology and principal functions of DC subsets. For instance, while most APCs generate an acidic endosomal pH to promote elimination of pathogens and

efficient generation of peptides for loading onto MHC-II, cDC1 actively maintain a neutral to alkaline endosomal pH, which is conducive to the partial protection of intact antigens for subsequent export to the cytoplasm for proteasomal degradation and eventual display via classical cross-presentation[219,222,227,312,314]. This fundamental property of cDC1 may also promote antigen presentation via MHC-dressing by increasing the likelihood that the donor pMHC-I molecule is recycled to the cell surface intact, as pMHC-I complexes are often unstable under acidic conditions[373,374]. This theory also fits well with the reported role of migratory $CD103^+$ cDC1 in transporting intact, pH-sensitive antigenic proteins acquired in the tumor environment back to the tdLN[255,256]. Indeed, migratory $CD103^+$ cDC1 are capable of transferring both intact tumor-derived fluorescent antigens, as well as MHC-I complexes, to other APC subsets in the tdLN[256]. While this seems to be the most logical explanation, more work must be done to fully elucidate the cDC1-intrinsic mechanism of antigen presentation via MHC-I-dressing.

4.4 MHC-dressing in human cancer

Finally, the role of MHC-I-dressing in human cancers must be addressed. Data presented in **Figure 3.19**, as well as published observations of others[338], demonstrate that APCs are capable of presenting exogenous human HLA molecules. However, the significance of this finding in regard to the subsequent activation of anti-tumor T cell responses in cancer patients remains unknown. For all the same reasons that studying MHC-I-dressing in syngeneic mouse models has been difficult, directly investigating this process in cancer patients is extremely challenging, especially when compounded with other known limitations of human immunology studies. A human tumor and its infiltrating immune cells always express identical HLA molecules, with the exception of HLA-mismatched bone marrow transplantation, which might represent one human cancer context in which MHC-dressing could be explored in the future.

One piece of circumstantial evidence suggesting a role for MHC-dressing in tumor antigen presentation is the existence of tumors which have down-regulated HLA-I presentation despite having no detectable $CD8^+$ T cell response[375–378]. While mutations in the HLA-I presentation pathway are typically considered to be a mechanism of immune evasion in response to $CD8^+$ T cell-mediated cytolysis[379], in these instances they might have inadvertently preempted a $CD8^+$ T cell response by eliminating MHC-dressing in the absence of any selective pressure. Unfortunately, due to the limitations described above, we cannot know whether HLA down-regulation in the absence of a $CD8^+$ T cell response is a mere passenger, one of many potential factors being controlled by a driver mutation[378], or a silhouette of MHC-dressing, whose importance is illuminated only in its absence.

4.5 Conclusions and limitations of the study

In conclusion, we have found that cDC1 utilize acquired cancer cell-derived pMHC-I molecules to prime anti-tumor $CD8^+$ T cell responses, even when classical cross-presentation is fully intact, and that MHC-dressing is associated with tumor antigen uptake. These unexpected observations challenge the current dogma and raise new questions about the mechanisms required to initiate anti-tumor $CD8^+$ T cell priming. Future studies are necessary to gain a complete understanding of the processes through which MHC-dressing occurs and how this impacts antigen presentation and adaptive immune responses, both in cancer and in other contexts.

One potential limitation of our results is the reliance on transplantable tumors and model antigens. It is possible that the impact of MHC-I dressing on anti-tumor $CD8^+$ T cell priming is over-estimated when analyzing responses against immunodominant antigens, such as SIY and SIINFEKL. SIY, in particular, has been found to not be representative of all tumor antigens in

disseminated leukemia[380]. MHC-I-dressing and its effect on antigen-specific $CD8^+$ T cell activation will need to be examined in more physiological models in future studies; however, the nature of the questions addressed in the current study necessitated the use of these models. Future studies will also be able to make use of β2m conditional knockout mice[381] to assess the role of MHC-I expression by APCs *in vivo*, rather than relying exclusively on *ex vivo* priming experiments.

References

1. Cooper, M. D. & Alder, M. N. The evolution of adaptive immune systems. *Cell* **124**, 815–822 (2006).

2. Horvath, P. & Barrangou, R. CRISPR/Cas, the immune system of bacteria and archaea. *Science.* **327**, 167–170 (2010).

3. Katiyar-Agarwal, S. & Jin, H. Role of small RNAs in host-microbe interactions. *Annu. Rev. Phytopathol.* **48**, 225–246 (2010).

4. Uehling, J., Deveau, A. & Paoletti, M. Do fungi have an innate immune response? An NLR-based comparison to plant and animal immune systems. *PLoS Pathog.* **13**, e1006578 (2017).

5. Janeway, C. A. J. & Medzhitov, R. Innate immune recognition. *Annu. Rev. Immunol.* **20**, 197–216 (2002).

6. Matzinger, P. The danger model: a renewed sense of self. *Science* **296**, 301–305 (2002).

7. Victora, G. D. & Nussenzweig, M. C. Germinal Centers. *Annu. Rev. Immunol.* **30**, 429–457 (2012).

8. Pancer, Z. & Cooper, M. D. The Evolution of Adaptive Immunity. (2006) doi:10.1146/annurev.immunol.24.021605.090542.

9. Kayama, H., Okumura, R. & Takeda, K. Interaction Between the Microbiota, Epithelia, and Immune Cells in the Intestine. *Annu. Rev. Immunol.* **38**, 23–48 (2020).

10. Chu, C., Artis, D. & Chiu, I. M. Neuro-immune Interactions in the Tissues. *Immunity* **52**, 464–474 (2020).

11. Ruterbusch, M., Pruner, K. B., Shehata, L. & Pepper, M. In Vivo CD4+ T Cell Differentiation and Function: Revisiting the Th1/Th2 Paradigm. *Annu. Rev. Immunol.* **38**, 705–725 (2020).

12. Campbell, C. & Rudensky, A. Roles of Regulatory T Cells in Tissue Pathophysiology and Metabolism. *Cell Metab.* **31**, 18–25 (2020).

13. Williams, M. A. & Bevan, M. J. Effector and Memory CTL Differentiation. *Annu. Rev. Immunol.* **25**, 171–192 (2007).

14. Cabeza-Cabrerizo, M., Cardoso, A., Minutti, C. M., Pereira da Costa, M. & Reis e Sousa, C. Dendritic Cells Revisited. *Annu. Rev. Immunol.* **39**, 131–166 (2021).

15. Worbs, T., Hammerschmidt, S. I. & Förster, R. Dendritic cell migration in health and disease. *Nat. Rev. Immunol.* **17**, 30–48 (2017).

16. Guermonprez, P., Valladeau, J., Zitvogel, L., Théry, C. & Amigorena, S. Antigen Presentation and T Cell Stimulation by Dendritic Cells. *Annu. Rev. Immunol.* **20**, 621–667 (2002).

17. Hilligan, K. L. & Ronchese, F. Antigen presentation by dendritic cells and their instruction of CD4+ T helper cell responses. *Cell. Mol. Immunol.* **17**, 587–599 (2020).

18. Burnet, F. M. *The clonal selection theory of acquired immunity*. (Vanderbilt University Press, 1959).

19. Bossen, C., Mansson, R. & Murre, C. Chromatin topology and the regulation of antigen receptor assembly. *Annu. Rev. Immunol.* **30**, 337–356 (2012).

20. Wucherpfennig, K. W. T cell receptor crossreactivity as a general property of T cell recognition. *Mol. Immunol.* **40**, 1009–1017 (2004).

21. Josefowicz, S. Z., Lu, L.-F. F. & Rudensky, A. Y. Regulatory T Cells: Mechanisms of Differentiation and Function. *Annu. Rev. Immunol.* **30**, 531–564 (2012).

22. Davis, M. M. & Bjorkman, P. J. T-cell antigen receptor genes and T-cell recognition. *Nature* **334**, 395–402 (1988).

23. Bradley, P. & Thomas, P. G. Using T Cell Receptor Repertoires to Understand the Principles of Adaptive Immune Recognition. *Annu. Rev. Immunol.* **37**, 547–570 (2019).

24. Fugmann, S. D., Lee, A. I., Shockett, P. E., Villey, I. J. & Schatz, D. G. The RAG Proteins and V(D)J Recombination: Complexes, Ends, and Transposition. *Annu. Rev. Immunol.* **18**, 495–527 (2000).

25. Schatz, D. G., Oettinger, M. A. & Baltimore, D. The V(D)J recombination activating gene, RAG-1. *Cell* **59**, 1035–1048 (1989).

26. Oettinger, M. A., Schatz, D. G., Gorka, C. & Baltimore, D. RAG-1 and RAG-2, adjacent genes that synergistically activate V(D)J recombination. *Science.* **248**, 1517–1523 (1990).

27. Zhou, L. *et al.* Transposition of hAT elements links transposable elements and V(D)J recombination. *Nature* **432**, 995–1001 (2004).

28. Fugmann, S. D., Messier, C., Novack, L. A., Cameron, R. A. & Rast, J. P. An ancient evolutionary origin of the Rag1/2 gene locus. *Proc. Natl. Acad. Sci. U. S. A.* **103**, 3728–3733 (2006).

29. Sakano, H., Huppi, K., Heinrich, G. & Tonegawa, S. Sequences at the somatic recombination sites of immunoglobulin light-chain genes. *Nature* **280**, 288–294 (1979).

30. Schatz, D. G. Antigen receptor genes and the evolution of a recombinase. *Semin. Immunol.* **16**, 245–256 (2004).

31. Fujimoto, S. & Yamagishi, H. Isolation of an excision product of T-cell receptor α-chain gene rearrangments. *Nature* **327**, 242–243 (1987).

32. McCormack, W. T. *et al.* Chicken IgL gene rearrangement involves deletion of a circular episome and addition of single nonrandom nucleotides to both coding segments. *Cell* **56**, 785–791 (1989).

33. Lafaille, J. J., DeCloux, A., Bonneville, M., Takagaki, Y. & Tonegawa, S. Junctional sequences of T cell receptor gamma delta genes: implications for gamma delta T cell lineages and for a novel intermediate of V-(D)-J joining. *Cell* **59**, 859–870 (1989).

34. Desiderio, S. V *et al.* Insertion of N regions into heavy-chain genes is correlated with expression of terminal deoxytransferase in B cells. *Nature* **311**, 752–755 (1984).

35. Komori, T., Okada, A., Stewart, V. & Alt, F. W. Lack of N regions in antigen receptor variable region genes of TdT-deficient lymphocytes. *Science.* **261**, 1171–1175 (1993).

36. Gilfillan, S., Dierich, A., Lemeur, M., Benoist, C. & Mathis, D. Mice lacking TdT: mature animals with an immature lymphocyte repertoire. *Science.* **261**, 1175–1178 (1993).

37. Schatz, D. G. & Ji, Y. Recombination centres and the orchestration of V(D)J recombination. *Nat. Rev. Immunol.* **11**, 251–263 (2011).

38. Starr, T. K., Jameson, S. C. & Hogquist, K. A. Positive and negative selection of T cells. *Annu. Rev. Immunol.* **21**, 139–176 (2003).

39. Rothenberg, E. V. Transcriptional control of early T and B cell developmental choices. *Annu. Rev. Immunol.* **32**, 283–321 (2014).

40. Murata, S., Takahama, Y., Kasahara, M. & Tanaka, K. The immunoproteasome and thymoproteasome: functions, evolution and human disease. *Nat. Immunol.* **19**, 923–931 (2018).

41. Singer, A., Adoro, S. & Park, J.-H. Lineage fate and intense debate: myths, models and mechanisms of CD4- versus CD8-lineage choice. *Nat. Rev. Immunol.* **8**, 788–801 (2008).

42. McDonald, B. D., Bunker, J. J., Erickson, S. A., Oh-Hora, M. & Bendelac, A. Crossreactive αβ T Cell Receptors Are the Predominant Targets of Thymocyte Negative Selection. *Immunity* **43**, 859–869 (2015).

43. Hogquist, K. A. & Jameson, S. C. The self-obsession of T cells: how TCR signaling thresholds affect fate 'decisions' and effector function. *Nat. Immunol.* **15**, 815–23 (2014).

44. Savage, P. A., Klawon, D. E. J. & Miller, C. H. Regulatory T Cell Development. *Annu. Rev. Immunol.* **38**, 421–453 (2020).

45. Xiong, N. & Raulet, D. H. Development and selection of gammadelta T cells. *Immunol.*

Rev. **215**, 15–31 (2007).

46. Arstila, T. P. *et al.* A Direct Estimate of the Human αβ T Cell Receptor Diversity. *Science.* **286**, 958 LP – 961 (1999).

47. Qi, Q. *et al.* Diversity and clonal selection in the human T-cell repertoire. *Proc. Natl. Acad. Sci.* **111**, 13139 LP – 13144 (2014).

48. Cyster, J. G. Chemokines, Sphingosine-1-Phosphate, and Cell Migration in Secondary Lymphoid Organs. *Annu. Rev. Immunol.* **23**, 127–159 (2005).

49. Förster, R. *et al.* CCR7 coordinates the primary immune response by establishing functional microenvironments in secondary lymphoid organs. *Cell* **99**, 23–33 (1999).

50. Mempel, T. R., Henrickson, S. E. & Von Andrian, U. H. T-cell priming by dendritic cells in lymph nodes occurs in three distinct phases. *Nature* **427**, 154–159 (2004).

51. Miller, M. J., Hejazi, A. S., Wei, S. H., Cahalan, M. D. & Parker, I. T cell repertoire scanning is promoted by dynamic dendritic cell behavior and random T cell motility in the lymph node. *Proc. Natl. Acad. Sci. U. S. A.* **101**, 998 LP – 1003 (2004).

52. Bousso, P. & Robey, E. Dynamics of CD8+ T cell priming by dendritic cells in intact lymph nodes. *Nat. Immunol.* **4**, 579–585 (2003).

53. Garcia, K. C. & Adams, E. J. How the T cell receptor sees antigen--a structural view. *Cell* **122**, 333–336 (2005).

54. Martin, P. J. *et al.* A 44 kilodalton cell surface homodimer regulates interleukin 2 production by activated human T lymphocytes. *J. Immunol.* **136**, 3282 LP – 3287 (1986).

55. Weiss, A., Manger, B. & Imboden, J. Synergy between the T3/antigen receptor complex and Tp44 in the activation of human T cells. *J. Immunol.* **137**, 819 LP – 825 (1986).

56. June, C. H., Ledbetter, J. A., Gillespie, M. M., Lindsten, T. & Thompson, C. B. T-cell proliferation involving the CD28 pathway is associated with cyclosporine-resistant interleukin 2 gene expression. *Mol. Cell. Biol.* **7**, 4472–4481 (1987).

57. Harding, F. A., McArthur, J. G., Gross, J. A., Raulet, D. H. & Allison, J. P. CD28-mediated signalling co-stimulates murine T cells and prevents induction of anergy in T-cell clones. *Nature* **356**, 607–609 (1992).

58. Freeman, G. J. *et al.* Engagement of the PD-1 immunoinhibitory receptor by a novel B7 family member leads to negative regulation of lymphocyte activation. *J. Exp. Med.* **192**, 1027–1034 (2000).

59. Okazaki, T., Chikuma, S., Iwai, Y., Fagarasan, S. & Honjo, T. A rheostat for immune responses: the unique properties of PD-1 and their advantages for clinical application.

Nat. Immunol. **14**, 1212–1218 (2013).

60. Lenschow, D. J. *et al.* Long-term survival of xenogeneic pancreatic islet grafts induced by CTLA4lg. *Science.* **257**, 789–792 (1992).

61. Azuma, M. *et al.* B70 antigen is a second ligand for CTLA-4 and CD28. *Nature* **366**, 76–79 (1993).

62. Freeman, G. J. *et al.* Cloning of B7-2: a CTLA-4 counter-receptor that costimulates human T cell proliferation. *Science.* **262**, 909–911 (1993).

63. Shiow, L. R. *et al.* CD69 acts downstream of interferon-alpha/beta to inhibit S1P1 and lymphocyte egress from lymphoid organs. *Nature* **440**, 540–544 (2006).

64. Bankovich, A. J., Shiow, L. R. & Cyster, J. G. CD69 suppresses sphingosine 1-phosophate receptor-1 (S1P1) function through interaction with membrane helix 4. *J. Biol. Chem.* **285**, 22328–22337 (2010).

65. Voskoboinik, I., Whisstock, J. C. & Trapani, J. A. Perforin and granzymes: function, dysfunction and human pathology. *Nat. Rev. Immunol.* **15**, 388–400 (2015).

66. Sutton, V. R. & Trapani, J. A. Proteases in lymphocyte killer function: redundancy, polymorphism and questions remaining. *Biol. Chem.* **391**, 873–879 (2010).

67. Gough, P. & Myles, I. A. Tumor Necrosis Factor Receptors: Pleiotropic Signaling Complexes and Their Differential Effects. *Front. Immunol.* **11**, 585880 (2020).

68. Hu, X. & Ivashkiv, L. B. Cross-regulation of Signaling Pathways by Interferon-γ: Implications for Immune Responses and Autoimmune Diseases. *Immunity* **31**, 539–550 (2009).

69. Schreiber, R. D., Lloyd, J. O. & Smyth, M. J. Cancer Immunoediting: Integrating Immunity's Roles in Cancer Suppression and Promotion. *Science.* **331**, 1565–1570 (2011).

70. Ehrlich, P. Ueber den jetzigen Stand der Karzinomforschung. *Ned Tijdschr Geneeskd* **5**, 273–290 (1908).

71. Gross, L. Intradermal Immunization of C3H Mice against a Sarcoma That Originated in an Animal of the Same Line. *Cancer Res.* **3**, 326 LP – 333 (1943).

72. Foley, E. J. Antigenic properties of methylcholanthrene-induced tumors in mice of the strain of origin. *Cancer Res.* **13**, 835–837 (1953).

73. Prehn, R. T. & Main, J. M. Immunity to Methylcholanthrene-Induced Sarcomas. *J. Natl. Cancer Inst.* **18**, 769–778 (1957).

74. Hellström, I., Hellström, K. E., Pierce, G. E. & Yang, J. P. Cellular and humoral immunity to different types of human neoplasms. *Nature* **220**, 1352–1354 (1968).

75. Hellström, I., Hellström, K. E., Sjögren, H. O. & Warner, G. A. Demonstration of cell-mediated immunity to human neoplasms of various histological types. *Int. J. Cancer* **7**, 1–16 (1971).

76. Vose, B. M., Vanky, F. & Klein, E. Lymphocyte cytotoxicity against autologous tumour biopsy cells in humans. *Int. J. Cancer* **20**, 512–519 (1977).

77. Vánky, F., Gorsky, T., Gorsky, Y., Masucci, M. G. & Klein, E. Lysis of tumor biopsy cells by autologous T lymphocytes activated in mixed cultures and propagated with T cell growth factor. *J. Exp. Med.* **155**, 83–95 (1982).

78. Vose, B. M. & Bonnard, G. D. Human tumour antigens defined by cytotoxicity and proliferative responses of cultured lymphoid cells. *Nature* **296**, 359–361 (1982).

79. Zinkernagel, R. M. & Doherty, P. C. Restriction of in vitro T cell-mediated cytotoxicity in lymphocytic choriomeningitis within a syngeneic or semiallogeneic system. *Nature* **248**, 701–702 (1974).

80. de Vries, J. E. & Spits, H. Cloned human cytotoxic T lymphocyte (CTL) lines reactive with autologous melanoma cells. I. In vitro generation, isolation, and analysis to phenotype and specificity. *J. Immunol.* **132**, 510–519 (1984).

81. Darrow, T. L., Slingluff, C. L. J. & Seigler, H. F. The role of HLA class I antigens in recognition of melanoma cells by tumor-specific cytotoxic T lymphocytes. Evidence for shared tumor antigens. *J. Immunol.* **142**, 3329–3335 (1989).

82. Townsend, A. R. M. *et al.* The epitopes of influenza nucleoprotein recognized by cytotoxic T lymphocytes can be defined with short synthetic peptides. *Cell* **44**, 959–968 (1986).

83. Bjorkman, P. J. *et al.* Structure of the human class I histocompatibility antigen, HLA-A2. *Nature* **329**, 506–512 (1987).

84. van der Bruggen, P. *et al.* A Gene Encoding an Antigen Recognized by Cytolytic T Lymphocytes on a Human Melanoma. *Science.* **254**, 1643–1647 (1991).

85. Kawakami, Y., Zakut, R., Topalian, S. L., Stötter, H. & Rosenberg, S. A. Shared human melanoma antigens. Recognition by tumor-infiltrating lymphocytes in HLA-A2.1-transfected melanomas. *J. Immunol.* **148**, 638–643 (1992).

86. Kawakami, Y. *et al.* Cloning of the gene coding for a shared human melanoma antigen recognized by autologous T cells infiltrating into tumor. *Proc. Natl. Acad. Sci. U. S. A.* **91**, 3515–3519 (1994).

87. Coulie, P. G. *et al.* A new gene coding for a differentiation antigen recognized by autologous cytolytic T lymphocytes on HLA-A2 melanomas. *J. Exp. Med.* **180**, 35–42

(1994).

88. Monach, P. A., Meredith, S. C., Siegel, C. T. & Schreiber, H. A unique tumor antigen produced by a single amino acid substitution. *Immunity* **2**, 45–59 (1995).

89. Yee, C., Savage, P. A., Lee, P. P., Davis, M. M. & Greenberg, P. D. Isolation of high avidity melanoma-reactive CTL from heterogeneous populations using peptide-MHC tetramers. *J. Immunol.* **162**, 2227–2234 (1999).

90. Schumacher, T. N., Scheper, W. & Kvistborg, P. Cancer Neoantigens. *Annu. Rev. Immunol.* **37**, 173–200 (2018).

91. Shankaran, V. *et al.* IFNgamma and lymphocytes prevent primary tumour development and shape tumour immunogenicity. *Nature* **410**, 1107–1111 (2001).

92. Vesely, M. D., Kershaw, M. H., Schreiber, R. D. & Smyth, M. J. Natural innate and adaptive immunity to cancer. *Annu. Rev. Immunol.* **29**, 235–271 (2011).

93. Kline, J., Zhang, L., Battaglia, L., Cohen, K. S. & Gajewski, T. F. Cellular and molecular requirements for rejection of B16 melanoma in the setting of regulatory T cell depletion and homeostatic proliferation. *J. Immunol.* **188**, 2630–2642 (2012).

94. Kaplan, D. H. *et al.* Demonstration of an interferon gamma-dependent tumor surveillance system in immunocompetent mice. *Proc. Natl. Acad. Sci. U. S. A.* **95**, 7556–7561 (1998).

95. Smyth, M. J. *et al.* Perforin-mediated cytotoxicity is critical for surveillance of spontaneous lymphoma. *J. Exp. Med.* **192**, 755–760 (2000).

96. Street, S. E. A., Trapani, J. A., MacGregor, D. & Smyth, M. J. Suppression of lymphoma and epithelial malignancies effected by interferon gamma. *J. Exp. Med.* **196**, 129–134 (2002).

97. Street, S. E. A., Cretney, E. & Smyth, M. J. Perforin and interferon-γ activities independently control tumor initiation, growth, and metastasis. *Blood* **97**, 192–197 (2001).

98. Wakita, D. *et al.* IFN-γ-dependent type 1 immunity is crucial for immunosurveillance against squamous cell carcinoma in a novel mouse carcinogenesis model. *Carcinogenesis* **30**, 1408–1415 (2009).

99. Wortzel, R. D., Urban, J. L. & Schreiber, H. Malignant growth in the normal host after variant selection in vitro with cytolytic T-cell lines. *Proc. Natl. Acad. Sci. U. S. A.* **81**, 2186–2190 (1984).

100. Restifo, N. P. *et al.* Identification of human cancers deficient in antigen processing. *J. Exp. Med.* **177**, 265–272 (1993).

101. Rooney, M. S., Shukla, S. A., Wu, C. J., Getz, G. & Hacohen, N. Molecular and genetic

properties of tumors associated with local immune cytolytic activity. *Cell* **160**, 48–61 (2015).

102. Baumeister, S. H., Freeman, G. J., Dranoff, G. & Sharpe, A. H. Coinhibitory Pathways in Immunotherapy for Cancer. *Annu. Rev. Immunol.* **34**, 539–573 (2016).

103. Philip, M. & Schietinger, A. CD8+ T cell differentiation and dysfunction in cancer. *Nat. Rev. Immunol.* (2021) doi:10.1038/s41577-021-00574-3.

104. Waldman, A. D., Fritz, J. M. & Lenardo, M. J. A guide to cancer immunotherapy: from T cell basic science to clinical practice. *Nat. Rev. Immunol.* **20**, 651–668 (2020).

105. van der Leun, A. M., Thommen, D. S. & Schumacher, T. N. CD8+ T cell states in human cancer: insights from single-cell analysis. *Nat. Rev. Cancer* **20**, 218–232 (2020).

106. Wölfel, T. *et al.* Analysis of antigens recognized on human melanoma cells by A2-restricted cytolytic T lymphocytes (CTL). *Int. J. Cancer* **55**, 237–244 (1993).

107. Matsushita, H. *et al.* Cancer exome analysis reveals a T-cell-dependent mechanism of cancer immunoediting. *Nature* **482**, 400–404 (2012).

108. Snyder, A. *et al.* Genetic basis for clinical response to CTLA-4 blockade in melanoma. *N. Engl. J. Med.* **371**, 2189–2199 (2014).

109. Linnemann, C. *et al.* High-throughput epitope discovery reveals frequent recognition of neo-antigens by CD4+ T cells in human melanoma. *Nat. Med.* **21**, 81–85 (2015).

110. Peters, B., Nielsen, M. & Sette, A. T Cell Epitope Predictions. *Annu. Rev. Immunol.* **38**, 123–145 (2020).

111. Le, D. T. *et al.* PD-1 Blockade in Tumors with Mismatch-Repair Deficiency. *N. Engl. J. Med.* **372**, 2509–2520 (2015).

112. Lauss, M. *et al.* Mutational and putative neoantigen load predict clinical benefit of adoptive T cell therapy in melanoma. *Nat. Commun.* **8**, 1738 (2017).

113. Simoni, Y. *et al.* Bystander CD8+ T cells are abundant and phenotypically distinct in human tumour infiltrates. *Nature* **557**, 575–579 (2018).

114. Scheper, W. *et al.* Low and variable tumor reactivity of the intratumoral TCR repertoire in human cancers. *Nat. Med.* **25**, 89–94 (2019).

115. Gee, M. H. *et al.* Antigen Identification for Orphan T Cell Receptors Expressed on Tumor-Infiltrating Lymphocytes. *Cell* **172**, 549-563.e16 (2018).

116. Miller, C. H. *et al.* Eomes identifies thymic precursors of self-specific memory-phenotype CD8+ T cells. *Nat. Immunol.* **21**, 567–577 (2020).

117. Park, S. L. *et al.* Tissue-resident memory CD8+ T cells promote melanoma–immune equilibrium in skin. *Nature* **565**, 366–371 (2019).

118. Park, S. L., Gebhardt, T. & Mackay, L. K. Tissue-Resident Memory T Cells in Cancer Immunosurveillance. *Trends Immunol.* **40**, 735–747 (2019).

119. Rosato, P. C. *et al.* Virus-specific memory T cells populate tumors and can be repurposed for tumor immunotherapy. *Nat. Commun.* **10**, (2019).

120. Cheng, Y. *et al.* Non-terminally exhausted tumor-resident memory HBV-specific T cell responses correlate with relapse-free survival in hepatocellular carcinoma. *Immunity* **54**, 1825-1840.e7 (2021).

121. Green, M. R. *et al.* Integrative analysis reveals selective 9p24.1 amplification, increased PD-1 ligand expression, and further induction via JAK2 in nodular sclerosing Hodgkin lymphoma and primary mediastinal large B-cell lymphoma. *Blood* **116**, 3268–3277 (2010).

122. Tumeh, P. C. *et al.* PD-1 blockade induces responses by inhibiting adaptive immune resistance. *Nature* **515**, 568–571 (2014).

123. Ansell, S. M. *et al.* PD-1 Blockade with Nivolumab in Relapsed or Refractory Hodgkin's Lymphoma. *N. Engl. J. Med.* **372**, 311–319 (2014).

124. Schalper, K. A. *et al.* In situ tumor PD-L1 mRNA expression is associated with increased TILs and better outcome in breast carcinomas. *Clin. Cancer Res.* **20**, 2773–2782 (2014).

125. Taube, J. M. *et al.* Association of PD-1, PD-1 ligands, and other features of the tumor immune microenvironment with response to anti-PD-1 therapy. *Clin. Cancer Res.* **20**, 5064–5074 (2014).

126. Taube, J. M. *et al.* Differential Expression of Immune-Regulatory Genes Associated with PD-L1 Display in Melanoma: Implications for PD-1 Pathway Blockade. *Clin. Cancer Res.* **21**, 3969 LP – 3976 (2015).

127. Topalian, S. L., Taube, J. M., Anders, R. A. & Pardoll, D. M. Mechanism-driven biomarkers to guide immune checkpoint blockade in cancer therapy. *Nat. Rev. Cancer* **16**, 275–287 (2016).

128. Godfrey, J. *et al.* PD-L1 gene alterations identify a subset of diffuse large B-cell lymphoma harboring a T-cell-inflamed phenotype. *Blood* **133**, 2279–2290 (2019).

129. Böttcher, J. P. & Reis e Sousa, C. The Role of Type 1 Conventional Dendritic Cells in Cancer Immunity. *Trends in Cancer* **4**, 784–792 (2018).

130. Wculek, S. K. *et al.* Dendritic cells in cancer immunology and immunotherapy. *Nat. Rev.*

Immunol. **20**, 7–24 (2020).

131. Chow, A., Brown, B. D. & Merad, M. Studying the mononuclear phagocyte system in the molecular age. *Nat. Rev. Immunol.* **11**, 788–798 (2011).

132. Adolfsson, J. *et al.* Identification of Flt3+ lympho-myeloid stem cells lacking erythro-megakaryocytic potential a revised road map for adult blood lineage commitment. *Cell* **121**, 295–306 (2005).

133. Naik, S. H. *et al.* Diverse and heritable lineage imprinting of early haematopoietic progenitors. *Nature* **496**, 229–232 (2013).

134. Shortman, K. & Naik, S. H. Steady-state and inflammatory dendritic-cell development. *Nat. Rev. Immunol.* **7**, 19–30 (2007).

135. Akashi, K., Traver, D., Miyamoto, T. & Weissman, I. L. A clonogenic common myeloid progenitor that gives rise to all myeloid lineages. *Nature* **404**, 193–197 (2000).

136. Manz, M. G., Traver, D., Miyamoto, T., Weissman, I. L. & Akashi, K. Dendritic cell potentials of early lymphoid and myeloid progenitors. *Blood* **97**, 3333–3341 (2001).

137. Wu, L. *et al.* Development of thymic and splenic dendritic cell populations from different hemopoietic precursors. *Blood* **98**, 3376–3382 (2001).

138. Schlenner, S. M. *et al.* Fate mapping reveals separate origins of T cells and myeloid lineages in the thymus. *Immunity* **32**, 426–436 (2010).

139. Satpathy, A. T., Wu, X., Albring, J. C. & Murphy, K. M. Re(de)fining the dendritic cell lineage. *Nat. Immunol.* **13**, 1145–1154 (2012).

140. Merad, M., Sathe, P., Helft, J., Miller, J. & Mortha, A. The dendritic cell lineage: ontogeny and function of dendritic cells and their subsets in the steady state and the inflamed setting. *Annu. Rev. Immunol.* **31**, 563–604 (2013).

141. Liu, Z. *et al.* Fate Mapping via Ms4a3-Expression History Traces Monocyte-Derived Cells. *Cell* **178**, 1509-1525.e19 (2019).

142. Fogg, D. K. *et al.* A clonogenic bone marrow progenitor specific for macrophages and dendritic cells. *Science.* **311**, 83–87 (2006).

143. Auffray, C. *et al.* CX3CR1+ CD115+ CD135+ common macrophage/DC precursors and the role of CX3CR1 in their response to inflammation. *J. Exp. Med.* **206**, 595–606 (2009).

144. Naik, S. H. *et al.* Intrasplenic steady-state dendritic cell precursors that are distinct from monocytes. *Nat. Immunol.* **7**, 663–671 (2006).

145. Diao, J. *et al.* In situ replication of immediate dendritic cell (DC) precursors contributes to conventional DC homeostasis in lymphoid tissue. *J. Immunol.* **176**, 7196–7206 (2006).

146. Liu, K. *et al.* In Vivo Analysis of Dendritic Cell Development and Homeostasis. *Science.* **324**, 392 LP – 397 (2009).

147. Ginhoux, F. *et al.* The origin and development of nonlymphoid tissue CD103+ DCs. *J. Exp. Med.* **206**, 3115–30 (2009).

148. Grajales-Reyes, G. E. *et al.* Batf3 maintains autoactivation of Irf8 for commitment of a CD8α(+) conventional DC clonogenic progenitor. *Nat. Immunol.* **16**, 708–717 (2015).

149. Schlitzer, A. *et al.* Identification of cDC1- and cDC2-committed DC progenitors reveals early lineage priming at the common DC progenitor stage in the bone marrow. *Nat. Immunol.* **16**, 718–728 (2015).

150. See, P. *et al.* Mapping the human DC lineage through the integration of high-dimensional techniques. *Science.* **356**, (2017).

151. McKenna, H. J. *et al.* Mice lacking flt3 ligand have deficient hematopoiesis affecting hematopoietic progenitor cells, dendritic cells, and natural killer cells. *Blood* **95**, 3489–3497 (2000).

152. Waskow, C. *et al.* The receptor tyrosine kinase Flt3 is required for dendritic cell development in peripheral lymphoid tissues. *Nat. Immunol.* **9**, 676–683 (2008).

153. Maraskovsky, E. *et al.* Dramatic increase in the numbers of functionally mature dendritic cells in Flt3 ligand-treated mice: multiple dendritic cell subpopulations identified. *J. Exp. Med.* **184**, 1953–1962 (1996).

154. Helft, J. *et al.* GM-CSF Mouse Bone Marrow Cultures Comprise a Heterogeneous Population of CD11c+MHCII+ Macrophages and Dendritic Cells. *Immunity* **42**, 1197–1211 (2015).

155. Ohl, L. *et al.* CCR7 governs skin dendritic cell migration under inflammatory and steady-state conditions. *Immunity* **21**, 279–288 (2004).

156. Ginhoux, F. *et al.* Blood-derived dermal langerin+ dendritic cells survey the skin in the steady state. *J. Exp. Med.* **204**, 3133–3146 (2007).

157. Bursch, L. S. *et al.* Identification of a novel population of Langerin+ dendritic cells. *J. Exp. Med.* **204**, 3147–3156 (2007).

158. Poulin, L. F. *et al.* The dermis contains langerin+ dendritic cells that develop and function independently of epidermal Langerhans cells. *J. Exp. Med.* **204**, 3119–3131 (2007).

159. Miller, J. C. *et al.* Deciphering the transcriptional network of the dendritic cell lineage. *Nat. Immunol.* **13**, 888–899 (2012).

160. Baratin, M. *et al.* Homeostatic NF-κB Signaling in Steady-State Migratory Dendritic Cells

Regulates Immune Homeostasis and Tolerance. *Immunity* **42**, 627–639 (2015).

161. Ardouin, L. *et al.* Broad and Largely Concordant Molecular Changes Characterize Tolerogenic and Immunogenic Article Broad and Largely Concordant Molecular Changes Characterize Tolerogenic and Immunogenic Dendritic Cell Maturation in Thymus and Periphery. *Immunity* 305–318 (2016) doi:10.1016/j.immuni.2016.07.019.

162. Ardouin, L. *et al.* Broad and Largely Concordant Molecular Changes Characterize Tolerogenic and Immunogenic Dendritic Cell Maturation in Thymus and Periphery. *Immunity* **45**, 305–318 (2016).

163. Zilionis, R. *et al.* Single-Cell Transcriptomics of Human and Mouse Lung Cancers Reveals Conserved Myeloid Populations across Individuals and Species. *Immunity* **50**, 1317-1334.e10 (2019).

164. Maier, B. *et al.* A conserved dendritic-cell regulatory program limits antitumour immunity. *Nature* **580**, 257–262 (2020).

165. Steinman, R. M. Decisions About Dendritic Cells: Past, Present, and Future. *Annu. Rev. Immunol.* **30**, 1–22 (2012).

166. Kashem, S. W. *et al.* Nociceptive Sensory Fibers Drive Interleukin-23 Production from CD301b + Dermal Dendritic Cells and Drive Protective Cutaneous Immunity. *Immunity* **43**, 515–526 (2015).

167. Perner, C. *et al.* Substance P Release by Sensory Neurons Triggers Dendritic Cell Migration and Initiates the Type-2 Immune Response to Allergens ll Article Substance P Release by Sensory Neurons Triggers Dendritic Cell Migration and Initiates the Type-2 Immune Response to . *Immunity* **53**, 1063-1077.e7 (2020).

168. Lai, N. Y. *et al.* Gut-Innervating Nociceptor Neurons Regulate Peyer's Patch Microfold Cells and SFB Levels to Mediate Salmonella Host Defense. *Cell* **180**, 33-49.e22 (2020).

169. Murphy, T. L. *et al.* Transcriptional Control of Dendritic Cell Development. *Annu. Rev. Immunol.* **34**, 93–119 (2016).

170. Carotta, S. *et al.* The transcription factor PU.1 controls dendritic cell development and Flt3 cytokine receptor expression in a dose-dependent manner. *Immunity* **32**, 628–641 (2010).

171. Wu, X. *et al.* Bcl11a Controls Flt3 Expression in Early Hematopoietic Progenitors and Is Required for pDC Development In Vivo. *PLoS One* **8**, e64800 (2013).

172. Ippolito, G. C. *et al.* Dendritic cell fate is determined by BCL11A. *Proc. Natl. Acad. Sci. U. S. A.* **111**, E998-1006 (2014).

173. Kueh, H. Y., Champhekar, A., Nutt, S. L., Elowitz, M. B. & Rothenberg, E. V. Positive feedback between PU.1 and the cell cycle controls myeloid differentiation. *Science.* **341**, 670–673 (2013).

174. Schönheit, J. *et al.* PU.1 level-directed chromatin structure remodeling at the Irf8 gene drives dendritic cell commitment. *Cell Rep.* **3**, 1617–1628 (2013).

175. Satpathy, A. T. *et al.* Zbtb46 expression distinguishes classical dendritic cells and their committed progenitors from other immune lineages. *J. Exp. Med.* **209**, 1135–52 (2012).

176. Meredith, M. M. *et al.* Expression of the zinc finger transcription factor zDC (Zbtb46, Btbd4) defines the classical dendritic cell lineage. *J. Exp. Med.* **209**, 1153–1165 (2012).

177. Meredith, M. M. *et al.* Zinc finger transcription factor zDC is a negative regulator required to prevent activation of classical dendritic cells in the steady state. *J. Exp. Med.* **209**, 1583–1593 (2012).

178. Hildner, K. *et al.* Batf3 deficiency reveals a critical role for CD8alpha+ dendritic cells in cytotoxic T cell immunity. *Science.* **322**, 1097–1100 (2008).

179. Edelson, B. T. *et al.* Peripheral CD103+ dendritic cells form a unified subset developmentally related to CD8alpha+ conventional dendritic cells. *J. Exp. Med.* **207**, 823–836 (2010).

180. Tussiwand, R. *et al.* Compensatory dendritic cell development mediated by BATF–IRF interactions. *Nature* **490**, 502–507 (2012).

181. Durai, V. *et al.* Cryptic activation of an Irf8 enhancer governs cDC1 fate specification. *Nat. Immunol.* **20**, 1161–1173 (2019).

182. Kashiwada, M., Pham, N.-L. L., Pewe, L. L., Harty, J. T. & Rothman, P. B. NFIL3/E4BP4 is a key transcription factor for CD8α+ dendritic cell development. *Blood* **117**, 6193–6197 (2011).

183. Hacker, C. *et al.* Transcriptional profiling identifies Id2 function in dendritic cell development. *Nat. Immunol.* **4**, 380–386 (2003).

184. Scott, C. L. *et al.* The transcription factor Zeb2 regulates development of conventional and plasmacytoid DCs by repressing Id2. *J. Exp. Med.* **213**, 897–911 (2016).

185. Wu, X. *et al.* Transcription factor Zeb2 regulates commitment to plasmacytoid dendritic cell and monocyte fate. *Proc. Natl. Acad. Sci.* **113**, 14775 LP – 14780 (2016).

186. Bagadia, P. *et al.* An Nfil3–Zeb2–Id2 pathway imposes Irf8 enhancer switching during cDC1 development. *Nat. Immunol.* **20**, 1174–1185 (2019).

187. Suzuki, S. *et al.* Critical roles of interferon regulatory factor 4 in CD11b^{high}CD8α^{-}

dendritic cell development. *Proc. Natl. Acad. Sci.* **101**, 8981 LP – 8986 (2004).

188. Vander Lugt, B. *et al.* Transcriptional programming of dendritic cells for enhanced MHC class II antigen presentation. *Nat. Immunol.* **15**, 161–7 (2014).

189. Wu, L. *et al.* RelB is essential for the development of myeloid-related CD8alpha- dendritic cells but not of lymphoid-related CD8alpha+ dendritic cells. *Immunity* **9**, 839–847 (1998).

190. Ichikawa, E. *et al.* Defective development of splenic and epidermal CD4+ dendritic cells in mice deficient for IFN regulatory factor-2. *Proc. Natl. Acad. Sci. U. S. A.* **101**, 3909 LP – 3914 (2004).

191. Mildner, A. & Jung, S. Development and function of dendritic cell subsets. *Immunity* **40**, 642–656 (2014).

192. Tussiwand, R. *et al.* Klf4 expression in conventional dendritic cells is required for T helper 2 cell responses. *Immunity* **42**, 916–928 (2015).

193. Lewis, K. L. *et al.* Notch2 receptor signaling controls functional differentiation of dendritic cells in the spleen and intestine. *Immunity* **35**, 780–791 (2011).

194. Satpathy, A. T. *et al.* Notch2-dependent classical dendritic cells orchestrate intestinal immunity to attaching-and-effacing bacterial pathogens. *Nat. Immunol.* **14**, 937–948 (2013).

195. Schlitzer, A. *et al.* IRF4 transcription factor-dependent CD11b+ dendritic cells in human and mouse control mucosal IL-17 cytokine responses. *Immunity* **38**, 970–983 (2013).

196. Persson, E. K. *et al.* IRF4 transcription-factor-dependent CD103(+)CD11b(+) dendritic cells drive mucosal T helper 17 cell differentiation. *Immunity* **38**, 958–969 (2013).

197. den Haan, J. M. M., Lehar, S. M. & Bevan, M. J. Cd8+ but Not Cd8− Dendritic Cells Cross-Prime Cytotoxic T Cells in Vivo. *J. Exp. Med.* **192**, 1685–1696 (2000).

198. Schulz, O. & Reis e Sousa, C. Cross-presentation of cell-associated antigens by CD8α+ dendritic cells is attributable to their ability to internalize dead cells. *Immunology* **107**, 183–189 (2002).

199. Iyoda, T. *et al.* The CD8+ Dendritic Cell Subset Selectively Endocytoses Dying Cells in Culture and In Vivo. *J. Exp. Med.* **195**, 1289–1302 (2002).

200. Valdez, Y. *et al.* Major Histocompatibility Complex Class II Presentation of Cell-associated Antigen Is Mediated by CD8α+ Dendritic Cells In Vivo. *J. Exp. Med.* **195**, 683–694 (2002).

201. Villadangos, J. A. & Schnorrer, P. Intrinsic and cooperative antigen-presenting functions

of dendritic-cell subsets in vivo. *Nat. Rev. Immunol.* **7**, 543–555 (2007).

202. Kline, D. E. *et al.* CD8α + Dendritic Cells Dictate Leukemia-Specific CD8 + T Cell Fates . *J. Immunol.* **201**, 3759–3769 (2018).

203. Schulz, O., Pennington, D. J., Hodivala-Dilke, K., Febbraio, M. & Reis e Sousa, C. CD36 or $\alpha_v\beta_3$ and $\alpha_v\beta_5$ Integrins Are Not Essential for MHC Class I Cross-Presentation of Cell-Associated Antigen by $CD8\alpha^+$ Murine Dendritic Cells. *J. Immunol.* **168**, 6057 LP – 6065 (2002).

204. Belz, G. T. *et al.* CD36 Is Differentially Expressed by $CD8^+$ Splenic Dendritic Cells But Is Not Required for Cross-Presentation In Vivo. *J. Immunol.* **168**, 6066 LP – 6070 (2002).

205. Schnorrer, P. *et al.* The dominant role of $CD8^+$ dendritic cells in cross-presentation is not dictated by antigen capture. *Proc. Natl. Acad. Sci.* **103**, 10729 LP – 10734 (2006).

206. Kreer, C., Rauen, J., Zehner, M. & Burgdorf, S. Cross-Presentation: How to Get there – or How to Get the ER. *Frontiers in Immunology* vol. 2 87 (2012).

207. Dudziak, D. *et al.* Differential Antigen Processing by Dendritic Cell Subsets in Vivo. *Science.* **315**, 107–111 (2007).

208. Burgdorf, S., Kautz, A., Böhnert, V., Knolle, P. A. & Kurts, C. Distinct Pathways of Antigen Uptake and Intracellular Routing in CD4 and CD8 T Cell Activation. *Science.* **316**, 612–616 (2007).

209. Geijtenbeek, T. B. H. & Gringhuis, S. I. Signalling through C-type lectin receptors: shaping immune responses. *Nat. Rev. Immunol.* **9**, 465–479 (2009).

210. Kamphorst, A. O., Guermonprez, P., Dudziak, D. & Nussenzweig, M. C. Route of Antigen Uptake Differentially Impacts Presentation by Dendritic Cells and Activated Monocytes. *J. Immunol.* **185**, 3426 LP – 3435 (2010).

211. Weck, M. M. *et al.* hDectin-1 is involved in uptake and cross-presentation of cellular antigens. *Blood* **111**, 4264–4272 (2008).

212. Giodini, A., Rahner, C. & Cresswell, P. Receptor-mediated phagocytosis elicits cross-presentation in nonprofessional antigen-presenting cells. *Proc. Natl. Acad. Sci.* **106**, 3324 LP – 3329 (2009).

213. Seitz, H. M., Camenisch, T. D., Lemke, G., Earp, H. S. & Matsushima, G. K. Macrophages and Dendritic Cells Use Different Axl/Mertk/Tyro3 Receptors in Clearance of Apoptotic Cells. *J. Immunol.* **178**, 5635 LP – 5642 (2007).

214. Theisen, D. J. *et al.* WDFY4 is required for cross-presentation in response to viral and tumor antigens. *Science.* **362**, 694–699 (2018).

215. Mahnke, K. *et al.* The Dendritic Cell Receptor for Endocytosis, Dec-205, Can Recycle and Enhance Antigen Presentation via Major Histocompatibility Complex Class II–Positive Lysosomal Compartments. *J. Cell Biol.* **151**, 673–684 (2000).

216. Gitlin, A. D., Shulman, Z. & Nussenzweig, M. C. Clonal selection in the germinal centre by regulated proliferation and hypermutation. *Nature* **509**, 637–640 (2014).

217. Gitlin, A. D. *et al.* T cell help controls the speed of the cell cycle in germinal center B cells. *Science.* **349**, 643–646 (2015).

218. Lennon-Duménil, A.-M. *et al.* Analysis of Protease Activity in Live Antigen-presenting Cells Shows Regulation of the Phagosomal Proteolytic Contents During Dendritic Cell Activation. *J. Exp. Med.* **196**, 529–540 (2002).

219. Delamarre, L., Pack, M., Chang, H., Mellman, I. & Trombetta, E. S. Differential lysosomal proteolysis in antigen-presenting cells determines antigen fate. *Science.* **307**, 1630–1634 (2005).

220. Savina, A. *et al.* NOX2 controls phagosomal pH to regulate antigen processing during crosspresentation by dendritic cells. *Cell* **126**, 205–218 (2006).

221. Jancic, C. *et al.* Rab27a regulates phagosomal pH and NADPH oxidase recruitment to dendritic cell phagosomes. *Nat. Cell Biol.* **9**, 367–378 (2007).

222. Savina, A. *et al.* The small GTPase Rac2 controls phagosomal alkalinization and antigen crosspresentation selectively in CD8(+) dendritic cells. *Immunity* **30**, 544–555 (2009).

223. Sancho, D. *et al.* Identification of a dendritic cell receptor that couples sensing of necrosis to immunity. *Nature* **458**, 899–903 (2009).

224. Ahrens, S. *et al.* F-Actin Is an Evolutionarily Conserved Damage-Associated Molecular Pattern Recognized by DNGR-1, a Receptor for Dead Cells. *Immunity* **36**, 635–645 (2012).

225. Zhang, J.-G. *et al.* The dendritic cell receptor Clec9A binds damaged cells via exposed actin filaments. *Immunity* **36**, 646–657 (2012).

226. Hanč, P. *et al.* Structure of the Complex of F-Actin and DNGR-1, a C-Type Lectin Receptor Involved in Dendritic Cell Cross-Presentation of Dead Cell-Associated Antigens. *Immunity* **42**, 839–849 (2015).

227. Canton, J. *et al.* The receptor DNGR-1 signals for phagosomal rupture to promote cross-presentation of dead-cell-associated antigens. *Nat. Immunol.* **22**, 140–153 (2021).

228. Maldonado-López, R. *et al.* CD8α+ and CD8α− Subclasses of Dendritic Cells Direct the Development of Distinct T Helper Cells In Vivo. *J. Exp. Med.* **189**, 587–592 (1999).

229. Hochrein, H. *et al.* Differential Production of IL-12, IFN-α, and IFN-γ by Mouse Dendritic Cell Subsets. *J. Immunol.* **166**, 5448 LP – 5455 (2001).

230. Mashayekhi, M. *et al.* CD8α+ Dendritic Cells Are the Critical Source of Interleukin-12 that Controls Acute Infection by Toxoplasma gondii Tachyzoites. *Immunity* **35**, 249–259 (2011).

231. Mattei, F., Schiavoni, G., Belardelli, F. & Tough, D. F. IL-15 Is Expressed by Dendritic Cells in Response to Type I IFN, Double-Stranded RNA, or Lipopolysaccharide and Promotes Dendritic Cell Activation. *J. Immunol.* **167**, 1179 LP – 1187 (2001).

232. Schulz, O. *et al.* Toll-like receptor 3 promotes cross-priming to virus-infected cells. *Nature* **433**, 887–892 (2005).

233. Yarovinsky, F. *et al.* TLR11 activation of dendritic cells by a protozoan profilin-like protein. *Science.* **308**, 1626–1629 (2005).

234. Zhou, B. *et al.* Thymic stromal lymphopoietin as a key initiator of allergic airway inflammation in mice. *Nat. Immunol.* **6**, 1047–1053 (2005).

235. Besnard, A.-G. *et al.* IL-33-activated dendritic cells are critical for allergic airway inflammation. *Eur. J. Immunol.* **41**, 1675–1686 (2011).

236. Gao, Y. *et al.* Control of T Helper 2 Responses by Transcription Factor IRF4-Dependent Dendritic Cells. *Immunity* **39**, 722–732 (2013).

237. Plantinga, M. *et al.* Conventional and Monocyte-Derived CD11b+ Dendritic Cells Initiate and Maintain T Helper 2 Cell-Mediated Immunity to House Dust Mite Allergen. *Immunity* **38**, 322–335 (2013).

238. Williams, J. W. *et al.* Transcription factor IRF4 drives dendritic cells to promote Th2 differentiation. *Nat. Commun.* **4**, 2990 (2013).

239. Halim, T. Y. F. *et al.* Group 2 Innate Lymphoid Cells Are Critical for the Initiation of Adaptive T Helper 2 Cell-Mediated Allergic Lung Inflammation. *Immunity* **40**, 425–435 (2014).

240. Halim, T. Y. F. *et al.* Group 2 innate lymphoid cells license dendritic cells to potentiate memory TH2 cell responses. *Nat. Immunol.* **17**, 57–64 (2016).

241. Lambrecht, B. N. & Hammad, H. The immunology of asthma. *Nat. Immunol.* **16**, 45–56 (2015).

242. Kumamoto, Y. *et al.* CD301b+ dermal dendritic cells drive T helper 2 cell-mediated immunity. *Immunity* **39**, 733–743 (2013).

243. Kinnebrew, M. A. *et al.* Interleukin 23 Production by Intestinal CD103+CD11b+

Dendritic Cells in Response to Bacterial Flagellin Enhances Mucosal Innate Immune Defense. *Immunity* **36**, 276–287 (2012).

244. Ota, N. *et al.* IL-22 bridges the lymphotoxin pathway with the maintenance of colonic lymphoid structures during infection with Citrobacter rodentium. *Nat. Immunol.* **12**, 941–948 (2011).

245. Miller, L. S. & Cho, J. S. Immunity against Staphylococcus aureus cutaneous infections. *Nat. Rev. Immunol.* **11**, 505–518 (2011).

246. Naik, S. *et al.* Commensal-dendritic-cell interaction specifies a unique protective skin immune signature. *Nature* **520**, 104–108 (2015).

247. Zheng, Y. *et al.* Interleukin-22, a TH17 cytokine, mediates IL-23-induced dermal inflammation and acanthosis. *Nature* **445**, 648–651 (2007).

248. Riol-Blanco, L. *et al.* Nociceptive sensory neurons drive interleukin-23-mediated psoriasiform skin inflammation. *Nature* **510**, 157–161 (2014).

249. Cohen, J. A. *et al.* Cutaneous TRPV1+ Neurons Trigger Protective Innate Type 17 Anticipatory Immunity. *Cell* **178**, 919-932.e14 (2019).

250. Perner, C. *et al.* Substance P Release by Sensory Neurons Triggers Dendritic Cell Migration and Initiates the Type-2 Immune Response to Allergens. *Immunity* **53**, 1063-1077.e7 (2020).

251. Fuertes, M. B. *et al.* Host type I IFN signals are required for antitumor CD8+ T cell responses through CD8{alpha}+ dendritic cells. *J. Exp. Med.* **208**, 2005–2016 (2011).

252. Spranger, S., Dai, D., Horton, B. & Gajewski, T. F. Tumor-Residing Batf3 Dendritic Cells Are Required for Effector T Cell Trafficking and Adoptive T Cell Therapy. *Cancer Cell* **31**, 711-723.e4 (2017).

253. Broz, M. L. *et al.* Dissecting the tumor myeloid compartment reveals rare activating antigen-presenting cells critical for T cell immunity. *Cancer Cell* **26**, 638–652 (2014).

254. Roberts, E. W. *et al.* Critical Role for CD103(+)/CD141(+) Dendritic Cells Bearing CCR7 for Tumor Antigen Trafficking and Priming of T Cell Immunity in Melanoma. *Cancer Cell* **30**, 324–336 (2016).

255. Salmon, H. *et al.* Expansion and Activation of CD103(+) Dendritic Cell Progenitors at the Tumor Site Enhances Tumor Responses to Therapeutic PD-L1 and BRAF Inhibition. *Immunity* **44**, 924–938 (2016).

256. Ruhland, M. K. *et al.* Visualizing Synaptic Transfer of Tumor Antigens among Dendritic Cells. *Cancer Cell* **37**, 786-799.e5 (2020).

257. Binnewies, M. *et al.* Unleashing Type-2 Dendritic Cells to Drive Protective Antitumor CD4(+) T Cell Immunity. *Cell* **177**, 556-571.e16 (2019).

258. Sánchez-Paulete, A. R. *et al.* Cancer Immunotherapy with Immunomodulatory Anti-CD137 and Anti–PD-1 Monoclonal Antibodies Requires BATF3-Dependent Dendritic Cells. *Cancer Discov.* **6**, 71 LP – 79 (2016).

259. Sancho, D. *et al.* Tumor therapy in mice via antigen targeting to a novel, DC-restricted C-type lectin. *J. Clin. Invest.* **118**, 2098–2110 (2008).

260. Ruffell, B. *et al.* Macrophage IL-10 Blocks CD8+ T Cell-Dependent Responses to Chemotherapy by Suppressing IL-12 Expression in Intratumoral Dendritic Cells. *Cancer Cell* **26**, 623–637 (2014).

261. Mikucki, M. E. *et al.* Non-redundant requirement for CXCR3 signalling during tumoricidal T-cell trafficking across tumour vascular checkpoints. *Nat. Commun.* **6**, 7458 (2015).

262. Diao, J., Zhao, J., Winter, E. & Cattral, M. S. Recruitment and Differentiation of Conventional Dendritic Cell Precursors in Tumors. *J. Immunol.* **184**, 1261 LP – 1267 (2010).

263. Böttcher, J. P. *et al.* NK Cells Stimulate Recruitment of cDC1 into the Tumor Microenvironment Promoting Cancer Immune Control. *Cell* **172**, 1022-1037.e14 (2018).

264. Spranger, S., Bao, R. & Gajewski, T. F. Melanoma-intrinsic β-catenin signalling prevents anti-tumour immunity. *Nature* **523**, 231–235 (2015).

265. Zelenay, S. *et al.* Cyclooxygenase-Dependent Tumor Growth through Evasion of Immunity. *Cell* **162**, 1257–1270 (2015).

266. Diamond, M. S. *et al.* Type I interferon is selectively required by dendritic cells for immune rejection of tumors. *J. Exp. Med.* **208**, 1989–2003 (2011).

267. Woo, S. R. *et al.* STING-Dependent cytoplasmic DNA Sensing Mediates Innate Immune Recognition of Immunogenic Tumors. *Immunity* **41**, 830–842 (2014).

268. Ghislat, G. *et al.* NF-kB–dependent IRF1 activation programs cDC1 dendritic cells to drive antitumor immunity. *Sci. Immunol.* **6**, (2021).

269. Trombetta, E. S. & Mellman, I. Cell Biology of Antigen Processing in Vitro and in Vivo. *Annu. Rev. Immunol.* **23**, 975–1028 (2005).

270. Blum, J. S., Wearsch, P. A. & Cresswell, P. *Pathways of Antigen Processing*. *Annu. Rev. Immunol* vol. 31 (2013).

271. Shastri, N., Schwab, S. & Serwold, T. Producing Nature's Gene-Chips: The Generation of

Peptides for Display by MHC Class I Molecules. *Annu. Rev. Immunol.* **20**, 463–493 (2002).

272. Shen, L., Sigal, L. J., Boes, M. & Rock, K. L. Important Role of Cathepsin S in Generating Peptides for TAP-Independent MHC Class I Crosspresentation In Vivo. *Immunity* **21**, 155–165 (2004).

273. Bochtler, M., Ditzel, L., Groll, M., Hartmann, C. & Huber, R. The Proteasome. *Annu. Rev. Biophys. Biomol. Struct.* **28**, 295–317 (1999).

274. Voges, D., Zwickl, P. & Baumeister, W. The 26S Proteasome: A Molecular Machine Designed for Controlled Proteolysis. *Annu. Rev. Biochem.* **68**, 1015–1068 (1999).

275. Wang, R. F., Parkhurst, M. R., Kawakami, Y., Robbins, P. F. & Rosenberg, S. A. Utilization of an alternative open reading frame of a normal gene in generating a novel human cancer antigen. *J. Exp. Med.* **183**, 1131–1140 (1996).

276. Coulie, P. G. *et al.* A mutated intron sequence codes for an antigenic peptide recognized by cytolytic T lymphocytes on a human melanoma. *Proc. Natl. Acad. Sci.* **92**, 7976 LP – 7980 (1995).

277. Yewdell, J. W., Antón, L. C. & Bennink, J. R. Defective ribosomal products (DRiPs): a major source of antigenic peptides for MHC class I molecules? *J. Immunol.* **157**, 1823 LP – 1826 (1996).

278. Schubert, U. *et al.* Rapid degradation of a large fraction of newly synthesized proteins by proteasomes. *Nature* **404**, 770–774 (2000).

279. Skipper, J. C. *et al.* An HLA-A2-restricted tyrosinase antigen on melanoma cells results from posttranslational modification and suggests a novel pathway for processing of membrane proteins. *J. Exp. Med.* **183**, 527–534 (1996).

280. Hanada, K., Yewdell, J. W. & Yang, J. C. Immune recognition of a human renal cancer antigen through post-translational protein splicing. *Nature* **427**, 252–256 (2004).

281. Vigneron, N. *et al.* An Antigenic Peptide Produced by Peptide Splicing in the Proteasome. *Science.* **304**, 587–590 (2004).

282. Androlewicz, M. J., Anderson, K. S. & Cresswell, P. Evidence that transporters associated with antigen processing translocate a major histocompatibility complex class I-binding peptide into the endoplasmic reticulum in an ATP-dependent manner. *Proc. Natl. Acad. Sci. U. S. A.* **90**, 9130–9134 (1993).

283. J., N. J., Frank, M. & J., H. G. Selective and ATP-Dependent Translocation of Peptides by the MHC-Encoded Transporter. *Science.* **261**, 769–771 (1993).

284. Shepherd, J. C. *et al.* TAP1-dependent peptide translocation in vitro is ATP dependent and peptide selective. *Cell* **74**, 577–584 (1993).

285. Heemels, M.-T. & Ploegh, H. GENERATION, TRANSLOCATION, AND PRESENTATION OF MHC CLASS I-RESTRICTED PEPTIDES. *Annu. Rev. Biochem.* **64**, 463–491 (1995).

286. Koopmann, J.-O., Post, M., Neefjes, J. J., Hämmerling, G. J. & Momburg, F. Translocation of long peptides by transporters associated with antigen processing (TAP). *Eur. J. Immunol.* **26**, 1720–1728 (1996).

287. Hammer, G. E., Gonzalez, F., Champsaur, M., Cado, D. & Shastri, N. The aminopeptidase ERAAP shapes the peptide repertoire displayed by major histocompatibility complex class I molecules. *Nat. Immunol.* **7**, 103–112 (2006).

288. Garbi, N. *et al.* Impaired immune responses and altered peptide repertoire in tapasin-deficient mice. *Nat. Immunol.* **1**, 234–238 (2000).

289. Grandea, A. G. *et al.* Impaired Assembly yet Normal Trafficking of MHC Class I Molecules in Tapasin Mutant Mice. *Immunity* **13**, 213–222 (2000).

290. Garbi, N., Tanaka, S., Momburg, F. & Hämmerling, G. J. Impaired assembly of the major histocompatibility complex class I peptide-loading complex in mice deficient in the oxidoreductase ERp57. *Nat. Immunol.* **7**, 93–102 (2006).

291. Gao, B. *et al.* Assembly and Antigen-Presenting Function of MHC Class I Molecules in Cells Lacking the ER Chaperone Calreticulin. *Immunity* **16**, 99–109 (2002).

292. Grant, B. D. & Donaldson, J. G. Pathways and mechanisms of endocytic recycling. *Nat. Rev. Mol. Cell Biol.* **10**, 597–608 (2009).

293. Vega, M. A. & Strominger, J. L. Constitutive endocytosis of HLA class I antigens requires a specific portion of the intracytoplasmic tail that shares structural features with other endocytosed molecules. *Proc. Natl. Acad. Sci.* **86**, 2688 LP – 2692 (1989).

294. Lizée, G. *et al.* Control of dendritic cell cross-presentation by the major histocompatibility complex class I cytoplasmic domain. *Nat. Immunol.* **4**, 1065–1073 (2003).

295. van Endert, P. Intracellular recycling and cross-presentation by MHC class I molecules. *Immunol. Rev.* **272**, 80–96 (2016).

296. Reid, P. A. & Watts, C. Cycling of cell-surface MHC glycoproteins through primaquine-sensitive intracellular compartments. *Nature* **346**, 655–657 (1990).

297. Grommé, M. *et al.* Recycling MHC class I molecules and endosomal peptide loading. *Proc. Natl. Acad. Sci.* **96**, 10326 LP – 10331 (1999).

298. Chiu, I., Davis, D. M. & Strominger, J. L. Trafficking of spontaneously endocytosed MHC proteins. *Proc. Natl. Acad. Sci.* **96**, 13944 LP – 13949 (1999).

299. Loredana, S. *et al.* IRAP Identifies an Endosomal Compartment Required for MHC Class I Cross-Presentation. *Science.* **325**, 213–217 (2009).

300. Duncan, L. M. *et al.* Lysine-63-linked ubiquitination is required for endolysosomal degradation of class I molecules. *EMBO J.* **25**, 1635–1645 (2006).

301. Wang, X. *et al.* Ubiquitination of serine, threonine, or lysine residues on the cytoplasmic tail can induce ERAD of MHC-I by viral E3 ligase mK3 . *J. Cell Biol.* **177**, 613–624 (2007).

302. Sallusto, F., Cella, M., Danieli, C. & Lanzavecchia, A. Dendritic cells use macropinocytosis and the mannose receptor to concentrate macromolecules in the major histocompatibility complex class II compartment: downregulation by cytokines and bacterial products. *J. Exp. Med.* **182**, 389–400 (1995).

303. Steinman, R. M. & Swanson, J. The endocytic activity of dendritic cells. *J. Exp. Med.* **182**, 283–288 (1995).

304. Swanson, J. A. & Watts, C. Macropinocytosis. *Trends Cell Biol.* **5**, 424–428 (1995).

305. Norbury, C. C., Chambers, B. J., Prescott, A. R., Ljunggren, H.-G. & Watts, C. Constitutive macropinocytosis allows TAP-dependent major histocompatibility compex class I presentation of exogenous soluble antigen by bone marrow-derived dendritic cells. *Eur. J. Immunol.* **27**, 280–288 (1997).

306. Mellman, I. ENDOCYTOSIS AND MOLECULAR SORTING. *Annu. Rev. Cell Dev. Biol.* **12**, 575–625 (1996).

307. Conner, S. D. & Schmid, S. L. Regulated portals of entry into the cell. *Nature* **422**, 37–44 (2003).

308. Harshyne, L. A., Watkins, S. C., Gambotto, A. & Barratt-Boyes, S. M. Dendritic Cells Acquire Antigens from Live Cells for Cross-Presentation to CTL. *J. Immunol.* **166**, 3717 LP – 3723 (2001).

309. Lindenbergh, M. F. S. & Stoorvogel, W. Antigen Presentation by Extracellular Vesicles from Professional Antigen-Presenting Cells. *Annu. Rev. Immunol.* **36**, 435–459 (2018).

310. Théry, C., Ostrowski, M. & Segura, E. Membrane vesicles as conveyors of immune responses. *Nat. Rev. Immunol.* **9**, 581–593 (2009).

311. Kovacsovics-Bankowski, M. & Rock, K. L. A Phagosome-to-cytoplasm Pathway for Exogenous Antigens Presented on MHC Class I Molecules. *Science.* **267**, 243–246

(1995).

312. Joffre, O. P., Segura, E., Savina, A. & Amigorena, S. Cross-presentation by dendritic cells. *Nat. Rev. Immunol.* **12**, 557–569 (2012).

313. Grotzke, J. E., Sengupta, D., Lu, Q. & Cresswell, P. The ongoing saga of the mechanism(s) of MHC class I-restricted cross-presentation. *Curr. Opin. Immunol.* **46**, 89–96 (2017).

314. Savina, A. *et al.* NOX2 Controls Phagosomal pH to Regulate Antigen Processing during Crosspresentation by Dendritic Cells. *Cell* **126**, 205–218 (2006).

315. Ackerman, A. L., Giodini, A. & Cresswell, P. A Role for the Endoplasmic Reticulum Protein Retrotranslocation Machinery during Crosspresentation by Dendritic Cells. *Immunity* **25**, 607–617 (2006).

316. Basha, G. *et al.* A CD74-dependent MHC class I endolysosomal cross-presentation pathway. *Nat. Immunol.* **13**, 237–245 (2012).

317. Nakayama, M. Antigen Presentation by MHC-Dressed Cells. *Front. Immunol.* **5**, 672 (2014).

318. Cone, R. E., Sprent, J. & Marchalonis, J. J. Antigen-Binding Specificity of Isolated Cell-Surface Immunoglobulin from Thymus Cells Activated to Histocompatibility Antigens. *Proc. Natl. Acad. Sci.* **69**, 2556 LP – 2560 (1972).

319. Sharrow, S. O., Ozato, K. & Sachs, D. H. Phenotypic expression of I-A and I-E/C subregion determinants on murine thymocytes. *J. Immunol.* **125**, 2263 LP – 2268 (1980).

320. Nepom, J. T., Benacerraf, B. & Germain, R. N. Acquisition of syngeneic I-A determinants by T cells proliferating in response to poly (Glu60Ala30Tyr10). *J. Immunol.* **127**, 888 LP – 892 (1981).

321. Sharrow, S. O., Mathieson, B. J. & Singer, A. Cell surface appearance of unexpected host MHC determinants on thymocytes from radiation bone marrow chimeras. *J. Immunol.* **126**, 1327 LP – 1335 (1981).

322. Lorber, M. I., Loken, M. R., Stall, A. M. & Fitch, F. W. I-A antigens on cloned alloreactive murine T lymphocytes are acquired passively. *J. Immunol.* **128**, 2798 LP – 2803 (1982).

323. Jing-Feng, H. *et al.* TCR-Mediated Internalization of Peptide-MHC Complexes Acquired by T Cells. *Science.* **286**, 952–954 (1999).

324. Hwang, I. *et al.* T Cells Can Use Either T Cell Receptor or Cd28 Receptors to Absorb and Internalize Cell Surface Molecules Derived from Antigen-Presenting Cells. *J. Exp. Med.*

191, 1137–1148 (2000).

325. Gu, P. *et al.* Trogocytosis of CD80 and CD86 by induced regulatory T cells. *Cell. Mol. Immunol.* **9**, 136–146 (2012).

326. Akkaya, B. *et al.* Regulatory T cells mediate specific suppression by depleting peptide–MHC class II from dendritic cells. *Nat. Immunol.* **20**, 218–231 (2019).

327. Joly, E. & Hudrisier, D. What is trogocytosis and what is its purpose? *Nat. Immunol.* **4**, 815 (2003).

328. Osborne, D. G. & Wetzel, S. A. Trogocytosis Results in Sustained Intracellular Signaling in $CD4^+$ T Cells. *J. Immunol.* **189**, 4728 LP – 4739 (2012).

329. Carlin, L. M., Eleme, K., McCann, F. E. & Davis, D. M. Intercellular Transfer and Supramolecular Organization of Human Leukocyte Antigen C at Inhibitory Natural Killer Cell Immune Synapses✪. *J. Exp. Med.* **194**, 1507–1517 (2001).

330. Sjöström, A. *et al.* Acquisition of External Major Histocompatibility Complex Class I Molecules by Natural Killer Cells Expressing Inhibitory Ly49 Receptors. *J. Exp. Med.* **194**, 1519–1530 (2001).

331. Zimmer, J., Ioannidis, V. & Held, W. H-2D Ligand Expression by Ly49A+ Natural Killer (NK) Cells Precludes Ligand Uptake from Environmental Cells : Implications for NK Cell Function. *J. Exp. Med.* **194**, 1531–1539 (2001).

332. Davis, D. M. Intercellular transfer of cell-surface proteins is common and can affect many stages of an immune response. *Nat. Rev. Immunol.* **7**, 238–243 (2007).

333. Viret, C., Barlow, A. K. & Janeway, C. A. On the intrathymic intercellular transfer of self-determinants. *Immunol. Today* **20**, 8–10 (1999).

334. Millet, V., Naquet, P. & Guinamard, R. R. Intercellular MHC transfer between thymic epithelial and dendritic cells. *Eur. J. Immunol.* **38**, 1257–1263 (2008).

335. Koble, C. & Kyewski, B. The thymic medulla: a unique microenvironment for intercellular self-antigen transfer. *J. Exp. Med.* **206**, 1505–1513 (2009).

336. Kroger, C. J., Spidale, N. A., Wang, B. & Tisch, R. Thymic Dendritic Cell Subsets Display Distinct Efficiencies and Mechanisms of Intercellular MHC Transfer. *J. Immunol.* **198**, 249–256 (2017).

337. Perry, J. S. A. *et al.* Transfer of Cell-Surface Antigens by Scavenger Receptor CD36 Promotes Thymic Regulatory T Cell Receptor Repertoire Development and Allo-tolerance. *Immunity* **48**, 923-936.e4 (2018).

338. Russo, V. *et al.* Acquisition of intact allogeneic human leukocyte antigen molecules by

human dendritic cells. *Blood* **95**, 3473–3477 (2000).

339. Wolfers, J. *et al.* Tumor-derived exosomes are a source of shared tumor rejection antigens for CTL cross-priming. *Nat. Med.* **7**, 297–303 (2001).

340. André, F. *et al.* Exosomes as potent cell-free peptide-based vaccine. I. Dendritic cell-derived exosomes transfer functional MHC class I/peptide complexes to dendritic cells. *J. Immunol.* **172**, 2126–2136 (2004).

341. Herrera, O. B. *et al.* A novel pathway of alloantigen presentation by dendritic cells. *J. Immunol.* **173**, 4828–4837 (2004).

342. Dolan, B. P., Gibbs, K. D. J. & Ostrand-Rosenberg, S. Dendritic Cells Cross-Dressed with Peptide MHC Class I Complexes Prime CD8 + T Cells . *J. Immunol.* **177**, 6018–6024 (2006).

343. Duong, E. *et al.* Type I interferon activates MHC class I-dressed CD11b+ conventional dendritic cells to promote protective anti-tumor CD8+ T cell immunity. *Immunity* 1–16 (2021) doi:10.1016/j.immuni.2021.10.020.

344. Wakim, L. M. & Bevan, M. J. Cross-dressed dendritic cells drive memory CD8+ T-cell activation after viral infection. *Nature* **471**, 629–632 (2011).

345. Smyth, L. A. *et al.* Acquisition of MHC:Peptide Complexes by Dendritic Cells Contributes to the Generation of Antiviral $CD8^+$ T Cell Immunity In Vivo. *J. Immunol.* **189**, 2274 LP – 2282 (2012).

346. Li, L. *et al.* Cross-dressed CD8α+/CD103+ dendritic cells prime CD8+ T cells following vaccination. *Proc. Natl. Acad. Sci. U. S. A.* **109**, 12716–12721 (2012).

347. Markey, K. A. *et al.* Cross-Dressing by Donor Dendritic Cells after Allogeneic Bone Marrow Transplantation Contributes to Formation of the Immunological Synapse and Maximizes Responses to Indirectly Presented Antigen. *J. Immunol.* **192**, 5426 LP – 5433 (2014).

348. Liu, Q. *et al.* Donor dendritic cell-derived exosomes promote allograft-targeting immune response. *J. Clin. Invest.* **126**, 2805–2820 (2016).

349. Marino, J. *et al.* Donor exosomes rather than passenger leukocytes initiate alloreactive T cell responses after transplantation. *Sci. Immunol.* **1**, (2016).

350. Bracamonte-Baran, W. *et al.* Modification of host dendritic cells by microchimerism-derived extracellular vesicles generates split tolerance. *Proc. Natl. Acad. Sci. U. S. A.* **114**, 1099–1104 (2017).

351. Zhang, L. *et al.* CD40 ligation reverses T cell tolerance in acute myeloid leukemia. *J.*

Clin. Invest. **123**, 1999–2010 (2013).

352. Hein, Z. *et al.* Peptide-independent stabilization of MHC class I molecules breaches cellular quality control. *J. Cell Sci.* **127**, 2885–2897 (2014).

353. Dougan, M., Dranoff, G. & Dougan, S. K. Cancer Immunotherapy: Beyond Checkpoint Blockade. *Annu. Rev. Cancer Biol.* **3**, 55–75 (2019).

354. Anderson, D. A., Dutertre, C.-A., Ginhoux, F. & Murphy, K. M. Genetic models of human and mouse dendritic cell development and function. *Nat. Rev. Immunol.* **21**, 101–115 (2021).

355. Sánchez-Paulete, A. R. *et al.* Antigen cross-presentation and T-cell cross-priming in cancer immunology and immunotherapy. *Ann. Oncol.* **28**, xii44–xii55 (2017).

356. Lee, M. Y., Jeon, J. W., Sievers, C. & Allen, C. T. Antigen processing and presentation in cancer immunotherapy. *J. Immunother. Cancer* **8**, (2020).

357. Overwijk, W. W. & Restifo, N. P. B16 as a Mouse Model for Human Melanoma. in *Current Protocols in Immunology* 20.1.1-20.1.29 (2000). doi:10.1002/0471142735.im2001s39.

358. LaBelle, J. L., Hanke, C. A., Blazar, B. R. & Truitt, R. L. Negative effect of CTLA-4 on induction of T-cell immunity in vivo to B7-1+, but not B7-2+, murine myelogenous leukemia. *Blood* **99**, 2146–2153 (2002).

359. Kline, J. *et al.* Homeostatic proliferation plus regulatory T-cell depletion promotes potent rejection of B16 melanoma. *Clin. Cancer Res.* **14**, 3156–3167 (2008).

360. de Witte, M. A. *et al.* Targeting self-antigens through allogeneic TCR gene transfer. *Blood* **108**, 870–877 (2006).

361. Schober, K. *et al.* Reverse TCR repertoire evolution toward dominant low-affinity clones during chronic CMV infection. *Nat. Immunol.* **21**, 434–441 (2020).

362. Böhm, W. *et al.* T cell-mediated, IFN-gamma-facilitated rejection of murine B16 melanomas. *J. Immunol.* **161**, 897–908 (1998).

363. Seliger, B., Wollscheid, U., Momburg, F., Blankenstein, T. & Huber, C. Characterization of the major histocompatibility complex class I deficiencies in B16 melanoma cells. *Cancer Res.* **61**, 1095–1099 (2001).

364. Van Kaer, L., Ashton-Rickardt, P. G., Ploegh, H. L. & Tonegawa, S. TAP1 mutant mice are deficient in antigen presentation, surface class I molecules, and CD4-8+ T cells. *Cell* **71**, 1205–1214 (1992).

365. Spiotto, M. T. *et al.* Increasing tumor antigen expression overcomes 'ignorance' to solid

tumors via crosspresentation by bone marrow-derived stromal cells. *Immunity* **17**, 737–747 (2002).

366. Nair-Gupta, P. *et al.* TLR signals induce phagosomal MHC-I delivery from the endosomal recycling compartment to allow cross-presentation. *Cell* **158**, 506–521 (2014).

367. Radhakrishna, H. & Donaldson, J. G. ADP-ribosylation factor 6 regulates a novel plasma membrane recycling pathway. *J. Cell Biol.* **139**, 49–61 (1997).

368. Montealegre, S. & van Endert, P. M. Endocytic recycling of MHC class I molecules in non-professional antigen presenting and dendritic cells. *Front. Immunol.* **9**, 1–11 (2019).

369. Bonifaz, L. *et al.* Efficient Targeting of Protein Antigen to the Dendritic Cell Receptor DEC-205 in the Steady State Leads to Antigen Presentation on Major Histocompatibility Complex Class I Products and Peripheral CD8 $^{+}$ T Cell Tolerance. *J. Exp. Med.* **196**, 1627–1638 (2002).

370. Tacken, P. J. *et al.* Targeting DC-SIGN via its neck region leads to prolonged antigen residence in early endosomes, delayed lysosomal degradation, and cross-presentation. *Blood* **118**, 4111–4119 (2011).

371. van Montfoort, N. *et al.* Antigen storage compartments in mature dendritic cells facilitate prolonged cytotoxic T lymphocyte cross-priming capacity. *Proc. Natl. Acad. Sci.* **106**, 6730 LP – 6735 (2009).

372. Tacken, P. J. *et al.* Effective induction of naive and recall T-cell responses by targeting antigen to human dendritic cells via a humanized anti–DC-SIGN antibody. *Blood* **106**, 1278–1285 (2005).

373. Reich, Z. *et al.* Stability of empty and peptide-loaded class II major histocompatibility complex molecules at neutral and endosomal pH: comparison to class I proteins. *Proc. Natl. Acad. Sci. U. S. A.* **94**, 2495–2500 (1997).

374. Chefalo, P. J. & Harding, C. V. Processing of Exogenous Antigens for Presentation by Class I MHC Molecules Involves Post-Golgi Peptide Exchange Influenced by Peptide-MHC Complex Stability and Acidic pH. *J. Immunol.* **167**, 1274–1282 (2001).

375. Ryschich, E. *et al.* Control of T-cell-mediated immune response by HLA class I in human pancreatic carcinoma. *Clin. Cancer Res.* **11**, 498–504 (2005).

376. Ogino, T. *et al.* HLA class I antigen down-regulation in primary laryngeal squamous cell carcinoma lesions as a poor prognostic marker. *Cancer Res.* **66**, 9281–9289 (2006).

377. Tsuchikawa, T. *et al.* Association of CD8+ T cell infiltration in oesophageal carcinoma lesions with human leucocyte antigen (HLA) class I antigen expression and survival. *Clin. Exp. Immunol.* **164**, 50–56 (2011).

378. Ennishi, D. *et al.* Molecular and Genetic Characterization of MHC Deficiency Identifies EZH2 as Therapeutic Target for Enhancing Immune Recognition. *Cancer Discov.* **9**, 546–563 (2019).

379. McGranahan, N. *et al.* Allele-Specific HLA Loss and Immune Escape in Lung Cancer Evolution. *Cell* **171**, 1259–1271 (2017).

380. Chen, X., MacNabb, B. W., Flood, B., Blazar, B. R. & Kline, J. Divergent fates of antigen-specific CD8+ T cell clones in mice with acute leukemia. *Cell Rep.* **37**, 109991 (2021).

381. Bern, M. D. *et al.* Inducible down-regulation of MHC class I results in natural killer cell tolerance. *J. Exp. Med.* **216**, 99–116 (2018).